University of Alberta

Crack Growth Behavior of Pipeline Steels in Near Neutral pH Soil Environment

by

Mohammad Hassan Marvasti

A thesis submitted to the Faculty of Graduate Studies and Research
in partial fulfillment of the requirements for the degree of

Master of Science
in
Materials Engineering

Department of Chemical and Materials Engineering

Spring 2010
Edmonton, Alberta

Examining Committee

Dr. Weixing Chen, Department of Chemical and Materials Engineering

Dr. Reg Eadie, Department of Chemical and Materials Engineering

Dr. Hao Zhang, Department of Chemical and Materials Engineering

Dr. Zihui Xia, Department of Mechanical Engineering

Abstract

Stress corrosion cracking (SCC) from the external surface of a buried pipeline is a serious matter and can cause significant economic and environmental losses. Despite of many research works which have been done on the understanding of crack initiation and propagation mechanisms, these mechanisms are still being debated. This research studied the crack growth behaviour of different pipeline steels including two types of X65, one X52 and one X80 pipeline steels in near-neutral pH environments. Crack growth behaviour of all steels has been found to be consistent with that of true corrosion fatigue. Crack growth rates were correlated with $(\Delta K)^2 K_{max}/f^{0.1}$. It was revealed that cracking behaviour of pipeline steels in near neutral pH environments is material dependent. Highest crack growth rate was seen in the steel which highest amount of hydrogen atoms could be generated and stored in its microstructure to contribute in cracking procedure due to hydrogen embrittlement effect.

Acknowledgements

I am extremely grateful to Dr Weixing Chen for his supervision, guidance and encouragement throughout the course of my thesis work. I am impressed by his knowledge in various aspects of Materials Engineering research and methods, as well as his friendly attitude.

I wish to thank Dr. Eadie and Dr. Zhang for their useful comments and feedbacks which was a great help for my research progression. I would also like to acknowledge US Department of Transportation, TransCanada Pipelines Ltd, Natural Science and Engineering Research Council of Canada for their financial support.

I am also thankful to Walter Boddez, Richard Cooper, Les Dean and Tina Barker form the University of Alberta for their technical support and advice throughout the progress of the work.

Kind helps of Lily Laser, Marion Pitchard and Heather Green is also appreciated.

Mohammad Hassan Marvasti

April 2010

Table of Contents

List of Tables

List of Figures

1. Introduction

Near-neutral pH SCC was first found in mid-1980s in Canada on TransCanada pipeline systems. Since then cracking of many other pipes were reported in Canada in the presence of near-neutral pH environment. The fact that there are more than 540,000 kilometers of buried oil and gas pipelines throughout Canada and high level of their failure due to cracking in near-neutral pH solutions has brought a great interest in investigation of cracking behavior of pipes in near-neutral pH environments.

Exposure of dilute ground water solution containing CO_2 with a pH range of 5.5-7.5 to the pipe surface is known to be responsible for cracking. Exposure occurs as a result of the pipe's coating disbondment. Many researchers indicated that this type of cracking involves anodic dissolution and hydrogen embrittlement. It is emphasized that hydrogen (corrosion's product) plays an important role in this type of cracking through hydrogen embrittlement effects.

Crack initiation on the pipe surface is inevitable but not all of these cracks can grow and cause failure. Many researchers have focused on the growth behavior of the existent cracks in the pipe structure to obtain an appropriate model which explains the growth behavior of cracks in different loading conditions. Using such a model helps pipe line operators to have a reasonable engineering expectation and prediction on the growth behavior of existent cracks. This helps that inspection and replacement of the section be done before the pipe failure occurs. To be efficient enough, different factors which influence cracking in a special environment should be considered in the proposed crack model.

Early studies on the cracking behavior of pipeline steels in near-neutral pH environments led to the introduction of the superposition model and strain rate model. It is believed that applied stresses to the pipe surface have the cyclic nature (fatigue) due to internal pressure fluctuations and cracking occurs due to synergistic interaction of corrosion and/or hydrogen and fatigue loading. Recently Chen and Sutherby used a combined factor $(\Delta K)^2 K_{max}/f^{\alpha}$ to relate the crack growth rate, da/dN. K_{max} is the maximum stress intensity factor, ΔK is the

changes of stress intensity factor due to cyclic stresses, f is the loading frequency and α represents the corrosivity of environment (environmental effect). This factor represents the synergistic interaction of fatigue loading effects $(\Delta K)^2 K_{max}$ and environmental effects $(1/f^{\alpha})$. Term $(\Delta K)^2 K_{max}/f^{\alpha}$ was used to analyze crack growth data of X65 TCPL in two different solutions. It was seen that all the growth data obtained by using different load ratios (R) and different frequencies could be rationalized by the combined term. The effect of hydrogen on corrosion fatigue crack growth could be well shown when the growth data analyzed using this factor. Threshold of the combined factor, demarcating the boundary between active growth and dormancy, could also be determined in each environment.

The objective of the current work was to investigate the crack growth behavior of different steels in near neutral pH environment and using the newly proposed combined term $(\Delta K)^2 K_{max}/f^{\alpha}$. With this purpose four different pipeline steels were used and their crack growth behavior further discussed using their microstructural and mechanical properties.

2. Literature Review

2.1. Environmentally Assisted Cracking

Environmentally assisted cracking is referred to any cracking process which can be enhanced due to environmental effects. Components failure due to their exposure to an aggressive environment is a common type of failure in industrial systems. In the presence of aggressive environment small flaws can be initiated in the components and failure potential of the component will be increased. Failure is commonly known to be caused by cracking. Usually an aggressive environment is referred to a chemical environment that causes corrosion. Offshore platforms in petroleum industry, buried pipeline steels and equipments in refineries are the examples of the components which are susceptible to corrosion as an aggressive environment that can cause failure. Environmentally assisted cracking phenomena include a wide range of materials with different cracking mechanisms and different environmental effects. The main focus of this thesis is on enhanced cracking occurrence in pipeline steels as a result of their exposure to the corrosive environment. The three most common types of environmentally assisted cracking observed in steels are recognized as:

- Stress Corrosion Cracking (SCC)
- Hydrogen Embrittlement (HE)
- Corrosion Fatigue (CF)

Failure due to all these three types is accompanied by facilitated crack initiation followed by enhanced crack growth behavior. Cracks propagate as a result of anodic dissolution in front of their tip in SCC processes while they propagate due to the embrittlement of their tip by hydrogen embrittlement mechanism and corrosion fatigue is known as enhanced fatigue crack growth by corrosion effects

[1]. These mechanisms which cause failure in pipeline steels will be discussed in details in this thesis.

2.1.1. Stress Corrosion Cracking

SCC is a type of environmentally assisted cracking that occurs when tensile stresses (mechanical factor) are applied to the susceptible material (metallurgical factor) which is exposed to the potent corrosive environment (electrochemical factor). Absence of any of these factors limits the occurrence of SCC. Tensile stresses may be supplied by service loads, cold work process, mismatch in fit-up, heat treatment or by wedging action of corrosion products. Stress intensity factor and strain rates at the crack tip due to external applied stresses influence cracking behavior significantly. Materials composition, its microstructure and deformation characteristics (yield strength) are some of the important metallurgical factors. It is noticeable that alloys are much more susceptible to SCC than pure metals because of more un-uniformity and microstructural flaws (second phases or inclusion particles). Finally important electrochemical parameters include oxidizing potential, critical pH values and temperature [**2**].

SCC crack grows through the anodic dissolution (corrosion reaction) at the tip of the crack. Simultaneous corrosion (dissolution) at the crack tip and on the crack walls will result in blunted crack and the crack can be changed to a corrosion pit. This shows that passive film generation on the crack walls to protect them from dissolution is a prerequisite need for SCC. It means that beside the anodic condition at the crack tip which should be thermodynamically possible, cathodic condition on the crack walls is also necessary to form a protective passive layer on the walls. Figure 2-1 shows SCC susceptibility zones on the anodic polarization curve. These zones represent the active to passive and passive to transpassive transition zones. SCC is probable in these zones because of changeable nature of passive film in these zones which undergoes rupture and re-formation repeatedly.

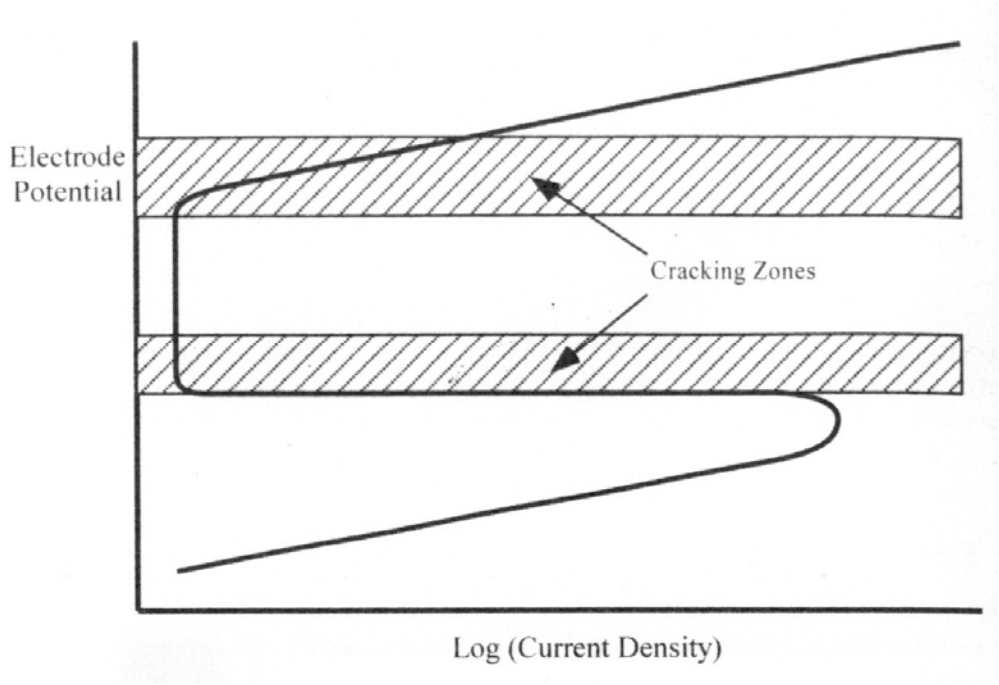

Figure 2-1: Polarization diagram which illustrates the zones that tend to favor SCC [3].

Passive layer on the crack tip can be ruptured due to available strain ahead of crack tip. Plastic strains (plastic deformations) can be caused due to triaxial stresses available in front of the crack tip. Plastic strains break the passive film at the crack tip so that material in the tip of the crack will be exposed to the environment (corrosive solution) and undergoes anodic dissolution while crack walls are protected. Schematic cracking behavior is illustrated in Figure 2-2:

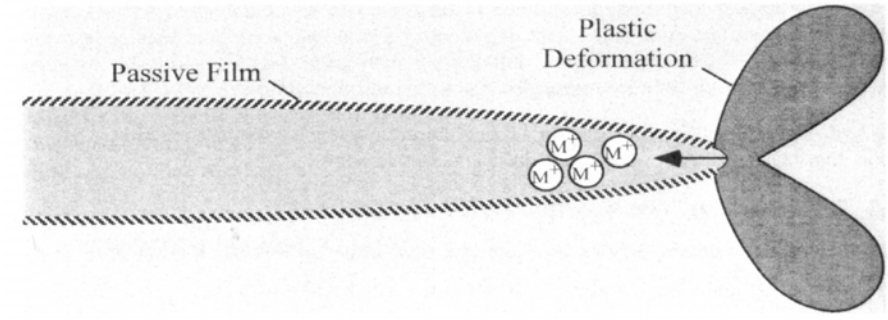

Figure 2-2: Film rupture model where plastic strain at the crack tip fractures the passive film at the crack tip [3].

Stress corrosion cracking process is known to consist of three stages of crack initiation, steady-state crack propagation and fracture failure.

SCC cracks can be either intergranular or transgranular and they propagate in the direction normal to the applied stress direction. Transgranular cracks propagate through the grains usually in specific crystal planes and intergranular cracks grow through the grain boundaries associated with the segregation of impurities in the grain boundaries [1].

2.2. SCC in Pipeline Steels

2.2.1. Introduction

There are more than 540000 kilometers of buried oil and gas pipelines throughout Canada. Pipe failure during its operation has a great probability and failure can occur either through leakage or rupture of the pipe. Pipe failure can be catastrophic and may cause significant economical losses and environmental damages [4]. Products transported through pipelines are generally hazardous and pipe failure can have serious consequences for people working or living close by the pipe environment. In the period from 1977 to 1996, 22 pipeline failures were reported in Canada including 12 ruptures and 10 leaks on both gas and liquid pipelines and death was caused in 1985 as a result of gas pipeline rupture. Since then many integrity research programs have been started to increase the understanding of SCC on pipeline systems to obtain prevention and safety operation procedures [5].

SCC can occur on both inner surface of the pipe and its outer surface. Corrosion can occur in the inner surface of the pipe as a result of gas or oil flow inside the pipe (erosion corrosion) or it can occur due to chemical reaction (dissolution) of pipe steel. On the other side outside surface of the pipe can also be corroded when it is exposed to its surrounded soil solution due to pipe's coating damages. This thesis focuses on the SCC occurrence on the outer surface of the pipe which can occur after pipes coating disbandment.

It is known that SCC begins on the outer surface of pipelines when small cracks develop on the outside surface of the buried pipe. These cracks are commonly found in colonies and can join each other along the length or depth of the pipe to form longer cracks. The joining process might take a long time over many years but when the crack size reaches the critical size it can cause failure. If the crack propagate through the whole thickness of the pipe wall before reaching its critical size (fracture mechanics calculations) it will cause leakage without rupture. On

the other hand passing the critical length on the pipe surface, the crack can cause rupture.

For stress corrosion cracking to occur three conditions of tensile stresses, susceptible material and potent environment (at the pipe surface) are necessary. These factors and some of their sources for pipelines are summarized in the Figure 2-3. Elimination of any of these conditions can lead to SCC prevention. Studying the individual effect of these factors on SCC and investigating their sources can help design prevention plans by controlling these factors in a way that make the pipeline less susceptible to SCC through an specific loading situation and environment which the pipe is operated in.

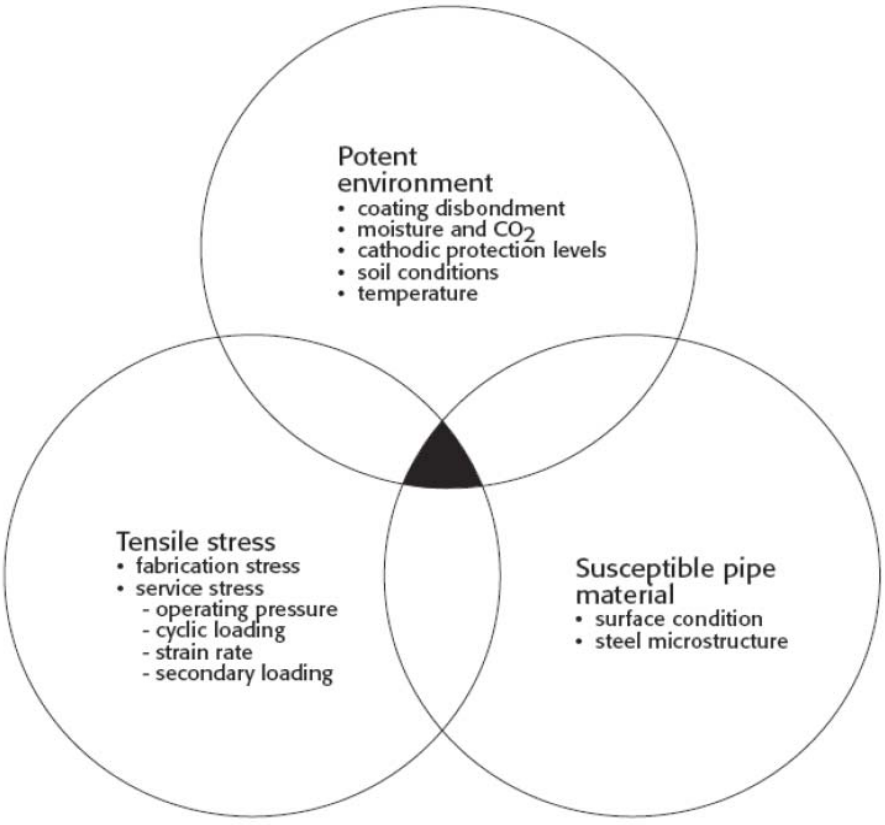

Figure 2-3: Factors required for SCC occurrence in pipeline steels [5].

2.2.2. Potent Environment

For SCC cracks to be initiated on the pipe outer surface it is necessary that the pipe surface be exposed to an appropriate environment that has the ability of causing corrosion. As it can be seen in Figure 2-4, when the pipe coating damages, pipe surface can be exposed to its surrounding environment. The water drainage can penetrate inside the gap under the coating which to causes SCC cracks initiation in the presence of appropriate stress. Factors such as pipe's coating condition, soil chemistry and cathodic current level, influence the environmental component of SCC [6].

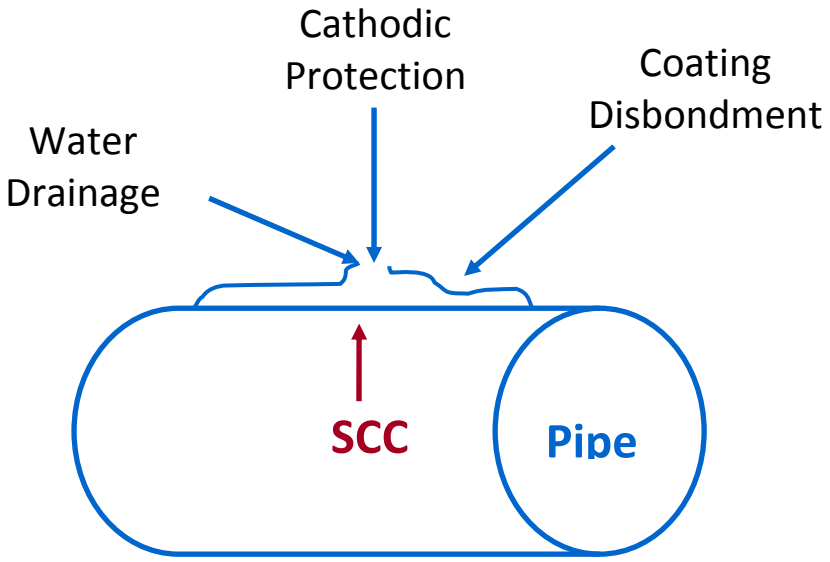

Figure 2-4: Potent environment for SCC.

Different coating types and conditions can represent different resistance to external stresses but it is reasonable to expect coating disbondment over the pass of time due to external loads such as soil movement or pipe surface roughness.
Soil chemistry is an important matter. Elements inside the soil affect the pH of the solution (water) in contact with the pipe surface. Based on the field observations

dilute carbonate-bicarbonate solution in water is a responsible environment that can cause SCC. Fracture surfaces of the pipes in the field are usually covered with black magnetite or iron carbonate film which proves the role of carbonate-bicarbonate environment on cracking. Decay of organic matters in the soil is known to be the source of CO_2 and different soil types can provide different levels of CO_2 in the water solution. Different CO_2 levels yields to different pH values. Certain aspects of CO_2-H_2O system that make suitable environment (solution) for cracking are summarized below [6].

2.2.2.1. Electro Chemistry of CO_2-H_2O System

Dissolution of CO_2 in the soil water generates carbonic acid (H_2CO_3). Carbonic acid can be dissociated to bicarbonate (HCO_3^-) and carbonate ion (CO_3^-) in different pH values which are defined based on the CO_2 concentration in the soil. Two different reactions that can happen in different pH values are shown below:

$$H_2CO_3 = HCO_3^- + H^+ \quad (1) \qquad ; \qquad HCO_3^- = CO_3^{2-} + H^+ \quad (2)$$

Figure 2-5 shows the dominancy boundaries of different species (H_2CO_3, HCO_3^- and CO_3^{2-}) in different solution pH using equilibrium constants of the reactions above:

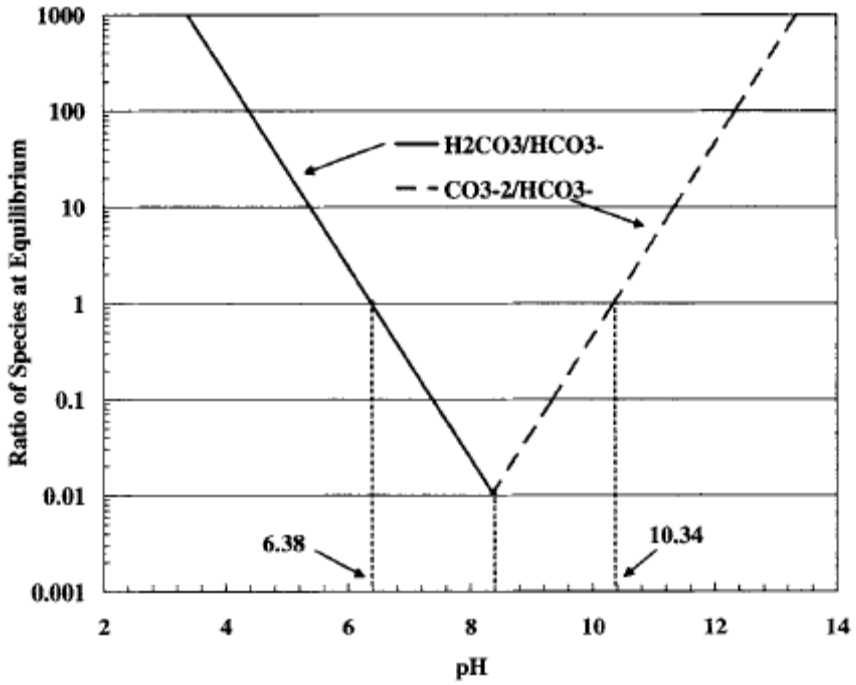

Figure 2-5: Solubility curves for predominant species in the CO_2-H_2O system [6].

CO_2 partial pressure in the soil (related to the soil type) and the amount of cathodic protection current applied to the pipe surface can obtain the specific pH value of the solution. Figure 2-5 shows that bicarbonate ion (HCO_3^-) is dominated in the intermediate pH region where the pH changes between 6.4 and 10.3. At pH values lower than 6.4, attributed to high partial pressure of CO_2 in the soil environment, H_2CO_3/HCO_3^- equilibrium goes in the reverse direction of equation (1) to generate more H_2CO_3 (acidic region with low pH values). In a highly concentrated H_2CO_3, corossivity of environment will be high enough to cause general corrosion on the pipe surface. On the other hand at low CO_2 partial pressures at pH values higher than 10.3, CO_3^{2-} will be generated form bicarbonate ions through equation (2). In this situation hydrogen ions of water reacts with the hydrogen ion released from equation (2) and OH^- ions of water make the local environment even more alkaline [6].

2.2.2.2. Cathodic Protection Current

Other than partial pressure of CO_2 in the soil, the degree of cathodic protection applied to the pipe surface is another factor that influences the pH value of the environment. When the pipe coating is damaged, pipe surface will be corroded due to its exposure to the environment. Corrosion happening on the pipe surface is an electrochemical reaction where iron on the surface of the pipe looses electron to be corroded in an anodic reaction. In cathodic protection process, an electric potential is applied to the pipe surface through the soil which can effectively prevent corrosion on the pipe surface when the surface gains a cathodic voltage and anodic dissolution will be limited.
However, cathodic current can increase the pH value of pipe surface by reducing Hydrogen ions which is accompanied with accumulation of hydroxyl ions:

$$2H_2O + 2e^- = H_2 + 2OH^- \quad , \quad O_2 + 2H_2O + 4e^- = 4OH^-$$

The amount of cathodic current reaches the pipe surface depends on the electrical resistivity of the soil, solution and the pipes coating. With high electrical resistivity the amount of cathodic current reaching the pipe surface won't be significant to cause pH increase of the environment [4].

2.2.3. SCC Categories

SCC is divided in two different groups based on the pH value of the environment that SCC occurs in. As discussed above different environment parameters such as coating type, soil chemistry (CO_2 partial pressure in the soil) and the amount of

cathodic protection can define the pH of the environment. SCC can happen in either high pH values or low (near-neutral pH) values. The former is being referred as high pH SCC and the latter is known as Near-Neutral pH SCC (NNPHSCC). These two kinds of cracking have many differences containing different cracking morphologies. Cracks which are known to be due to high pH SCC are intergranular while transgarnular cracks are found in near-neutral pH SCC (Figure 2-6). Difference in cracks morphologies suggests different cracking mechanisms in these two types of SCC.

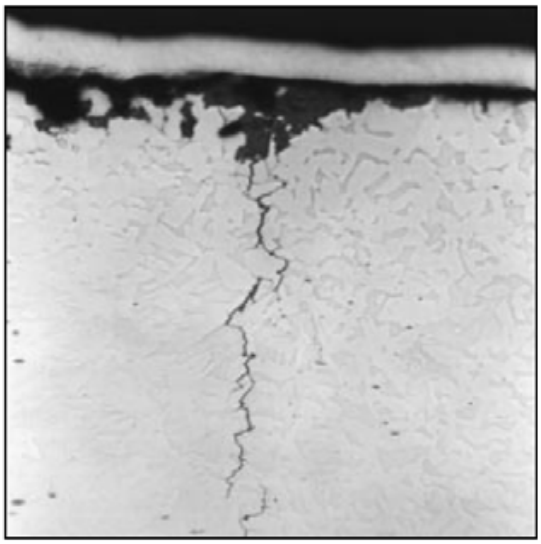

(a)

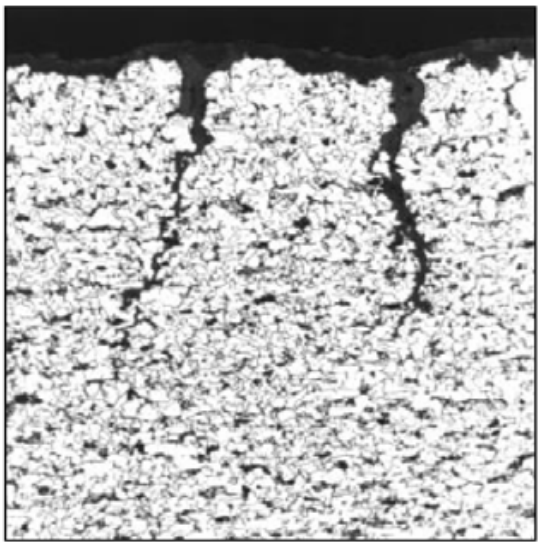

(b)

Figure 2-6: Crack morphology of a) high pH SCC and b) NNpHSCC [5].

Parkins Developed a general four-stage cracking procedure model applied to both types of SCC (Figure 2-7). First stage represents the crack initiation stage when necessary conditions for crack initiation such as coating disbandment and formation of appropriate electrolyte composition (solution) established. Cracks will form in stage two in stations of high local strain energies that decreases the strain level and limits the growth of initiated cracks to cause crack dormancy. Coalescence of neighboring cracks increases the probability of cracking re-initiation and finally in the last stage (stage four) large coalesced cracks can continue the growth leading to failure as the stress intensity factor at their tip exceeds a threshold value [7].

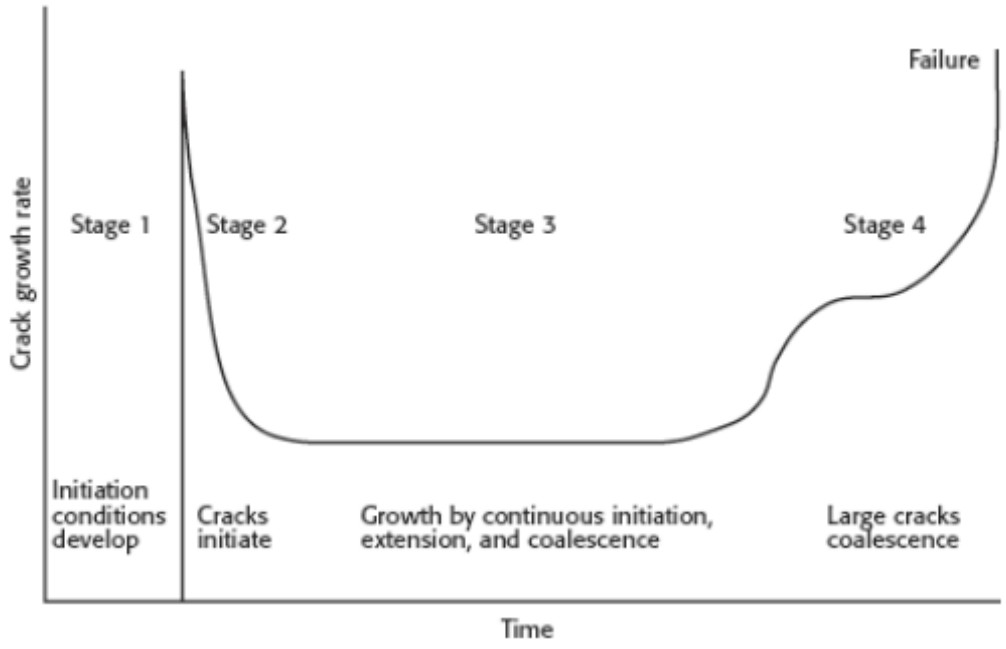

Figure 2-7: Model for a SCC crack that would grow to failure [7].

2.2.3.1. High pH SCC

This type of SCC is quite well known as it was investigated long time ago in 1960s and it occurs in high pH environments (pH= 8.5-11.5) as its name represents. High partial pressure of CO_2 in the soil environment and high amount of cathodic current (generation of hydroxyl ions) reaching the pipe surface (low current resistance of the soil and pipe coating) can be responsible for local increase of pH in the environment to make high pH type of SCC to occur.

Intergranular sharp narrow cracks with little evidence of corrosion happening on the crack walls are some of the characteristics of the cracks found due to high pH SCC. High pH SCC occurs in a limited potential range of about 100 mV wide which is centered on about -720 mV $Cu/CuSO_4$ (CSE) at 75^oC. This potential range represents the active-passive transition zone on potentiodynamic polarization curves of steels which reflect the fact that passivation behavior should play a great role in the cracking procedure [8].

The mechanism of cracking in high pH SCC is known to be related to the passive film formation and anodic dissolution. Passive film (thin oxide layer that forms from electrochemical reactions on this specified potential range) on the crack walls and its tip prevents the exposure of crack tips and walls to the environment (corrosive solution). This limits the anodic dissolution. The passive film can be ruptured due to high amount of plastic deformation and strain rate at the crack tip zone as a result of high magnitude of triaxial local stresses available at that region. Rupture of passive layer on the crack tip exposes the fresh metal to the corrosive solution and anodic dissolution occurs. When the crack propagates, passive film will be formed continuously on the crack walls. Presence of passive layer on the crack walls keeps the crack crevice narrow with little evidence of corrosion on the crack walls.

Considering the mechanism of high pH SCC as a repeated passive film rupture, anodic dissolution and re-passivation of new crack walls, it can be concluded that anodic dissolution rate, passive film formation rate and re-passivation rate can

influence the cracking rate in high pH SCC. Re-passivation rate and plastic strain rate are also in competition at the crack tip. Plastic strain rate can be investigated through creep deformation process at the crack tip. With high film formation rate and low creep (plastic strain) rate passive film maintenance will be expected that limits the crack advancement. On the other hand high creep (plastic strain) rate and low re-passivation rate enhances the crack tip exposure to the corrosive environment and crack growth.

Intergranular crack morphology which is seen in high pH SCC regime is attributed to cracking mechanism. Impurities and some alloying elements such as carbon, sulfur or phosphorus tend to segregate to the grain boundaries in ferritic steels which influence re-passivation and creep behavior of the steel. Segregation of these elements in grain boundaries cause the grain boundaries to go through preferential dissolution in high pH regimes. The dissolution can continue farther by the presence of stresses with an appropriate magnitude. As a final result grain boundaries will be the preferential cracking cites and cracking morphology is mainly intergranular cracking in high pH SCC regimes [4, 8, 9].

2.2.3.2. Near-Neutral pH SCC

Near-neutral pH SCC was first founded in mid-1980s in Canada on TransCanad pipeline systems. Dilute ground water solution containing CO_2 with pH range of 5.5-7.5 is responsible in this type of SCC. When the pipe coating ruptures the solution will get in contact with the pipe surface and cracking occurs in a wide range of potentials. Relatively high amount of CO_2 pressure and lack of cathodic protection current reaching the pipe limits the pH increase of the environment.

Crack morphology in this type of SCC contains transgranular cracks with a quasi-cleavage fracture surface and secondary internal cracks on the fracture surface. These transgranular cracks have a wide crevice with the evidence of large amount of corrosion on their walls [9].

Active-passive transition behavior is absent in these low pH ranges and corrosion can happen easily on the crack walls and the crack tip. The corrosion happening on the crack walls makes the crack crevice wider due to dissolution of crack walls dissolution. The significant amount of white powders (predominantly iron carbonate, $FeCO_3$) found near transgranular crack failures is a sign of high amount of corrosion happening in this pH regime.

Different cracking morphology and the absence of active-passive transition behavior, represents the different cracking mechanism of near-neutral pH SCC from the high pH mechanism. The most plausible mechanism is known to be hydrogen related mechanism which is supported by the presence of quasi-cleavage fracture with secondary cracks.

Parkins [10, 11] indicated that near-neutral pH SCC crack growth involves anodic dissolution and hydrogen embrittlement. This idea was supported by other researches such as Leis, Wilmott and Jack, Lambert and Plumtree and Beavers [12]. Parkins announced that SCC cracks in near-neutral pH environment probably initiate at the bottom of the corrosion pits formed on the pipe surface where the localized low pH environment is available to produce atomic hydrogen with continuous dissolution.

Hydrogen is generated as a product of corrosion (equations below) happening on the pipe surface. Then it diffuses to the highly plastically distorted areas in the microstructure such as the crack tip and enhances the crack due to hydrogen embrittlement effect [6].

$$
\begin{array}{lcllll}
H_2CO_3 & \leftrightarrow & HCO_3^- & + & H^+ \\
 & & + & & + \\
Fe & \leftrightarrow & Fe^{2+} & + & 2e^- \\
 & & \downarrow & & + \\
 & & FeCO_3 & + & H^+ \\
 & & & & \downarrow \\
 & & & & 2H(ads)
\end{array}
$$

As a conclusion the mechanism of cracking in near-neutral pH environment is the synergistic interaction of anodic dissolution (hydrogen generator) and hydrogen embrittlement.

This type of SCC has a great importance in Canada as all the Canadian pipelines are susceptible to this type of SCC so that many integrity researches have been started sinne near-neutral pH SCC was found first in mid 1980s. Investigation the effect of different parameters on the growth behavior of the cracks initiated in near-neutral pH environment can lead to the efficient way of monitoring the growth to establish prevention behaviors to replace or repair the pipes before the pipe fails [5]. More details will be provided on the cracking mechanisms and important factors influence cracking in Near-neutral pH environment after short discussion on the role of applied stresses and susceptible pipe material on SCC occurrence of pipelines.

2.2.4. Applied Stresses

Buried pipelines are always under different types of stresses. The main stresses that are applied to the pipe are due to internal pressure of the gas or liquid which is transported in the pipe. These stresses have a cyclic nature (fatigue) because of the gas or liquid pressure fluctuation inside. Pressure changes in gas lines is affected by the rate at which the gas is injected into the system and withdrawn by delivery systems. Internal pressure can fluctuate more widely in liquid pipelines due to fluid density changes from the pumps in internal stations.

Internal pressure inside the pipe can apply either hoop stresses (circumferentially) or axial stresses (lengthwise) to the pipe body. Cracks found on the buried pipeline surface contain two different types of axial (longitudinal) and circumferential cracks. Cracks usually grow in perpendicular direction to the applied tensile stresses. It can be concluded that axial cracks are the most serious cracks on the pipe surface as they are due to the main stress applied to the pipe (internal pressure) which is applied more circumferentially (Figure 2-8). Parkins

also represented that SCC cracks usually occur on the outside surface of the pipe in colonies mostly oriented longitudinally along the pipe [13]. Field observations showed that 73 per cent (16 out of 22) of the failures that have occurred on pipelines in Canada involved axial cracks indicating that hoop stresses controlled the failure.

It seems that reducing the internal pressure of the gas or liquid in the pipe can be an important key in reducing the susceptibility of pipe line to SCC but it is not economical for the purpose of transportation. On natural gas pipelines, the maximum allowable hoop or operating stress ranges between 44 and 80 per cent SMYS (specified minimum yield strength) depending on the environmental condition that the pipe is operated in while the minimum pressure is typically in the range of 85 per cent of the maximum operating pressure.

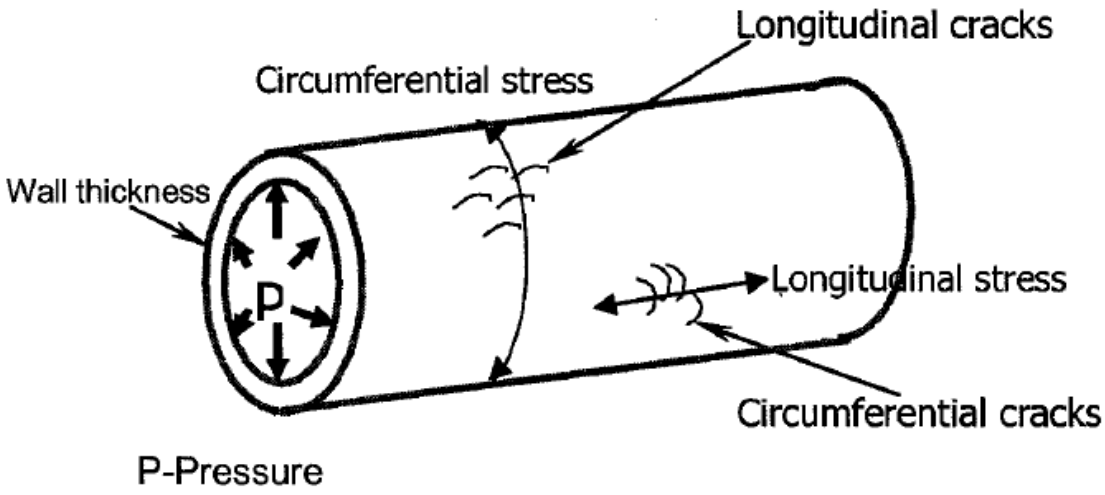

Figure 2-8: Stresses and cracks in pipeline steels [5].

Residual stresses are the second important source of applied stresses. Residual stresses usually introduced to the pipe structure due to fabrication processes on the pipe such as rolling and welding. The level of residual stresses depends on the manufacturing process used to produce the pipe but it is known that operating

pipelines can contain residual stresses of at least 25 per cent of their yield strength [5]. These residual stresses influence cracking as they can elevate stress levels in localized areas to enhance SCC cracks initiation. Residual stresses are known to contribute more in circumferential direction which enhances cracking in axial direction on the pipe surface. So it sounds reasonable to think about the ways to decrease the level of residual stresses in the pipe. Other than using fabrication processes which cause less amount of residual stresses, thermally stress reliving of the pipe during fabrication is known to reduce residual stresses. Introducing compression stresses by increasing expansion (high-pressure hydrostatic tests) during the fabrication process can be another option to reduce residual tensile stresses mechanically although residual stresses can not be eliminated completely [5].

Other than internal pressure and residual stresses, soil environment of the pipe can be mentioned as another source of stresses which are applied to the pipe surface. Movement of the soil surrounded the pipe can apply tension tresses to its surface and this can be accompanied by the stresses applied due to seasonal temperature changes on the pipe surface. Thermal stresses and stresses from the soil surface are mainly in the axial direction of the surface and have minor contribution in the stress level that can increase the susceptibility of SCC.

2.2.5. Susceptible Material

From the field observations SCC has occurred on a wide variety of pipes and it can be said that all of different pipe types are susceptible to SCC independent of their manufacturing methods. Pipe surface condition, pipe chemistry and its mechanical characteristics have a great influence on its susceptibility to SCC.

Pipe's surface condition affects the bonding quality of the pipe coating. Macroscopic discontinuities on the pipe surface can generate some gaps between the surface and the coating that can be counted as a preferred spots for the corrosive solution (water drainage) to penetrate in and be exposed to the pipe

surface cracking initiation site. Corrosion pits can be generated on the surface of the pipe as a result of its direct exposure to the corrosive environment. These pits are usually formed on the microscopic surface discontinuities. Pits are counted as a preferred spots for stress concentration and many cracks have been observed, that have been initiated at the bottom of surface pits. Pipe cleanliness and composition characteristics also affect cracking. Susceptibility of the pipe will be decreased when less amount of inclusions appear in the pipe microstructure. Inclusions are known to act as stress risers that can cause stress concentration to increase the stress state of the pipe. Corrosion resistance of the steel is known to be affected by steel's composition. Addition of some elements such as chromium, nickel and molybdenum between two to six per cent can increase the general corrosion resistance of the pipe to corrosion.

Other important characteristic of pipe steel is its mechanical (plastic deformation) characteristics. Mechanical behavior is represented as the material's response to the applied stresses affecting crack initiation and propagation. SCC cracks can be initiated easily in microplastic deformed areas. These microplastic deformations can occur at the stresses range between 85 to 95 per cent of the steel yield strength. Cyclic loads can help to cause localized microplastic deformations in lower stress states (cyclic softening). It seems that increasing the yield strength of the pipe steel can prevent the formation of microplastic deformation in lower stresses but it was seen that increasing the yield strength does not decrease the SCC susceptibility of the pipe. This might be explainable as the magnitude of the triaxial stresses present in deformed area is proportional to the yield strength of the material.

2.3. Hydrogen Embrittlement

It was mentioned before that besides the anodic dissolution occurrence, hydrogen is known to have a big role in near-natural pH cracking of pipeline steels by causing hydrogen embrittlement effect in the pipe steel. A brief introduction to

hydrogen embrittlement as other environmentally assisted cracking mechanisms in steels seems to be necessary for further discussion on the cracking behavior in near-neutral pH environments. Hydrogen embrittlement is probable to occur in the environments which are capable of introducing hydrogen into the component material. Hydrogen embrittlement cracks are more preferentially transgranuler cracks which grow fast with planar appearance in a brittle quasi-cleavage fracture mode. The mechanism due which hydrogen causes embrittlement in the metals and alloys is represented by different theories known as decohesion theory and internal pressure theory.

2.3.1. Decohesion Theory

According to this theory which was developed by Toriano [14], hydrogen atoms tend to diffuse into the alloy microstructure as a result of their relatively small size compared to most of other metallic atoms such as iron, aluminum and titanium. Locations with more lattice defects (distortion) such as fracture process zone ahead of the crack tip, localized plastic deformed areas and grain boundaries are the preferred spots for hydrogen accumulation in the material microstructure.
Toughness and ductility of the metal are reduced dramatically when hydrogen is introduced to the microstructure and cracking potential is increased. Hydrogen reduces the bond strength between the metal atoms by penetrating in the interstitial sites in the lattice. Triaxial stresses at the crack tip form a highly distorted plastically deformed area with high local hydrogen solubility. Accumulation of hydrogen in these regions embrittles the region and enhances the growth of crack in the presence of the same amount of triaxial stresses [15].

2.3.2. Internal Pressure Theory:

This theory was proposed by Zapffe and Sims [16]. These authors argued that hydrogen atoms accumulate at voids and lattice defects in the microstructure of the metal until an equilibrium pressure is obtained. Metal embrittlement occurs

when this pressure reaches a value close to the yield strength of the metal. Griffith theory of brittle fracture can be used to explain crack growth through this mechanism. According to this theory, for a stable crack to grow, cracking system must undergo a total decrease in the local energy content. Considering internal pressure theory, crack growth is facilitated by the energy release by hydrogen gas expansion in crack crevice. Gas expansion energy supplies the portion of strain energy required for crack to grow and the strain energy which should be supplied for crack to propagate is decreased so that cracking process continues easier [15].

2.3.3. Factors Affecting Hydrogen Embrittlement

Any factor related to hydrogen generation and absorption process in the metal microstructure influence hydrogen embrittlement cracking. Environment of which the component is used in is the main source of the hydrogen. Hydrogen diffusion into the metal structure will become more probable with higher amount of available hydrogen generated by the environment. On the other hand materials tendency in welcoming the hydrogen to its lattice can define the level of its susceptibility to hydrogen embrittlement. Generally hydrogen can diffuse to any kind of material microstructures because of its small atomic size but more un-uniformities inside the structure such as impurities, inclusions, precipitates and second phase particles increases the diffusion and accumulation of hydrogen in the microstructure as their interfaces are appropriate welcoming areas for hydrogen accumulation because of local distortion at that regions. Yield strength of the material is known as a reprehensive of its mechanical characteristics. It is revealed that the increase in the yield strength of the material increases the probability of hydrogen damage. The best explanation may be related to the magnitude of the stresses present in the fracture process zone ahead of crack tip. Magnitude of the triaxial stresses present in the fracture process zone ahead of the crack tip is proportional to the yield strength value of the material. Higher yield strength results in higher magnitude of triaxial which can form larger plastically deformed area with higher amount of distortion which represents more welcoming

spots for hydrogen to diffuse and accumulate in. Figure 2-9 illustrates the increase of hydrogen embrittlement cracking rate with increasing yield strength:

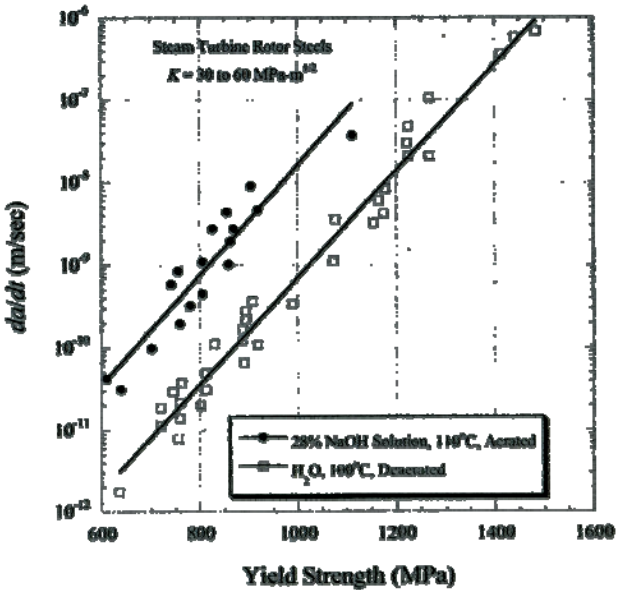

Figure 2-9: Effect of yield strength on crack growth rate in steam turbine rotor steel [1].

Temperature is another factor that affects hydrogen embrittlement process significantly. Kinetics of the cracking process is affected by temperature. The rate of hydrogen assisted cracking is controlled by the diffusion rate of hydrogen to the fracture process zones. Hydrogen can be concentrated in Cottrell atmospheres of dislocations and transported along with dislocation movements. Dislocation movement rate is a great function of diffusion rate which is directly related to the temperature. Hydrogen diffusion rate can be represented by Arrhenius law: $D=D_oe^{-Q/RT}$ where Q=activation energy, R=gas constant and T=absolute temperature. Figure 2-10 below shows the effect of temperature on hydrogen assisted crack growth rate and cracking threshold.

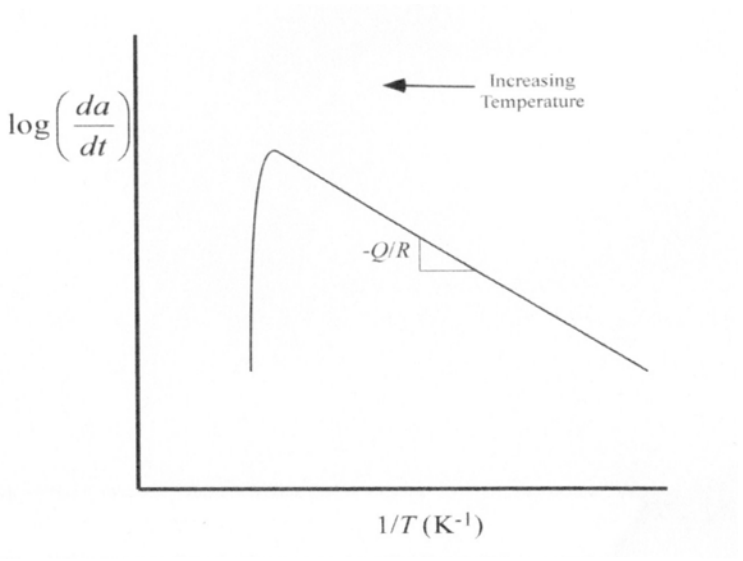

Figure 2-10: Effect of temperature on cracking velocity for hydrogen induced cracking [1].

It can be seen that cracking velocity is increased by increasing temperature and the disappearance of hydrogen embrittlement at low temperatures can be explained by the decrease of hydrogen diffusivity in lower temperatures.

2.4. Crack Growth Behavior of Pipeline Steels in Near-Neutral pH Environments

2.4.1. Introduction

Stresses applied to the pipe and the corrosion occurring on the surface of the pipe are known to be the two synergistic driving forces for crack growth in near-neutral pH environment. The influence of both stresses and corrosion can not be considered individually as both interact with each other and affect crack growth. Stresses applied to the pipe are classified as mechanical factors and are mainly divided in to residual and operational stresses.

The role of stresses primarily consists of generation, concentration and emission of dislocations through the occurrence of plastic deformation which results in metal flow and material removal that facilitates the environment exposure to the fresh metal. Distorted area in front of the crack tip as a result of plastic deformation and dislocation concentration enhances the hydrogen diffusion in front of the crack tip to readily cause local embrittlement. On the other hand high amount of plastic deformations occurs due to creep (time-dependent plastic deformation at a constant stresses below the yield strength) can cause crack tip blunting due to plasticity closure effect.

Maximum stress intensity factor at the crack tip (K_{max}) and stress intensity factors changes at the crack tip (ΔK) are used to represents the mechanical driving forces for crack growth. Stress intensity factor reflects the effects of applied stresses, crack length and shape of the component. K_{max} and ΔK are representatives of rupture of crack tip bonds and cyclic plastic damage at the crack tip respectively.

Corrosion occurring on the pipe surface is classified as environmental factor that influence cracking. Corrosion products (iron carbonate) resulted form extensive dissolution at the crack tip can blunt the crack tip. Corrosion is also the main source of hydrogen generation. Hydrogen enhances crack growth due to embrittlement effect in crack tip area. It has also an effective role in re-sharpening

the blunted crack tip caused by either high amount of plasticity or corrosion products [17].

As mentioned before there is a great synergistic interaction between stress, corrosion and hydrogen. Figure 2-11 illustrates the interaction present on the crack growth schematically. Although environmental and mechanical effects on the crack growth can not be discussed separately, it is generally believed that crack growth is influenced more by environmental effects on the early stages of growth while mechanical effects become dominant in later stages when crack tip conditions become more severe.

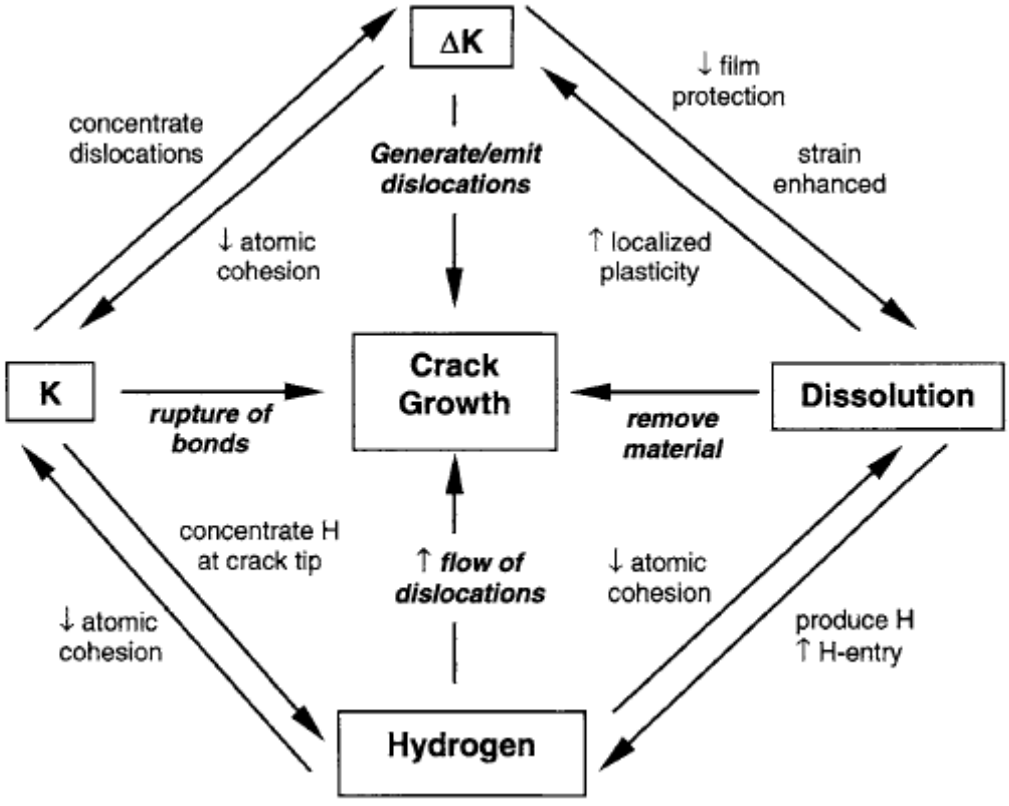

Figure 2-11: Schematic illustration of interactions between the driving forces behind crack growth [17].

2.4.2. Mechanical Factors Affecting Crack Growth

The growth ability of a single crack in the pipe system depends significantly on the amount of maximum stress intensity that can be reached on its tip due to mechanical loading condition. Crack can grow when maximum stress intensity factor ahead of its tip K_{max} (represents the highest magnitude of local stresses ahead of its tip) reaches the critical value of stress intensity factor called fracture toughness which is a material dependent parameter.

J-integral values are used to report stress intensity factors of materials which represent considerable amount of plastic deformation in their cracking process. Reversely the amount of plastic deformation can be evaluated using J-integral values.

Harle et al., [18], used J-integral test technique to investigate the driving force of crack growth in X65 pipeline steel in simulated near-neutral pH corrosion solution. The plot of crack velocity vs. J values (Figure 2-12) represents that J was dominated by the plastic component. This indicates that crack propagated with significant amount of plastic deformation and the linear increase of crack velocity with J-integral values confirms that J (plastic deformation) can be counted as a good driving force for cracking process in near-neutral pH environments.

Plastic deformation can make distortion in the lattice which prepares best sites for hydrogen to diffuse. Plastic deformation is accompanied by dislocation generation and dislocation movements which results in increase of dislocation density. Dislocations are known as easy paths that can trap hydrogen atoms to make embrittlement.

Increase of dislocation density increases the yield strength of the material and the hydrostatic stress filed around the crack tip increases results in the higher magnitude of triaxial stress in front of the crack tip and larger distorted area that hydrogen can diffuses in and enhances the crack growth [19].

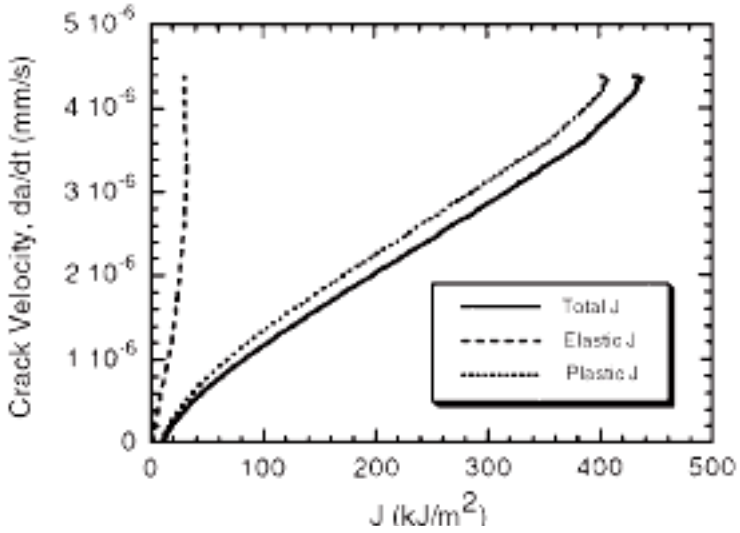

Figure 2-12: Crack velocity as a function of elastic J, plastic J and total J [18].

Some extent of internal energy will be stored in the steel when it is plastically deformed. This stored energy is mainly due to strain energy associated with dislocations. This amount of energy is released on dissolution, makes it to occur easier. Easier dissolution enhances the corrosion occurrence and hydrogen generation. As these two factors are the two main factors influencing cracking in near-neutral pH environment, it can be concluded that near-neutral pH cracking will be enhanced by plastic deformation.

The tests done by Li et al. [20], confirmed the critical role of plastic deformation on cracking process in near-neutral environment. Their results showed that in all X52 pipeline steels samples used, stress corrosion rates enhanced by plastic deformation. They also saw an increase of corrosion current as a result of increased plastic deformation in their samples in electrochemical tests which reflect the enhancement of corrosion occurrence with plastic deformation occurrence.

Considering the above discussion it seems necessary to investigate the contribution of mechanical parameters that can make plastic deformation in the pipe. Stresses applied to the pipe are responsible for plastic deformation of the

pipe. A high positive tensile stress gradient higher than yield strength of the pipe steel is required to generate plastic deformation. Tensile residual stresses and stress concentrators can have a great contribution in preparing the tensile stress gradient in the pipe other than external stresses applied to the pipe. Van Boven et al. [21, 22], found the strong correlation between tensile residual stresses and presence of cracks. They found that micro-pits can be formed preferentially in areas where tensile residual stresses were the highest and then the growth ability of the crack from the bottom of the pits is related to residual stress state at the local area at the bottom of the pit. Their results had a good consistency with the filed data which showed the great correlation between tensile residual stresses and the presence of cracks. As a result residual stress gradient represents a high mechanical driving force for crack initiation and growth.

Plastic deformation can also be caused by local stress concentrations due to stress risers such as inclusions and lattice defect interfaces. Stress concentration can cause local micro plastic deformation at stress levels higher than yield strength of steel which increases the dislocation density locally and facilitates hydrogen ingress and accumulation preferably on the slip bands formed by plastic deformation and dislocations strain energy fields [19, 23].

Crack advancement and plastic deformation occurrence probability can be represented by K_{max} and ΔK values which reflect the stress state at the crack tip. Mechanical factors which affect these values should be investigated.

Mechanical overloads, crack deflection, strain hardening and crack closure effect can influence cracking by decreasing ΔK. Crack closure effect is known as the most important phenomena which contains the corrosion effects as well. Crack closure effect reduces ΔK due to contact of the crack surfaces near the minimum stress of the cycle. Crack closure effect can occur due to several mechanisms but among those, oxide (corrosion products) induced closure and plasticity closure are known to be important in near-neutral pH environments. Oxide induced closure in this case is related to accumulation of corrosion products in the crack crevice ahead of crack tip that can contact the crack faces and plasticity induced closure can be related to the excessive amount of plastic deformation at the crack tip that

can happen due to creep deformation at the crack tip which results in the bluntness of the crack tip.

It has been shown that pipeline steels are susceptible to creep deformation at room temperature. Time-dependent plastic deformation can occur under a constant stress higher than yield strength due to creep deformation. The amount of creep deformation occurring at the crack tip depends on the time duration which it is affected under sufficient stress. Fluctuation's (loading) frequency and crack growth rate have a great effect on creep behavior due to its time dependence behavior. When the crack grows slowly (due to general mechanical and environmental effects) or when the frequency is low, there will be higher amount of time that crack tip can be affected by sufficient stress to cause creep deformation. Excessive plastic deformation occurred by creep can have a dual effect on cracking in near-neutral pH environment. It can cause plastic induced closure effect and dormancy but in the other hand it can enhance hydrogen diffusion through the crack tip due to dislocation movements and crack tip morphologies changes due to plastic deformation [25, 25].

2.4.3. Environmental Factors Affecting Crack Growth

Mechanism of pipeline steels cracking in near-neutral pH environments is known to be based on combination of crack-tip dissolution and hydrogen embrittlement. Environmental factors affecting crack growth should be considered based on their effect on these two phenomena. For cracking to be occurred in near-neutral pH environment the pipe surface should be exposed to an appropriate environment (solution). Ground water which penetrates inside the disbandment coating is considered as the solution. Different solutions represent different corrosion behaviors and hydrogen generating abilities. Relative aggressiveness of different soil solutions depends on the soil chemistry (initial concentration of HCO_3^- in the soil) and the level of CO_2 in the soil solution which can determine the pH of the solution [26].

Chen et al. [25] investigated the effect of soil solution chemistry on the crack growth rate of pipeline steels using X65 pipeline steels CT specimens in different corrosive solutions with different pH values (according to various content of $CaCO_3$) known as C2 (pH=6.29) and NOVATW (pH=7.11). They found out that more corrosive solutions (lower pH) represent higher crack growth rate due to their higher dissolution capacity which can generate higher amount of hydrogen. Crack tip of the specimen which was cracked in more aggressive solution (C2) was very sharp while it was curved and blunted for the specimen cracked in less aggressive solution (NOVATW). Sharpness of crack tip is a representative of amount of hydrogen available at the crack tip to cause micro cracks formation by embrittling effects. This shows that solution with lower pH value is able to produce higher amount of hydrogen due to its higher aggressiveness. Relatively crack growth rate in C2 solution was found to be three orders of magnitude higher than its rate in NOVATW solution.

Environmental effects on crack growth behavior in near-neutral pH environments is dominant at lower mechanical conditions and as the mechanical loading conditions become more aggressive, environmental effects on crack growth will become minor. Tests done by Chen et al. [27] showed this behavior clearly (Figure 2-13). No significant crack growth rate difference was observed between the X65 CT specimens cracked in C2 and NOVATW soil solutions when aggressive mechanical loading condition was used (ΔK=16 $MPam^{0.5}$, Kmax=47 $MPam^{0.5}$ and f=0.0025 Hz). However, different growth curves were observed when initial loading conditions changed to less aggressive situation (Kmax=35 $MPam^{0.5}$, ΔK=12 $MPam^{0.5}$ and f=0.0025 Hz) it can be concluded that effect of hydrogen on crack growth will become minor as the loading condition becomes more aggressive but still growth rate will be enhanced in near-neutral pH environment compared to crack growth in air.

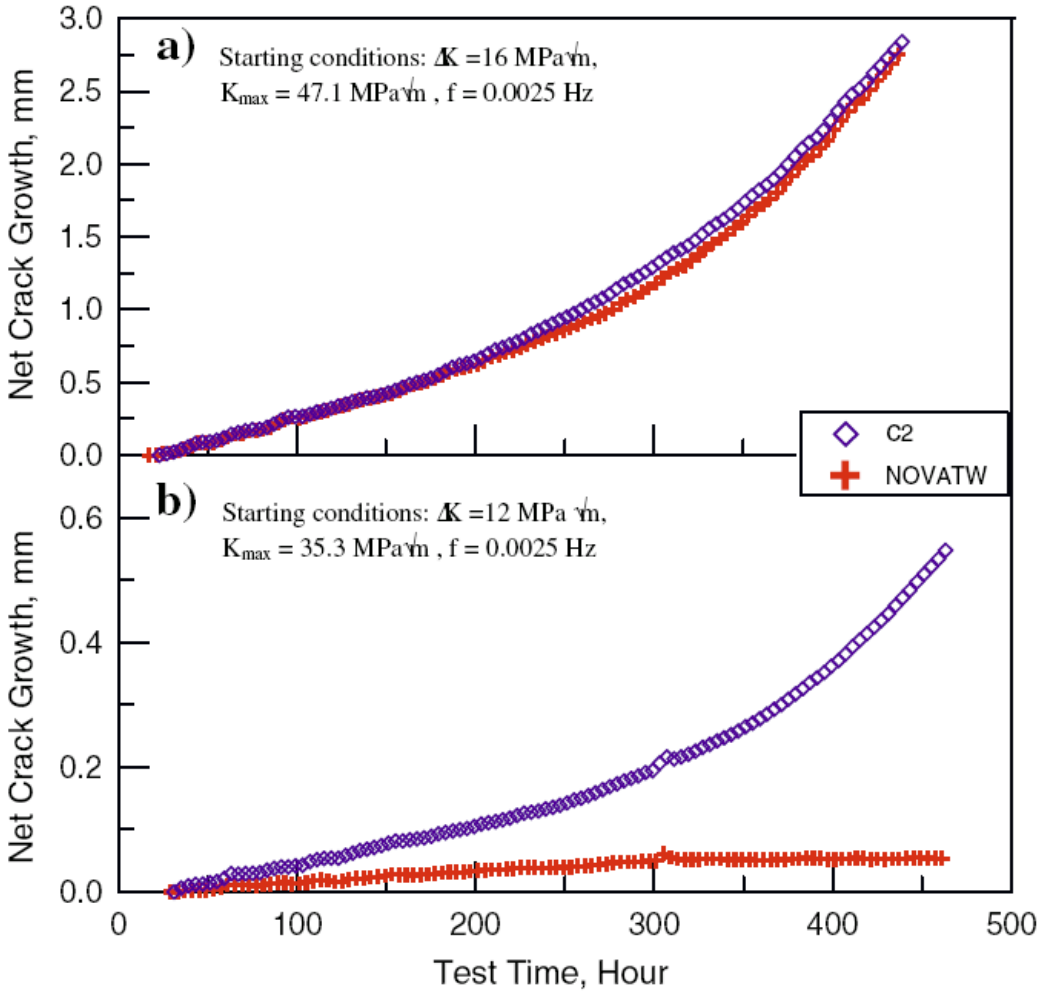

Figure 2-13: Comparison of crack growth behavior under a) benign and b) aggressive loading situations in C2 and NOVATW solutions [27].

2.4.4. Role of Hydrogen in Near-Neutral pH SCC Crack Growth

The hydrogen which is generated due to corrosion is absorbed by the steel and transported to highly-stressed plastic zones and locations with highly-concentrated trapping energy such as the crack tip. Hydrogen enhances the crack growth in near-neutral pH environment in two different ways. Mainly it can decrease the metal bond strength and cause embrittlement in front of the crack tip to enhance the growth of the crack. Hydrogen can also increase the amount of plastic deformation and facilitate the flow of dislocations that can increase the

dislocation density in the pipe which reversely facilitates hydrogen absorption and movement.

Been et al. [28] used slow strain rate tests with X65 pipeline samples in simulated groundwater solution to investigate the effect of hydrogen in near-neutral pH environment. Slow strain rate tests were frequently used to evaluate materials resistance to environmentally assisted cracking by using tensile specimens and considering the degree of cross-sectional area (%RA) upon failure. According to their results ductility of the pipe material will be decreased significantly with the presence of hydrogen with no change in steel tensile strength. In other work, Cialone et al. [29] tested samples of low-strength; carbon-manganese API-5LX grade X42 pipeline steels in high pressure hydrogen and nitrogen environments using cyclic loads. It was seen that presence of hydrogen could decrease the fatigue life of the samples. Crack growth was accelerated with the increase of hydrogen pressure and decrease of cyclic frequency. This was known to be related to the hydrogen-induced reduction of fracture toughness (J_{IC}). They observed that growth acceleration decreased by increasing stress ratio (R) in cyclic loads possibly due to reduced influence of plasticity-induced crack closure effects. J-resistance curves form growth data in hydrogen and nitrogen environment were used for to explain the effect of plasticity on the results. In Figure 2-14 reduction of 65 per cent observed in fracture toughness (J_{IC}) values of specimens tested in hydrogen environment. Reduction of fracture toughness by hydrogen was also accompanied by a change of fracture mode from ductile to cleavage or quasi-cleavage mode.

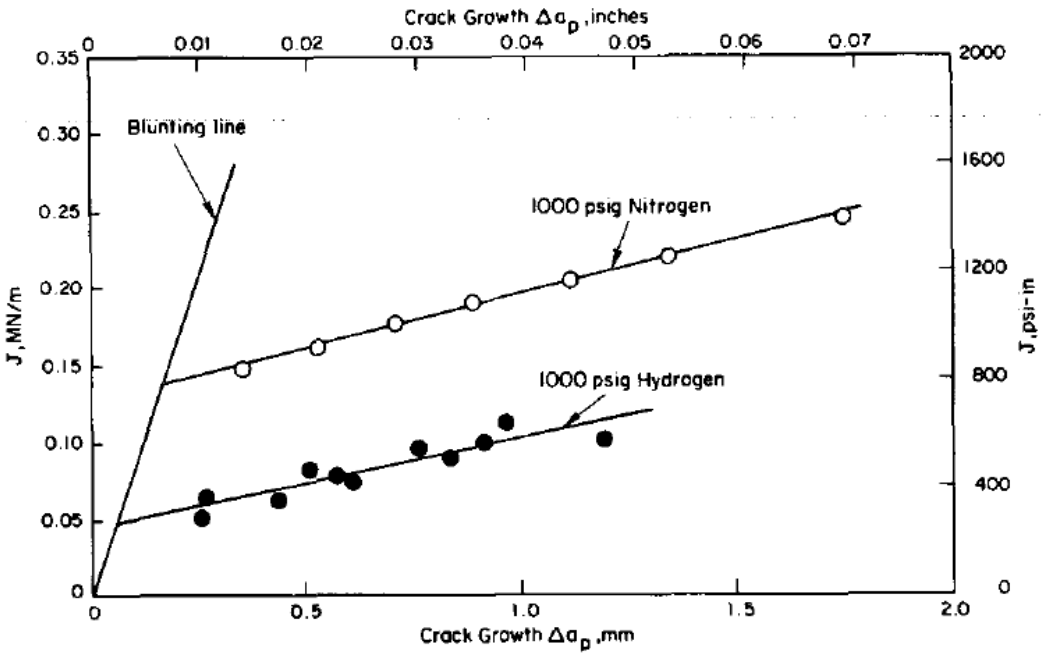

Figure 2-14: Crack growth resistance data for X42 pipe steel tested in 6.9 MPa hydrogen and 6.9 MPa nitrogen gases [29].

Hydrogen influences the anodic dissolution in the steels as well. Gu et al [30] used polarization curves of X52 pipeline steel to investigate the effect of hydrogen on anodic current. They precharged some X52 samples by hydrogen in different solutions and compared their polarization curves with non-precharged sample's curves. They found out that hydrogen precharging greatly increases the anodic current and the active potential range which can even make the passive zone to be disappeared in some solutions. Hydrogen also has a big contribution in crack growth by its tendency of re-sharpening the blunted crack tips by generating micro cracks due to embrittlement effect. In less aggressive mechanical (loading) situations that environmental effects on crack growth in near-neutral pH environment are more dominant. Chen et al. [31] reported crack growth reactivation after dormancy in C2 solution which is believed to be able to provide enough hydrogen to cause embrittlement because of its low pH. CT specimens of X65 pipeline steels were used in C2 (pH=6.29) and NOATW (pH=7.11) test solutions. Crack dormancy occurred when the cyclically loading condition

changed to loading hold for a week. Resuming the cyclic loadings, growth was seen in the specimen exposed to C2 solution while crack remained dormant in the specimen which was exposed to NOVATW solution. This behavior can be explained by higher hydrogen generating ability of C2 solution due to its lower pH. Enough amount of hydrogen at the crack tip in C2 solution could re-sharpen the crack tip in the presence of mechanical loading situation. However, non aggressive cyclic loads could not make the crack tip with sharp again in the absence of enough amount of hydrogen at the crack tip in the sample used in NOVATW solution and the crack remained blunted and dormant even when the cyclic loading resumed. As it is illustrated in Figure 2-15, when the loading situations shifted to more aggressive one, mechanical cyclic loading can re-sharpen the blunted crack tip, results in resuming the crack growth after dormancy even in the specimen tested in NOVATW solution with less amount of hydrogen concentrated around the crack tip. This was evidence for the dominant role of mechanical loadings than hydrogen (environmental factors) in crack growth and re-sharpening effect in the aggressive mechanical loading situations.

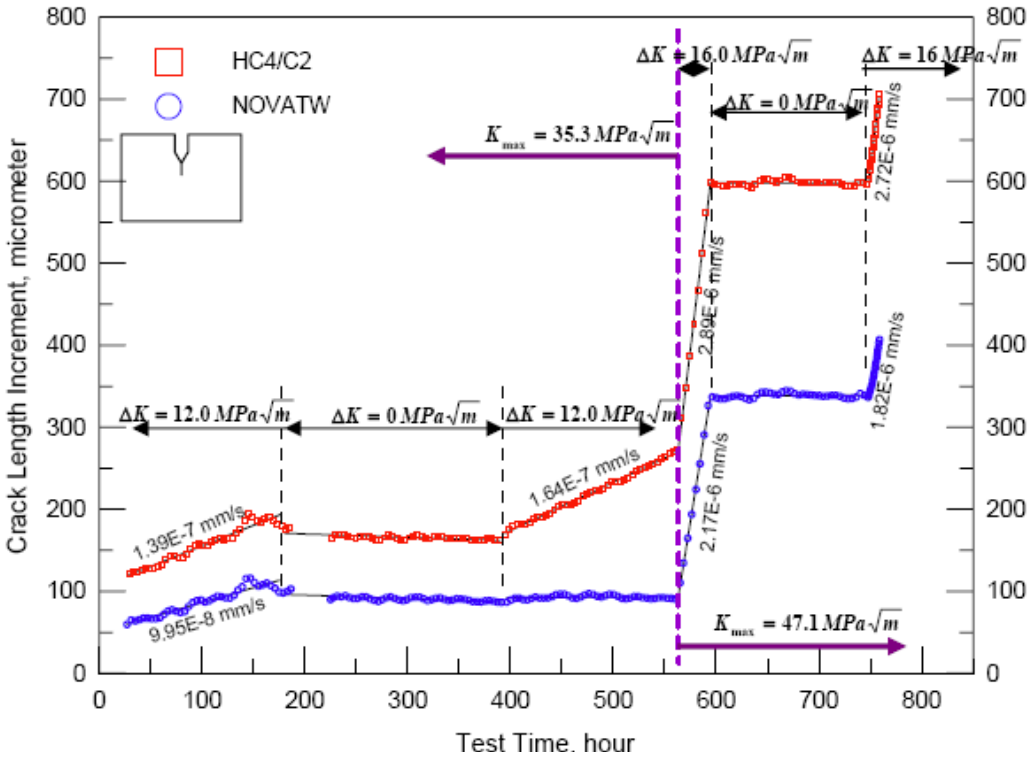

Figure 2-15: Crack growth length as a function of test time in C2 and NOVATW solutions [31].

2.4.5. Metallurgical and Microstructural Effects

Metallurgical factors influence crack growth behavior in near-neutral pH environment. It was discussed before that anodic dissolution and hydrogen embrittlement are responsible for cracking in near-neutral pH environment. Metallurgical and microstructural features should be considered with their effects on anodic dissolution occurrence and hydrogen generation and accumulation in the microstructure.

In general it can be said that any metallurgical discontinuity in the structure can enhance crack growth in near-neutral pH environment. Discontinuities and lattice defects in the structure act as stress risers and increase the strain energy of the microstructure locally. The chance of local micro-plastic deformation happening in the interfaces will be increased due to different mechanical behavior characteristics of inclusions and their surroundings such as their hardness or strength. As a result crack growth is enhanced due to the role of plasticity in crack growth behavior. Dislocation density and strain energy will be increased in discontinuities interfaces with the matrix which makes them preferable cites for hydrogen to be absorbed and trapped.

According to Chu et al. [32] metallurgical discontinuities in the steel microstructure are responsible for microcracks initiation. They believed that selective corrosion related to galvanic effect can happen between the discontinuity and its surrounding matrix and the hydrogen generated as a result of this localized corrosion can be easily trapped at high strain energy areas in the interface.

One of the most important inhomogenites in the structure is the presence of second phase particles in the structure. Second phases can generate local galvanic cells with their surrounding phases because of their differences in anodic nature. These galvanic cells can make local corrosion that increases the concentration of hydrogen locally in the microstructure. The hydrogen which is generated can be trapped easily in the interface of the phase and its matrix because of high local amount of strain energy stored at the interface as a result of micro plastic deformation. Concentration of hydrogen in the interfaces makes them preferential

sites of cracking due to embrittlement effect of hydrogen and stress concentration. Kushida et al. [33] and Bulger et al. [34] observed in their researches that small cracks were more likely to initiate and propagate in the pearlite colonies or along the pearlite-ferrite boundaries. They explained this behavior based on the fact that pearlite structures can promote non-uniform micro-plastic deformation since they possesses higher strength and hardness than ferrite and also galvanic cells can be generated in their interfaces with surrounding ferrite. Kushida also observed that uniform microstructures in steels such as ferrite or bainite are more resistant to Cracking than mixed non-uniform structures. The same observation was made by Martinez et al. [35]. They found pearlite/ferrite interface as the prime site for hydrogen occlusion in steels. They believed that a field of tensional energy with a high dislocation density in ferrite/pearlite interface as a result of volume change taking place during the transformation of final austenite to pearlite is responsible for hydrogen occlusion enhancement in the interface.

Lu et al. [36] discussed that the relation between yield strength and near-neutral pH cracking is also microstructure dependent. They investigated the effect of different pipe yield strength on their cracking susceptibility in near-neutral pH environment. They observed that generally cracking susceptibility increases with increase in the yield strength of steels. This is related to the increase in the magnitude of stresses in triaxial stresses zone in plastic deformed zones such as crack tips. But they also emphasized that yield strength comparisons for crack growth behavior prediction should be done between the steels with same type of microstructures. They reported that pipelines with microstructures of fine grained bainite + ferrite are less susceptible to cracking than those with ferrite-pearlite structures. This can be another prove that cracking susceptibility increases as the structure becomes more un-uniform.

Grain boundaries are known as other important sites for hydrogen trapping. Grain boundaries are the area with lattice misorientation and high dislocation density that hydrogen can be easily trapped in due to the distortion. It can be concluded that hydrogen uptake of the microstructure will be increased as the grain boundary area is increased [37]. This introduces the influence of grain size on hydrogen

uptake and relatively cracking susceptibility of steel in near-neutral pH environment. Sammy [38] investigated the effects of microstructure on hydrogen trapping ability in pure iron and steels by hydrogen-charging them in the NACE H_2S-saturated saline solution for different period of times. He found that hydrogen uptake of steels is generally increased by decrease in their grain sizes which reflects the increase in grain boundary area but he also found some exceptions in large grain size steels as well. Martinez et al. [35] were also investigated the effect of grain size on the hydrogen content of pure iron and steels after hydrogen charging. They observed a critical grain size (~70μm for pure iron) that hydrogen content decreased with increasing the grain size below this critical size, while it was increased by increasing the grain size for grains larger than this critical value. Decrease of hydrogen content by increasing grain size before this specific grain size was not unreasonable as grain boundary length become shorter with larger grains and available sites for hydrogen storage become less. The reverse behavior of material after the critical grain size seemed to be unreasonable at first. They etched the samples and used polarized light microscopy for further microstructural analysis. Optical microscopy pictures are shown in Figures 2-16 and 2-17:

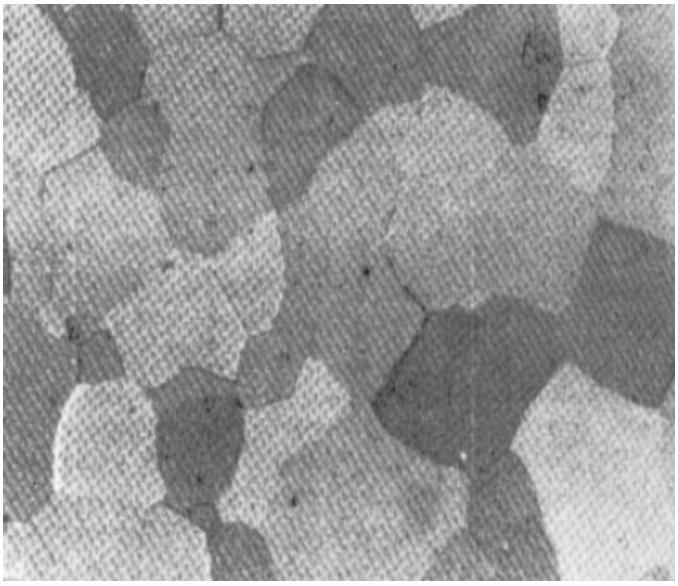

Figure2-16: Small ferritic grain size showing low contrast under polarized light (280X) [35].

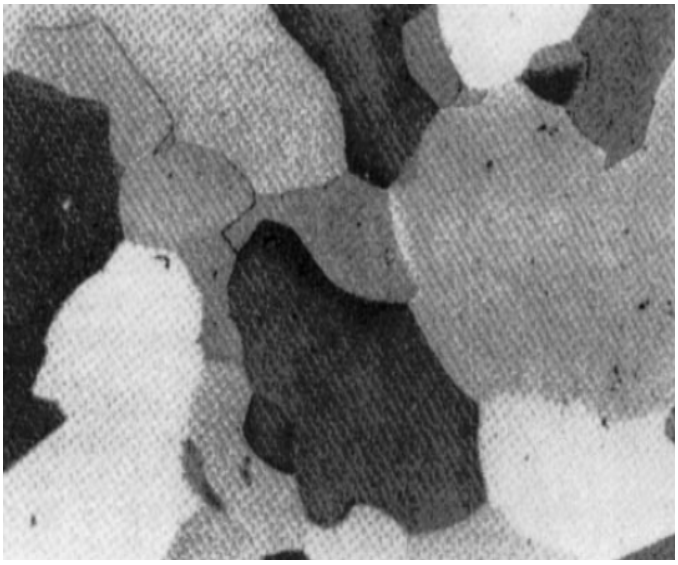

Figure 2-17: Large ferritic grain size showing large contrast under polarized light (150X) [35].

Very noticeable contrast is seen in specimens with larger grains which reflect the large lattice misorientation between the grains and grain boundaries as a result of high angle nature of large grains. Large mismatch between the grains enhance the hydrogen trapping in the area between the grains in grain boundary. On the other

hand samples with small grains showed only slight contrast and small mismatch from one grain to another. It can be concluded that beside the grain size, the nature of grain boundary also influences the hydrogen trapping ability in the steels microstructure. Coarse grain microstructures with high angle grain boundaries may occlude a large amount of hydrogen even though they have relatively less grain boundary areas.

Non-metallic inclusions and precipitates are other sensitive metallurgical defects. These defects can act as stress risers and stress can be concentrated at their interfaces to make locally plastic deformed areas in their interfaces. Inclusion interfaces are known as preferential sites for corrosion attack due to the high strain energy stored in these sites which enhance anodic dissolution between inclusions and their surrounding matrix [39]. Localized galvanic corrosion cells at the interfaces cause corrosion pitting in the interface and micro cracks can be formed as a result of stress concentration at the bottom of the formed pits. Parkins et al. [13] indicated that transgranular cracks are associated with pits that had formed at inclusions exposed to the surface. Van Boven et al. [22] also reported that cracking was observed at the bottom of corrosion pits where enough amount of tensile stress gradient is available. It is believed that inclusions significantly affect the hydrogen generating and hydrogen trapping ability of the microstructure. Cracking can occur if the critical amount of hydrogen is accumulated and stress concentration reaches the critical value required for crack propagation.

2.5. Crack Growth Models

There is a great interest in introducing an appropriate model that can show the growth behavior of an initiated crack in pipe steel in near-neutral pH environment. The model is useful if it considers influences of the pipes environmental and operational situations (applied mechanical loadings). Using such a model helps pipe line operators to have a reasonable engineering expectation and prediction on the growth behavior of an existent crack. This helps

inspection intervals or section replacements to be done at the appropriate time before further damages occur.

Crack growth models were proposed previously based on SCC mechanism. It was believed that SCC is responsible for cracking in near-neutral pH environments. Strain rate model is an example of the crack growth model which was proposed based on SCC mechanism. Critical strain rate is introduced in this model which is needed to break the passive film formed at the crack tip so that crack propagation can continue [40].

2.5.1. Strain Rate Model

Strain rate at the crack tip has a great influence on cracking in high pH environments. Plastic strain accumulation at the crack tip can rupture the oxide (passive) film and crack advances trough anodic dissolution until the protective film be formed again. Effect of strain rate on crack growth behavior in near-neutral pH environment is less obvious but still it can influence both dissolution rate and plastic deformation occurrence. Generally strain and strain energy increases the dissolution in order of magnitude by providing energy and enhances the hydrogen uptake of the steel by increasing the active amount of plastic deformation in the steel.

J. Beavers [40] believed that a critical strain rate is required at the crack tip to cause crack growth. Strain rate can be related to the stress ratio (R) and loading frequency (f). Representing a critical strain rate value required for cracking, it can be predicted that whether specific loading condition can leads to growth or dormancy. Beavers tried to propose a strain rate model that can reflect the crack growth and dormancy behavior according to cyclic loading conditions. He used the relation between the crack tip opening displacement (CTOD) and crack growth driving force parameter (J_{IC}) in small yielding situation (which neglects the plastic component of J). Considering the relation between K_{max}, ΔK and R,

($\Delta K = K_{max}$ (1-R)) strain rate at the crack tip was correlated to loading frequency and stress ratio in the equation which is shown bellow:

$$\dot{\varepsilon} = 4\, f\, (1\text{-}R)$$

This model shows that strain rate for cyclic loading situation is proportional to the frequency and (1-R). Crack tip strain rate will go to zero when R=1 or f=0 (static loading). Zero strain rate with static loads (f=0 and R=1) agrees with the fact that cyclic loading situation is necessary for crack growth. However, it seems unreasonable to expect this model to be used for crack growth behavior predictions in near-neutral pH environment. The main reason is that plastic component of J was ignored and analysis was done based on the small scale yielding which does not reflect the main role of plasticity in near-neutral pH cracking of pipeline steels.

On the other effort Shoji et al. [41] developed an equation describing strain rate for cyclic loading in distance (r) ahead of crack tip:

$$\dot{\varepsilon}_{ct} = \left(\frac{\beta \cdot \sigma_{ys}}{E}\right)\left(\frac{n}{n-1}\right)\left(\ln\left(\frac{K^2}{3\pi \cdot \sigma_{ys}^2 \cdot r}\right)\right)^{1/n-1}\left(\frac{2}{K}\cdot\frac{dK}{dt} + \frac{1}{r}\cdot\frac{da}{dt}\right)$$

This equation reflects material properties such as yield strength and elastic modulus and also strain hardening coefficient (it is known that time dependent processes such as strain hardening can affect the crack tip strain rate) in the first term. Dependency of strain rate on crack growth rate (da/dt) and its balance with time-dependent crack plasticity (dK/dt, K: stress intensity factor ahead of crack tip) were also included in the second part of the equation.

Parkins and Beavers [42] and also Been and Sutherby [43] applied the above equation to their crack growth data. They found that there is a linear relationship

between crack growth rate and crack tip strain rate. They compared their data with various pipelines steels references data (Figure 2-18). It was generally revealed that strain rate is related to the frequency and lower frequencies represent lower strain rates at the crack tip which results in decrease of cracking velocity.

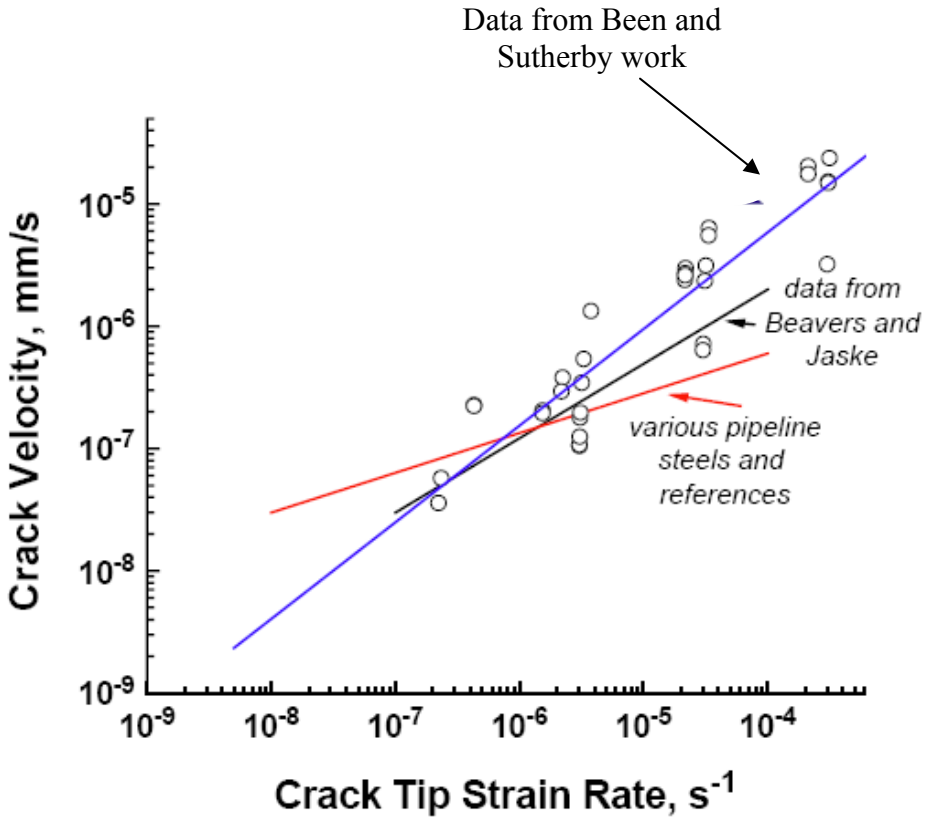

Figure 2-18: Fitted experimental crack velocity as a function of the calculated $\acute{\varepsilon}_{ct}$ [43].

Field data could not be correlated to this model and it could not be applied to cracking behavior in near-neutral pH environments.

It was discussed before that pressure fluctuations inside the pipe is the main source of applied loads which has the cyclic nature. Stress corrosion cracking can not explain the cracking behavior as it mainly deals with static loading and can not reflect the effect of cyclic nature of the loads applied to the pipe. The cyclic

nature of applied loads should be considered for proposing the growth model as it was seen that pre-existing cracks came to a dormant state (blunt crack tip) under monotonic loading in a near-neutral pH environments [31]. This is possibly because of anodic dissolution at the crack tip and corrosion products closure effect which blunts the crack tip and static loads are not able to make the crack tip sharp again for further growth.

In further attempt, superposition model was introduced by considering the combined effect of SCC and fatigue loading.

2.5.2. Superposition Model

This model was first introduced by Wei and Landes as early as 1969. They modeled the growth of crack in near-neutral pH environment on the basis of fatigue crack growth (mechanical factor) with contribution of SCC as an environmental corporation in crack growth:

$$(da/dN)_{total} = (da/dN)_{fatigue} + 1/f\,(da/dt)_{SCC}$$

Including the SCC part in the model seemed natural as it was initially believed that cracking of pipeline steels in near-neutral pH environments can be explained by SCC and monotonic loading. If the effect of monotonic loading be neglected in the model the SCC part will be negligible and the model can just consider the effect of fatigue loading. This means that the effect of environment (corrosion) will be neglected and hydrogen contribution in crack growth (hydrogen embrittlement effect) won't be considered.

In addition to environmental effects, this model is not able to represent the crack growth due to fatigue load as well. Paris law was suggested to be used for fatigue growth rate. Paris law correlates the growth rate to change of stress intensity factor at the crack tip due to equation below where C and m are constant values:

$$(da/dN)_{fatigue} = C\,(\Delta K)^{m}$$

Effects of maximum stress intensity factor in front of the crack tip (K_{max}) and loading frequency on the crack growth is ignored in this model. Using this model for crack growth predictions will lead to underestimation of the crack growth rate in near-neutral pH environment as this model is not able to show the synergistic interaction between environmental (corrosion) and mechanical (fatigue) factors affecting the crack growth. Many researchers have compared their crack growth results with this model. Experimental crack growth data obtained by Plumtree et al., Zhang et al., Beavers and Jaske could not be fitted to superposition model while the general trend was consistent with the model in some cases [17, 27, 44].
An appropriate growth model should represent the synergistic interaction between environmental factor and mechanical (loading) factor. The above model could not represent this interaction. Crack grows in near-neutral pH environments with the interaction of corrosion on the surface of the pipe (source of hydrogen) and cyclic loading. Cyclic loading nature represents the fatigue loading behavior which is enhanced by corrosion occurrence. Hydrogen (corrosion's product) enhances fatigue growth due to its embrittlement effect. It can be concluded that crack growth behavior in pipeline steels in near-neutral pH environments can be best explained by the behavior of corrosion fatigue which is another environmentally assisted cracking mechanisms.

2.6. Corrosion Fatigue

Corrosion fatigue is a type of environmentally assisted cracking which occurs due to synergistic interaction of corrosion and fluctuating (cyclic) stresses. Corrosion fatigue is also known as an enhanced fatigue failure due to corrosion. There is a high probability that engineering components fail through corrosion fatigue cracking phenomena as the stress level do vary to some extent in almost all of them. Corrosion fatigue damage is almost always much greater than the sum of the damage caused by corrosion or fatigue individually. Figure 2-19 shows an

example of the reduction of a fatigue life of the high-strength steel in presence of aggressive sodium chloride solution [45].

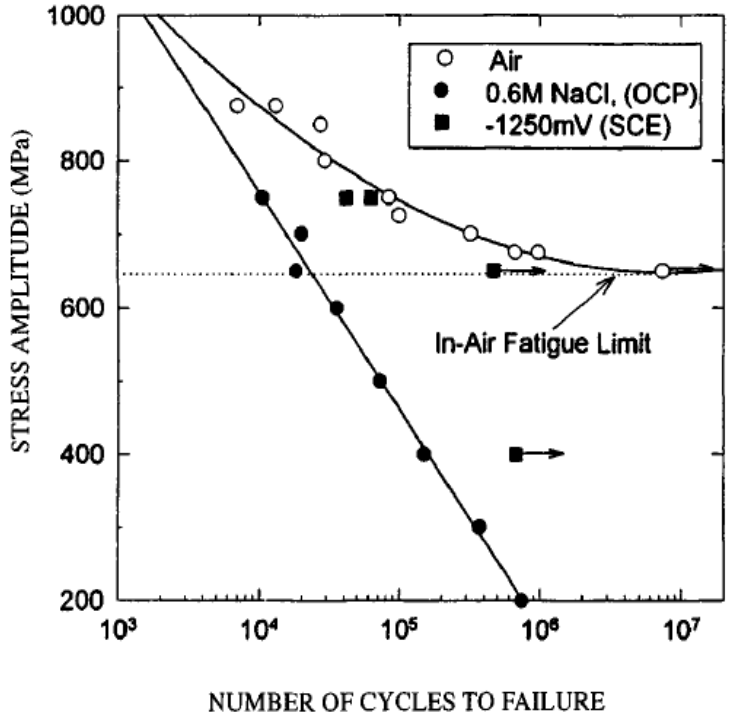

Figure 2-19: Fatigue life data, S-N curves, for high-strength steel in air and corrosive environment [45].

Corrosion fatigue cracks can be transgranular, intergranular or a combination of both depending on the mechanical and environmental conditions applied to the component. Corrosion fatigue damage accumulates with increasing load cycles in four stages of cyclic plastic deformation, microcrack initiation, small cracks growth and coalescence and finally macrocrack propagation. This type of environmentally assisted cracking is known to be the most complicated one which many different factors and mechanisms can possibly play role in its occurrence. Contribution of different mechanisms on cracking is controversial and dependent to the metallurgical and environmental variables. Among various mechanisms

anodic slip dissolution and hydrogen embrittlement are known as the main categories of mechanisms associated with corrosion fatigue cracking.

2.6.1. Factors Controlling Corrosion Fatigue

2.6.1.1. Mechanical Factors

Mechanical factors affecting corrosion fatigue are usually investigated in relation with fatigue loading processes. All the mechanical factors that influence the fatigue behavior of the components also influence the occurrence of corrosion fatigue. Corrosion fatigue cracking behavior (crack growth rate) is defined by the usage of linier elastic fracture mechanics same as fatigue cracking behavior. Crack growth rate per cycles of both fatigue and corrosion fatigue is reported using stress intensity factors ahead of the crack tip which can represent the effect of external applied stress, crack length and the shape of the component.

Crack closure effect which is a well known phenomenon in fatigue affects corrosion fatigue cracking rate. This phenomenon is based on the contact of crack surfaces during unloading process at low stress intensity levels above zero. Crack closure effect occurs due to the presence of corrosion products in the crack crevice, plasticity, crack path roughness or phase transformation. This behavior will decrease the value of effective stress intensity factor ahead of the crack tip and decrease in the crack growth rate relatively. Fatigue loadings frequency, magnitude of fatigue stresses and their ratio and also the amount of corrosion that can happen due to the environment affect the amount of crack closure [45, 46].

2.6.1.2. Metallurgical Factors

Metallurgical factors have a great influence on cracking process of corrosion fatigue failure. As of their same role in other environmentally assisted cracking processes, metallurgical features such as metallurgical discontinuities can prepare

preferential localized sites for selective environmental corrosion attacks. Impurities, non-metallic inclusions, grain boundaries and second phase particles are common types of metallurgical discontinuities that increase the chance of corrosion occurrence in the microstructure due to galvanic cells formation in their interfaces with the matrix. These galvanic cells enhance the localized anodic dissolution in the microstructure and corroded spots will become the preferential sites for crack initiation and growth [46].

2.6.2. Corrosion Fatigue Crack Propagation

The propagation behavior of corrosion fatigue cracks is often described using fracture mechanics concepts with the plots of crack growth rate per cycle (da/dN) as a function of applied stress intensity factor range. Under the cyclic loadings, corrosion fatigue cracks can propagate even with the maximum stress intensity factors lower than the threshold fatigue crack growth stress intensity factor. Cyclic crack growth in corrosive environment has also a higher rate than the crack growth rate of fatigue cracking in an inert environment.

Corrosion fatigue cracking behavior can be divided in three different groups of cycle-dependent corrosion fatigue, time-dependent corrosion fatigue or a combination of both. Cycle dependent corrosion fatigue represents a simple acceleration of the fatigue crack growth due to corrosive environment exposure to the component. In this type of corrosion fatigue, loading frequency has no contribution to the environmental factors affecting the crack growth. On the other hand frequency relates the environmentally assisted crack growth rate to the inert fatigue crack growth rate in time-dependent corrosion fatigue. Cycle-time-dependent corrosion fatigue represents the most material-environment combination in cracking process. Crack growth behaviors and cracking rate equations for these three types of corrosion fatigue are illustrated in Figure 2-20:

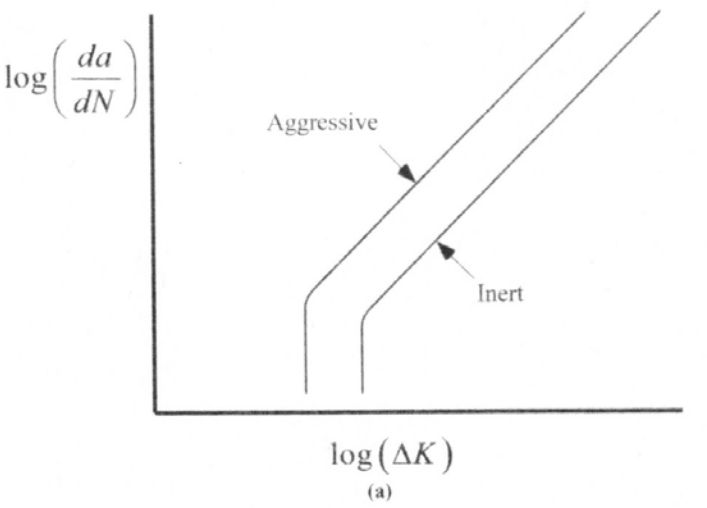

$(da/dN)_{aggressive} = \varphi\,(da/dN)_{inert}$

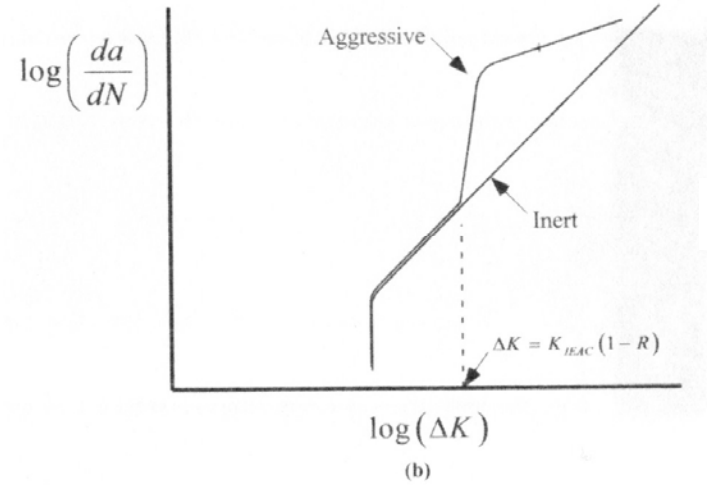

$(da/dN)_{aggressive} = (da/dN)_{inert} + 1/f\,(da/dt)_{EAC}$

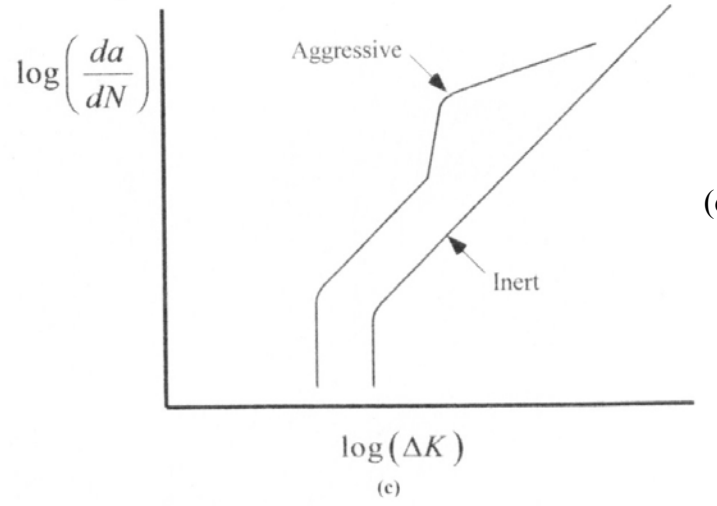

$(da/dN)_{aggressive} = \varphi\,(da/dN)_{inert} + 1/f\,(da/dN)$

Figure 2-20: Three types of corrosion fatigue behavior and their related crack growth rate equations: a) cycle-dependent corrosion fatigue b) time-dependent corrosion fatigue and c) cycle-time-dependent corrosion fatigue [1].

As it can be seen in crack growth rate equations above, there are three possible frequency responses for corrosion fatigue crack growth behavior. Cycle dependent corrosion fatigue is independent of the loading frequency while crack growth per cycle (da/dN) decreases with increasing frequency in time-dependent and time-cycle-dependent corrosion fatigue.

Figure 2-21 illustrates the predicted effect of loading frequency on crack growth rate of corrosion fatigue based on superposition equations above. It can be see that due to these equations cycle-time-dependent and time dependent corrosion fatigue behavior approach to cycle dependent corrosion fatigue and inert fatigue in high frequencies respectively which means in high frequencies environmental effects will become minor on crack growth behavior [1].

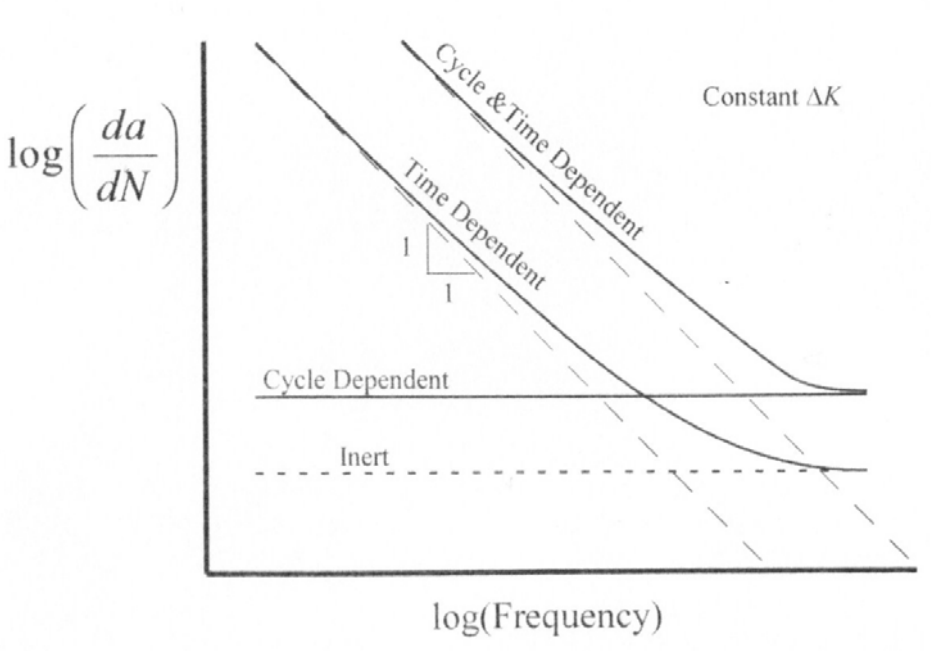

Figure 2-21: Effect of frequency on various types of corrosion fatigue [1].

2.6.3. Relationship between Corrosion Fatigue and SCC

SCC and corrosion fatigue are related but different from each other. Their main difference is in their loading situations. Static loading regimes is responsible for SCC failures while corrosion fatigue failures is attributed to varying loading (fatigue) situations. Cyclic loading characteristic of corrosion fatigue makes it more general than SCC in the same environment because most of the engineering components work under the state of fluctuating stresses. Environmental effects on both of these cracking behaviors is related to the corrosivity of the environment but the cyclic nature of applied stresses to the component in corrosion fatigue causes more potent situation for cracking. Cyclic loading can cause more strain rate and plastic deformation in front of the crack tip and also can contribute in re-sharpening of the crack tip which were blunted by anodic dissolution (corrosion). Movement of dislocation will also be easier in corrosion fatigue processes due to higher strain rate and plastic deformation. Dislocations are the preferred sites for hydrogen diffusion and diffusion of hydrogen through the microstructure will be enhanced by increase of dislocation density. According to this discussion hydrogen embrittlement effect will also be enhanced in corrosion fatigue and more severe failure is expected due to corrosion fatigue [46].

2.7. Corrosion Fatigue Model

Environmentally enhanced crack growth behaviour can be categorized in four different groups of stress corrosion cracking, corrosion fatigue, combination of SCC and inert fatigue crack growth and synergy of the latter two. As discussed before cracking behaviour of pipeline steels in near-neutral pH environments can be best explained by the behaviour of corrosion fatigue. Crack growth rate data from research done by Beaver and Jaske and Zhang et al. has been compared with both superposition and corrosion fatigue model. Corrosion fatigue predicted a

lower crack growth rate than superposition model initially but as the cracks become deeper corrosion fatigue crack growth prediction exceeds both superposition and constant crack growth rate prediction with predicting more crack growth per cycle especially during later stages of crack growth [17].

Chen et al. [27] conducted several tests using CT specimens of X65 pipeline steel in C2 (pH=6.29) and NOVATW (pH=7.11) synthetic soil solutions to investigate the effects of mechanical loading conditions on crack growth rate of pipeline steels in near-neutral pH environment. They used da/dN vs. ΔK curves to report their data as a usual way reported in literature, but their data could not been rationalized by ΔK in different tests with same frequency and different K_{max} or R values. It can be seen in Figure 2-22 that crack growth rates per cycles (da/dN) were increased by increasing Kmax or R values (K_{max} and R are related due to equation Kmax=ΔK / (1-R)).

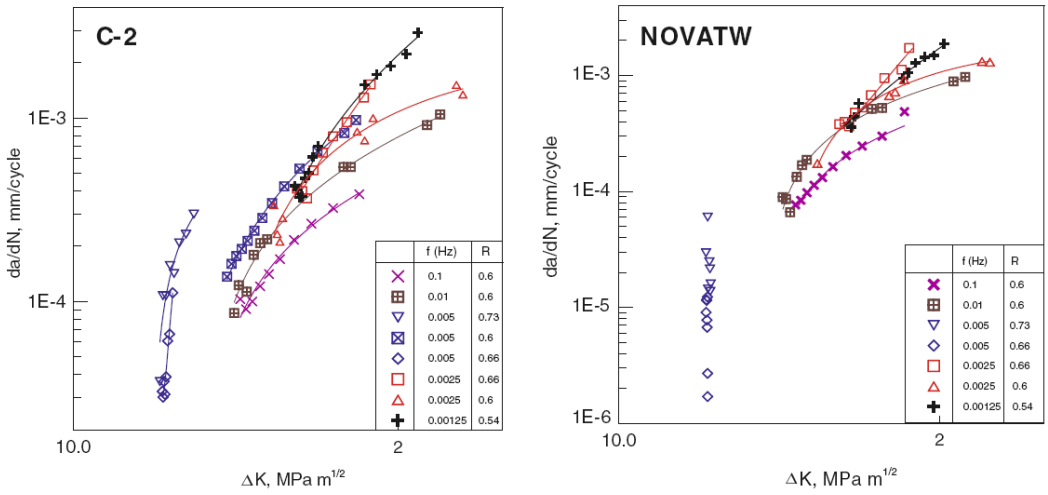

Figure 2-22: Crack growth rate da/dN as a function of ΔK obtained from testing in (a) C2 solution and b) NOVATW solution [27].

Plotting the same results as crack growth by time (da/dt) vs. ΔK could not rationalized the data either but it showed a big clue of the role of corrosion fatigue in the crack growth behavior. Figure 2-23 shows that time-dependent growth rate was increased with the decrease in loading frequency.

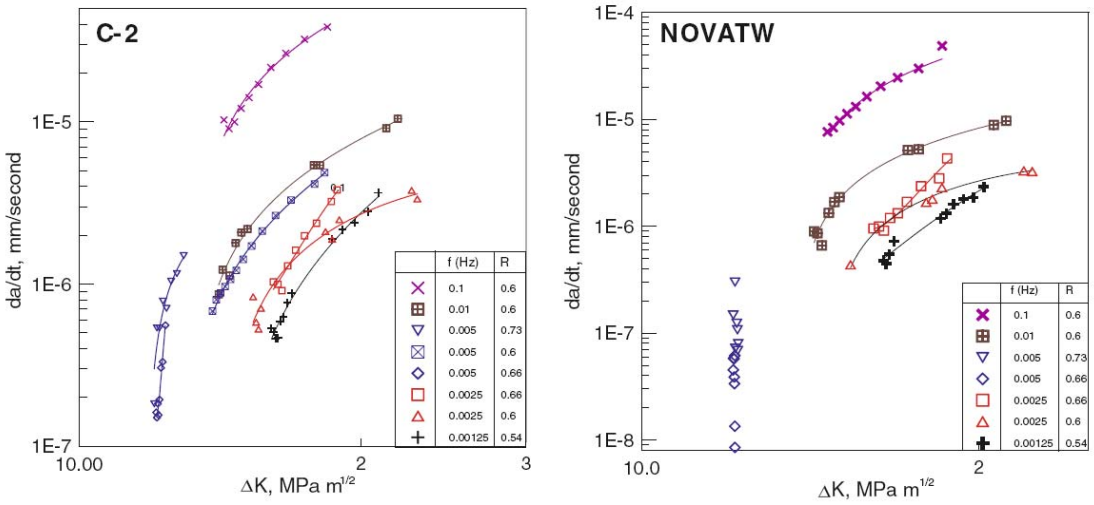

Figure 2-23: Crack growth rate da/dt as a function of ΔK obtained from testing in (a) C2 solution and (b) NOVATW solution [27].

Increase of crack growth rate with decrease of frequency is seen in both corrosion fatigue and near-neutral pH cracking environments. Chen et al. thought of using corrosion fatigue concept to analyze their data. They also concluded that both effects of ΔK and K_{max} should be considered in their analysis as the growth data could not be rationalized by either of them separately (Figure 2-24).

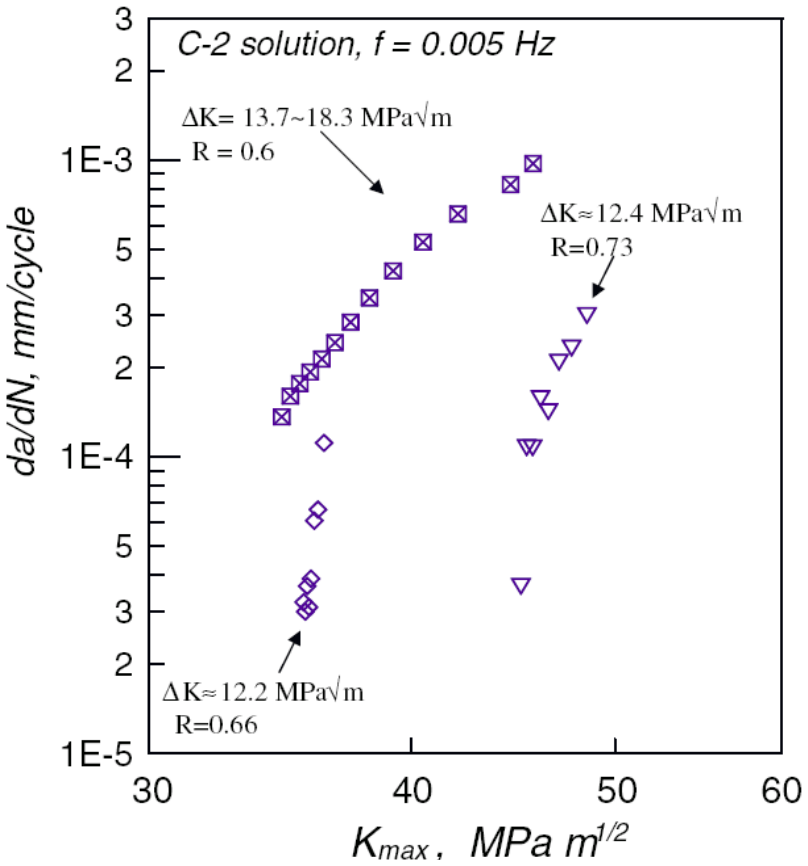

Figure 2-24: Effect of K_{max} on crack growth rate da/dN in C2 solution [27].

Using both K_{max} and ΔK for crack growth data analysis reflects the consideration of two-criterion model proposed by Vasudevan et al. [47] for fatigue crack growth behavior.

Vasudevan et al. showed that both K_{max} and ΔK influence fatigue crack growth rate as two essential single driving forces. They argued that these two parameters contain intrinsic thresholds for cracking. ΔK represents the cyclic behavior of loading situation and is related to R (cyclic stress ratio). K_{max} is a primary driving force which is known as a fundamental fracture mechanics parameter needed to quantify fracture in different cracking processes. According to these authors any reduction of data in terms of a single driving force, either ΔK or K_{max} provides an incomplete description of fatigue crack growth rate behavior.

2.7.1. New Corrosion Fatigue Model

Considering the behavior of corrosion fatigue and two-criteria model, Chen et al. attempted to use the combined effect of K_{max}, ΔK and loading frequency (showing time dependency of crack growth) with respect of environmental effects to analysis their crack growth data in near-neutral pH environment. They formulated these parameters to a single term of $(\Delta K)^2 K_{max}/f^{\alpha}$ through trial and error. It can be seen that four different driving forces for corrosion fatigue crack growth are included in this term. This model can reflect the synergistic interaction between mechanical loading situation and environmental effects. First part of this term, $(\Delta K)^2 K_{max}$, represents the fatigue crack growth behavior which is consistent with Paris law and two-criteria model. Second part, $1/f^{\alpha}$, reflects the environment effect where α value shows the corrosivity of environment and its tendency in generating hydrogen. Frequency (f) reflects the crack exposure time to the corrosive environment and can be the basis of loading parameters interaction with environmental parameter α in this term.

Plotting the data of their research with using new established parameter, Chen et al. observed fewest scatter and the data could be rationalized with the parameter as it can be seen in Figure 2-25:

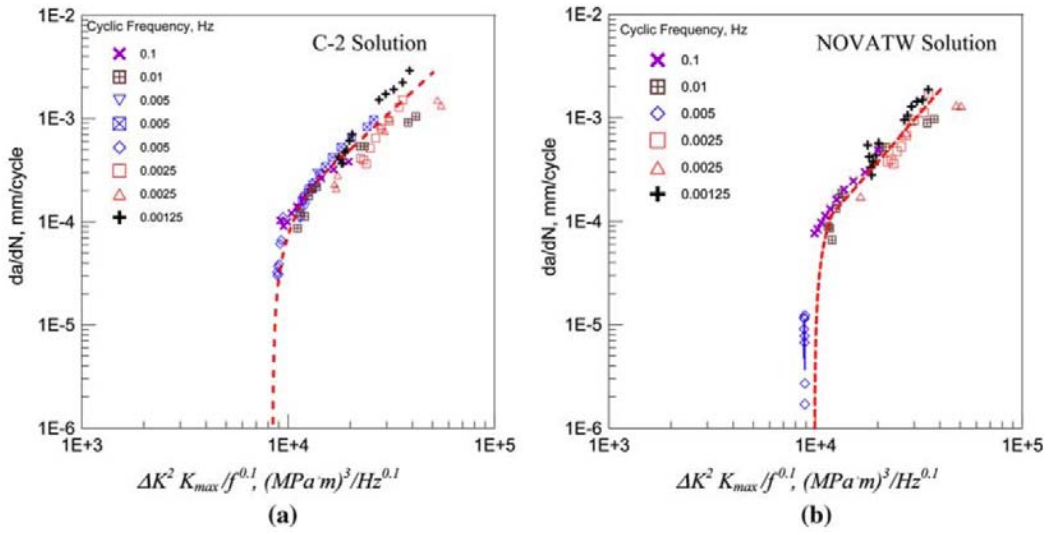

Figure 2-25: Crack growth rate da/dN as a function of $\Delta K^2 K_{max}/f^{0.1}$ obtained from testing in (a) C2 solution and (b) NOVATW solution [27].

The above curves brought the idea that this factor can represent the threshold value (critical $(\Delta K)^2K_{max}/f^{0.1}$ value) to reflect a boundary between crack growth and dormancy. The idea was approved when they provided the test below the threshold value in both environments which resulted in blunted crack tip and dormant growth. Threshold value can be defined as threshold $(\Delta K)^2K_{max}$ for the fatigue (which suggest the inverse relationship between ΔK and K_{max} under a constant frequency consistent with two-criteria model) part and $(\Delta K)^2K_{max}/f^{0.1}$ threshold for corrosion fatigue part.

In low frequencies there will be a more time-dependent contribution of corrosion to crack growth. On the other hand the general belief is that cracking threshold value is lower in corrosion fatigue than its value in fatigue in inert environments. These facts can be interestingly seen in $(\Delta K)^2K_{max}/f^{0.1}$ parameter as it predicts a lower $(\Delta K)^2K_{max}$ threshold when the loading frequency is reduced. When crack growth data of both solutions were plotted together (Figure 2-26), it could be seen that the parameter can properly reflect the environmental effects.

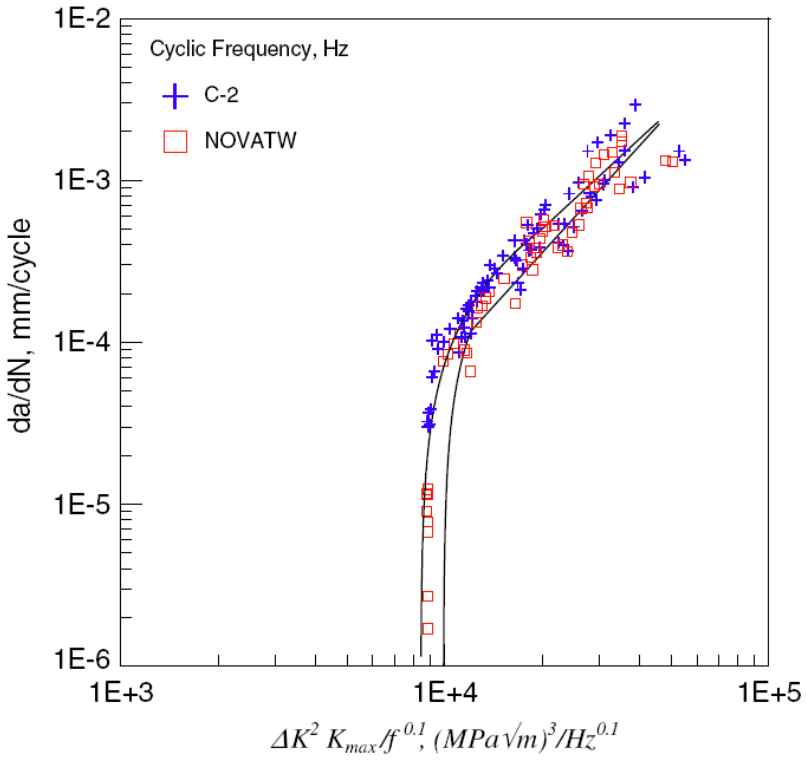

Figure 2-26: Comparison of growth rate da/dN as a function of $\Delta K^2K_{max}/f^{0.1}$ in two different solutions [27].

Cracking threshold value is lower for C2 solution which reflects the lower pH value of C2 solution and its higher corrosivity that generates higher amount of hydrogen and makes the cracking to become easier.

Chen et al.'s observations showed that new corrosion fatigue model can successfully explain the pipelines cracking behavior in near-neutral environment. This model can also support the fact that mechanical factors will become dominant over environmental factors in more aggressive loading conditions. It can be seen in figure above that by the increase in $(\Delta K)^2K_{max}/f^{0.1}$ value crack growth curves of both different solutions converge to each other representing similar cracking behavior in aggressive loading situations.

2.7.2. Investigation of Hydrogen Role in Crack Growth Behavior of Pipeline Steels in Near-Neutral pH Environment Based on New Corrosion Fatigue Model

It is believed that hydrogen has a great role in cracking of pipeline steels in near-neutral pH environment. New set of crack growth tests were designed by Chen et al [31] using same type of samples (CT samples of X65 pipeline steels) with different surface conditions to investigate the tendency of $(\Delta K)^2K_{max}/f^{0.1}$ factor in showing the hydrogen effect in crack growth behavior.

Crack growth behavior of bare, partially coated with epoxy and completely coated CT specimens were obtained in comparative tests using C2 solution and same less aggressive cyclic loading condition slightly higher than threshold $(\Delta K)^2K_{max}/f^{0.1}$ value of crack growth in C2 solution. Potential changes as a result of crack growth for these samples are illustrated in Figures 2-27:

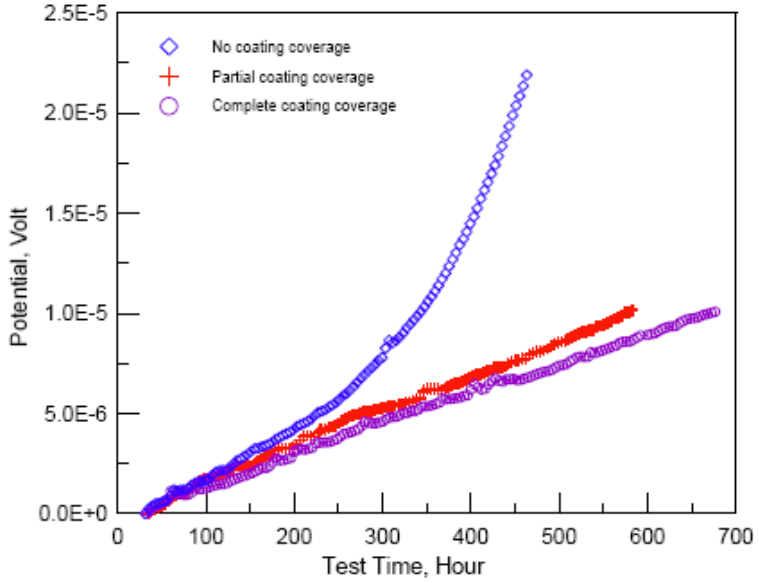

Figure 2-27: Change of measured potential as a function of test time for three specimens tested in C2 solution [31].

The results showed that bare sample had the highest amount of crack growth, much higher than crack growth seen in coated and partially coated samples. Partially coated sample showed slightly higher amount of growth than completely coated samples. Crack growth per cycle vs. time curves of these three samples can be seen in Figure 2-28:

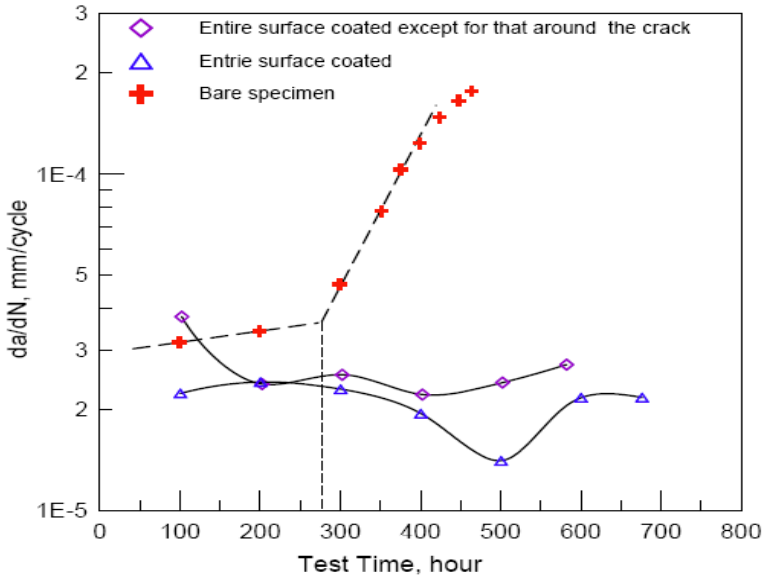

Figure 2-28: Crack growth rate as a function of test time for three specimens tested in C2 solution [31].

Different crack growth behavior can be seen in these different samples. Cracking process of uncoated sample can be divided to three different stages. Insensitive growth rate to time in the first stage was followed by rapid growth rate after 275 hours in stage two and again turned back to the insensitive behavior of crack growth by time in the last stage (stage three). Partially coated and completely coated samples showed almost the same cracking behavior except that partially coated samples represented slightly higher growth amount than completely coated sample. Chen et al. explained the cracking behavior of bare specimen using hydrogen effect on crack growth behavior. Using the hydrogen diffusion coefficient in steels ($2\times10^{-7}cm^2/s$) and diffusion equation of "X (distance) = $(Dt)^{0.5}$", they found out that 275 hours is the time required for hydrogen to transfer from its generation source (surface) to the crack tip, diffusing through entire sample's thickness (4.45 mm). As a result they explained that the sudden growth attributed to the onset of hydrogen embrittling effect on the crack growth which is a true reflection of environmental effects on crack growth behavior.

Results of the same kind of tests in more aggressive loading conditions showed no transition in growth rate after 275 hours in either C2 or NOVATW solutions (Figure 2-29).

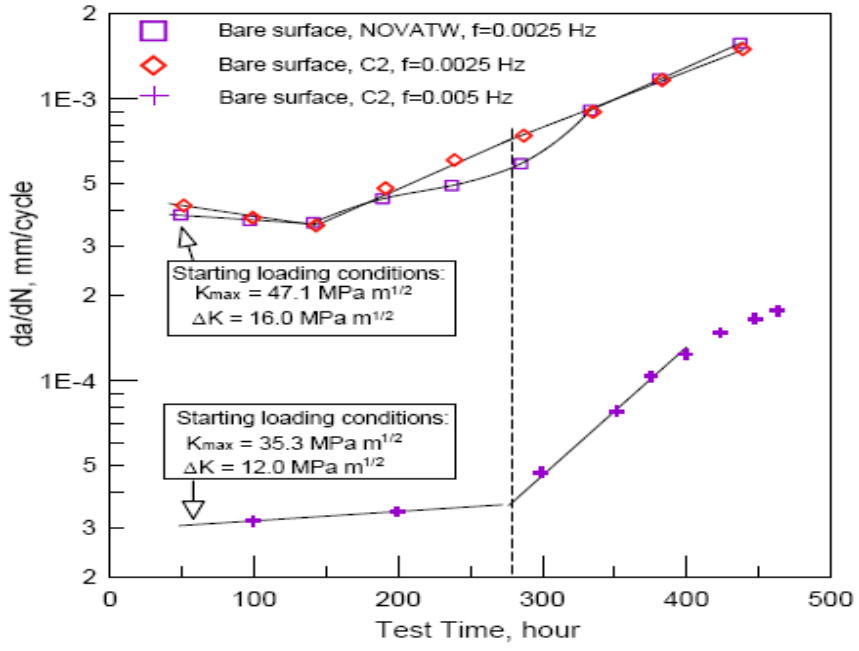

Figure 2-29: Crack growth rate as a function of test time [31].

Absence of hydrogen transition was not surprising as it was discussed before that effect of hydrogen (environment) will be benign in aggressive loading conditions. It was also noted that although hydrogen role will be benign, but it still enhances the growth rate of cracks in aggressive loading conditions. Chen et al. new corrosion fatigue model was so helpful to see this fact. Hydrogen effect in aggressive loading situations became clear when they normalized their data by $(\Delta K)^2K_{max}/f^{0.1}$ factor as it can be seen in Figure 2-30:

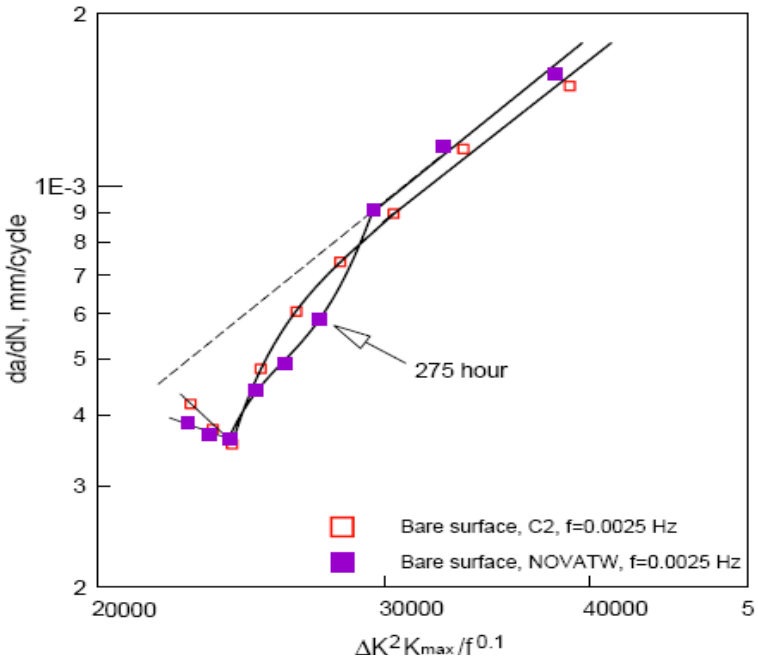

Figure 2-30: Crack growth rate as a function of $\Delta k^2K_{max}/f^{0.1}$ [31].

It can be concluded that $(\Delta K)^2K_{max}/f^{0.1}$ can successfully reflect the combination of environmental and mechanical factors on crack growth behavior. The effect of hydrogen on crack growth rate in near-neutral pH environment can also be seen properly by analyzing growth data using this factor. Plotting the data of coated samples using $(\Delta K)^2K_{max}/f^{0.1}$ (Figure 2-31), it could be seen that with the absence of hydrogen effect in coated samples, their growth rate was much lower than that

of bare samples. This emphasizes the role of hydrogen in enhancing the fatigue crack growth rate by its emberittling effect in near-neutral pH environments.

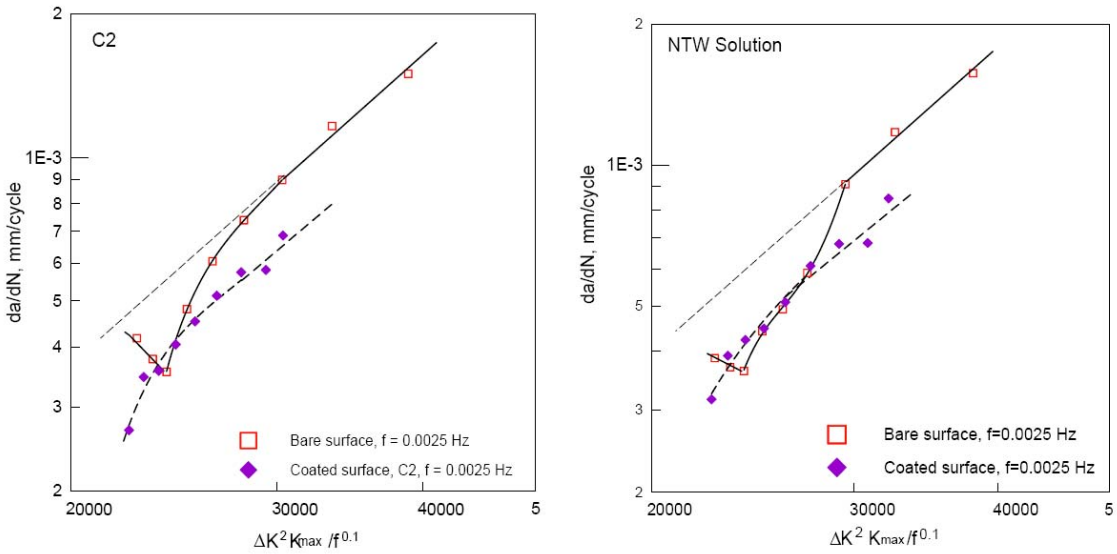

Figure 2-31: Comparison of crack growth behavior between bare CT specimen and the coated CT specimen in C2 and NOVATW solutions [31].

Chen et al. made the last discussion on the decreasing growth rate with time in the first stage of crack growth before hydrogen effect being started. They believed that high growth rate at the beginning was due to the sharp crack tip resulted from pre-cracking procedure before the test and corrosion was responsible for the decrease in growth rate by increasing time before the effect of hydrogen being started. High rate of corrosion at the beginning of the crack exposure to the corrosive environment tends to blunt the crack tip due to high amount of dissolution and the hydrogen has not reached the crack tip to apply its re-sharpening effect and the crack tip tends to become blunted which will result in decrease of crack growth rate.

2.8. Summary

Anodic dissolution and hydrogen embrittlement were believed to be responsible mechanisms for crack growth of pipeline steels in near neutral pH environments. Applied stresses can cause plastic deformation to build preferential sites for hydrogen atoms to be stored in. Environmental factors such as soil chemistry and the amount of cathodic protection in addition to metallurgical and mechanical properties of the pipe steel such as the level of un-uniformity of the steels microstructure can define the level of hydrogen generation and trapping in the steels microstructure. Crack growth behavior in near neutral pH environments can be well explained based on the behavior of corrosion fatigue cracking. Pipelines crack growth data were well rationalized using a newly introduced $(\Delta K)^2 K_{max}/f^{\alpha}$ combined factor which reflects the synergistic interaction of mechanical situation (fatigue) and environmental effects (corrosion) on cracking procedure. Significant role of hydrogen in cracking procedure can also be revealed in data analysis using this factor. Further research required to obtain the effectiveness of using the newly introduced factor on analysis of crack growth rate of different steels.

3. Materials and Experimental Details

3.1. Materials

Four different pipeline steels including two types of X65, one X52 and one X80 pipeline steels were selected to be tested. These steels were selected among the steels which are commonly used in oil and gas pipelines and were susceptible to cracking in near-neutral pH environments. As it can be seen in Table 3-1, these steels have different chemical composition with different carbon contents.

Table 3-1: Chemical composition of different steels.

Steel	C	Mn	Cu	Nb	Cr	Mo	V	Ni	Al	Ti	N
X80	0.06	1.75	0.27	0.31	0.04	0.03	0.005	0.08	0.026	0.011	0.003
X65(I)	0.13	1.55	0.05	0.05	0.08	0.01	0.002	0.05	0.042	0.002	0.009
X65(II)	0.03	1.49	0.27	0.06	0.08	0.21	0.003	0.01	0.001	0.001	0.012
X52	0.07	0.80	0.28	0.09	0.05	0.01	0.002	0.01	0.031	0.019	0.001

* P=0.01, B=0.0002, Si=0.3, S=0.01 and Ca<0.003 for all steels.

3.2. Methods Used For Characterizing the Steels:

3.2.1. Metallography (Microstructures)

Small coupons were cut from all different steels for metallography purposes to investigate the steel's microstructures. All the samples were polished to 1200 sand grit paper followed by polishing on cloth. Polished surface of the samples were etched using Nital (2%). Scanning Electron Microscope (SEM) was used to investigate the microstructures.

3.2.2. Tensile Tests (Mechanical Properties)

Mechanical properties of the steels were determined using tensile tests. Mechanical properties such as yield strength, tensile strength and total elongation of steels were reported using the stress-strain (load-displacement) curves obtained from tensile testing of tensile specimens which were cut from the pipes sections.

3.3. Corrosion Tests

3.3.1. Test Solution

To investigate the growth behavior of pipeline steels in near-neutral pH environment a synthetic soil solution with the pH in the range of near-neutral pH values (5.5-7.5) was selected (C2 solution [25]). As the focus of this research was to investigate the material dependence of crack growth behavior, all the tests were done in C2 solution. Chemical composition of the solution is listed in Table 3-2. The solution was purged for 48 hours with the $N_2/5\%CO_2$ gas mixture to obtain the pH value of 6.29 before being used.

Table3-2: C2 solution (pH=6.29).

Chemicals	Composition (g/L)
$MgSO_4.7H_2O$	0.0274
$CaCl_2$	0.0255
KCl	0.0035
$NaHCO_3$	0.0195
$CaCO_3$	0.0606

3.3.2. Weight Loss Tests

Small coupons of 10×10×1mm were cut from all the steels to be used in coupon weight loss tests to evaluate the corrosion resistance of different steels in C2 solution. Twenty four small coupons were distributed in six flasks. All the flasks were filled with C2 solution and each flask contains 4 coupons of different steels. All the coupons were weighed before exposure to the solution for three times and their average weight were obtained. Coupons of first flask were taken out after 5 days of exposure. The coupons in next flasks removed after each 5 days and final coupons (sixth flask) were removed after 30 days of exposure and weighed. Weight changes values of steels (amount of dissolution) were plotted versus the time of their exposure to the solution. Figure 3-1 shows the coupon test's set up. It should be noted that coupons in each flask were not connected to each other and the solutions were purged by N_2-5%CO_2 gas mixture to keep the pH of the solutions constant (pH= 6.29) during the exposure time.

Figure 3-1: Weight loss coupon test.

3.4. Corrosion Fatigue Tests

3.4.1. Sample Preparation Procedures

Compact Tension (CT) specimens were used for corrosion fatigue tests. CT specimens were cut from the pipes with the notch perpendicular to the circumferential direction of the pipe (Figure 3-2). Dimensions of CT specimens were selected based on ASTM E647-93. It was expected that the size of plastic zone created in front of the crack tip be small compared to specimen dimensions so that linear elastic fracture mechanics concepts and formulas can be used for crack growth measurements. Dimensions of the CT specimens used in this research are shown in Figure 3-3:

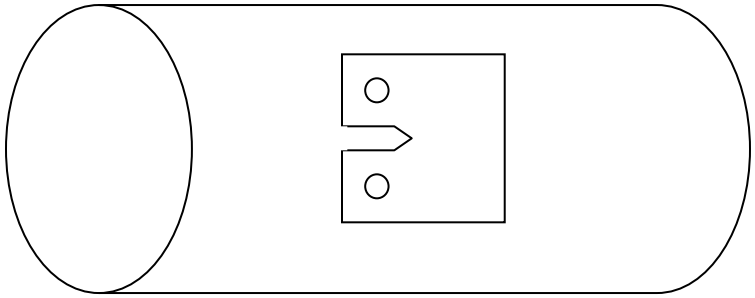

Figure 3-2: Directions of the CT specimen cut from the pipe.

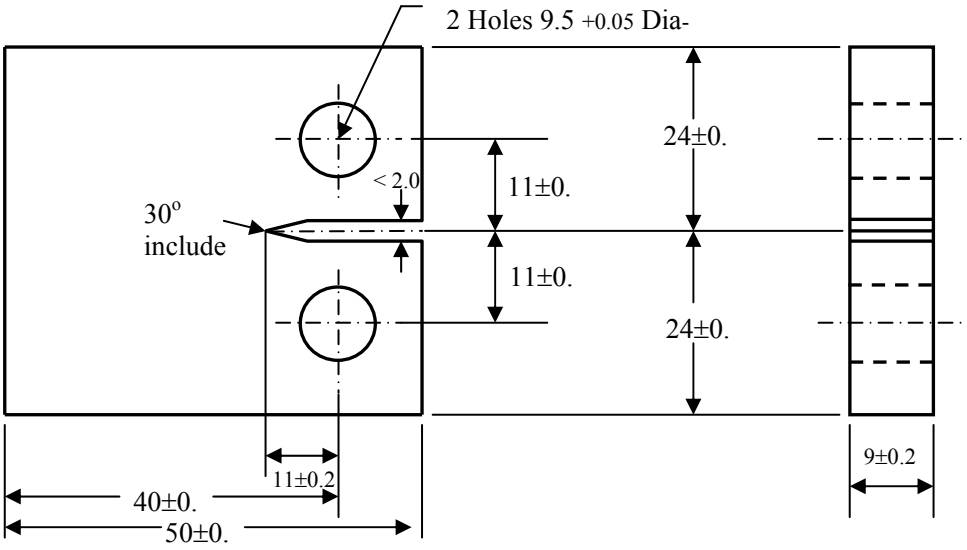

Figure 3-3: Dimensions of CT specimens used in this research.

According to linear elastic-plastic fracture mechanics, stress intensity factor values (K) for CT specimens can be defined using equation below (ASTM E647-93):

$$K = P\,(2+\alpha)\,(0.886+4.46\alpha-13.32\alpha^2+14.72\alpha^3-5.6\alpha^4) \,/\, [BW^{1/2}(1-\alpha)^{3/2}]$$

Where P is the applied load, B is the thickness of the specimen and α= a/W is defined as crack length (a) to specimen width (W) ratio. After being cut from the pipes, all CT specimens were polished to 600 sand grit paper to be ready for pre-cracking procedure.

3.4.1.1. Pre-Cracking Procedure

CT specimens were pre-cracked using the MTS machine before being used for the actual tests. Pre-cracking was done with the maximum load lower than the maximum load used in the actual test and pre-crack size was controlled using optical microscope to be between 2 and 3 mm with crack length difference of less than 0.1 mm on the sides of the specimens.

3.4.1.2. Wire Attachments

Four different wires were soldered to pre-cracked CT samples so that potential drop system could be used to monitor the crack length changes during the tests. As it can be seen in Figure 3-4 two wires were soldered to the sides of the sample (current wires) and other two wires (signal wires) were soldered on the sides of the specimen's notch.

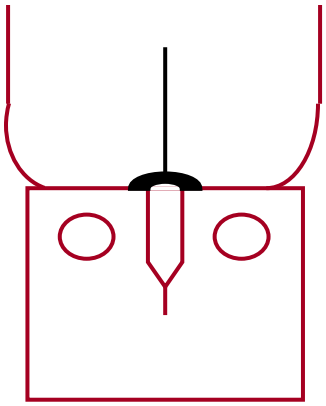

Figure 3-4: Current and Signal wires.

3.4.2. Test's Apparatus and Set-up

Pre-cracked CT specimens were pin hole loaded in corrosion cells filled with C2 solution to the middle of the specimen's notch. The test set up is shown in Figure 3-5. Pneumatic loading frame was used to apply cyclic loads to the samples. Loading cells were controlled by computer with minimum load, maximum load, frequency and number of cycles as inputs. Two corrosion cells were used so that two different samples could be used in each test. Corrosion cells were sealed and the solution purged with N_2+5%CO_2 gas mixture during the tests so that oxygen could not penetrate inside the cells to cause extra corrosion and the pH remained constant (pH=6.29).

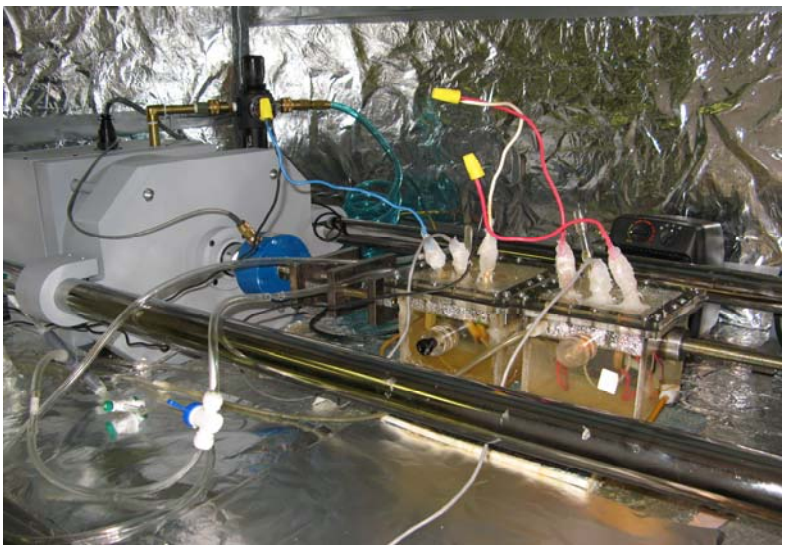

Figure 3-5: Pneumatic cyclic loading frame and test set up.

3.4.3. Testing Conditions

All the pre-cracked specimens were cyclically loaded using triangle waveform. Loading frequency was in the range of 0.1 to 0.00125 Hz and R ratio (minimum load/maximum load ratio) in the range of 0.4 to 0.65. K_{max} and ΔK were

controlled to achieve a value in the range of 35 to 55 and 10 to 28 $MPam^{0.5}$, respectively. Different loading conditions led to different initial K_{max}, ΔK, f and $(\Delta K)^2K_{max}/f^{0.1}$ values for each test. A summary of the test conditions is shown in Table 3-3. Tables 3-4, 3-5, 3-6 and 3-7 show testing conditions at which X65(I), X52, X65(II), and X80 samples were tested:

Table 3-3: Corrosion fatigue testing conditions.

Test No.	**Steels**	**K_{max}**	**ΔK**	**R**	**f**	**$(\Delta K)^2K_{max}/f^{0.1}$**
1	X65(I)	35	14	0.6	0.01	10872.4
2	X52	35	14	0.6	0.01	10872.4
3	X65(I)	35	14	0.6	0.005	11652.7
	X52	38	14.8			14138.7
4	X65(I)	41	16	0.6	0.005	18732.7
5	X80	35	14	0.6	0.005	11652.7
	X65(II)	36.6	14.6			13252.2
6	X80	40.5	16.2	0.6	0.005	18054.6
	X65(II)	43	17.2			21608.6
7	X80	43.13	18.05	0.58	0.00125	27418.4
	X52	43	18			27184.6
8	X80	35	18.05	0.48	0.00125	22250.1
	X52	35	18			22126.9
9	X65(I)	35	12	0.65	0.005	8561.2
	X65(II)	35	12			8561.2
10	X80	35	12	0.65	0.005	8561.2
	X52	35	12			8561.2

Table 3-4: Testing conditions of X65(I) pipeline steel.

Pre-crack (mm)	**Max/Min Loads (KN)**	**K_{max} ($MPa.m^{0.5}$)**	**ΔK ($MPa.m^{0.5}$)**	**f (Hz)**	**$(\Delta K)^2 K_{max}/f^{0.1}$ $MPa^3m^{1.5}Hz^{-0.1}$**
3.43	8.52/5.12	35	14	0.01	10872.4
2.51	9.04/5.42	35	14	0.005	11652.7
2.46	10.62/6.37	41	16	0.005	18732.7
2.45	9.08/5.97	35	12	0.005	8561.25

Table 3-5: Testing conditions of X52 pipeline steel.

Pre-crack (mm)	**Max/Min Loads (KN)**	**K_{max} ($MPa.m^{0.5}$)**	**ΔK ($MPa.m^{0.5}$)**	**f (Hz)**	**$(\Delta K)^2 K_{max}/f^{0.1}$ $MPa^3m^{1.5}Hz^{-0.1}$**
2.45	9.07/5.44	35	14	0.005	11652.7
2.45	10.502/6.301	40.5	16.2	0.005	18054.6
2.49	11.15/6.48	43.13	18.05	0.00125	27418.4
2.52	9.03/4.37	35	18.05	0.00125	22250.1
2.45	9.08/5.97	35	12	0.005	8561.2

Table 3-6: Testing conditions of X65(II) pipeline steel.

Pre-crack Size	**Max/Min Loads (KN)**	**K_{max} ($MPa.m^{0.5}$)**	**ΔK ($MPa.m^{0.5}$)**	**f (Hz)**	**$(\Delta K)^2 K_{max}/f^{0.1}$ $MPa^3m^{1.5}Hz^{-0.1}$**
3.18	9.07/5.44	36.6	14.6	0.005	13252.2
3.37	10.502/6.301	43	17.2	0.005	21608.6
2.43	9.08/5.97	35	12	0.005	8561.25

Table 3-7: Testing conditions ofX80 pipeline steel.

Pre-crack (mm)	Max/Min Loads (KN)	K_{max} (MPa.m$^{0.5}$)	ΔK (MPa.m$^{0.5}$)	f (Hz)	$(\Delta K)^2 K_{max}/f^{0.1}$ MPa^{3}m$^{1.5}$Hz$^{-0.1}$
3	8.76/5.26	35	14	0.01	10872.4
3.36	9.04/5.42	38	14.8	0.005	14138.7
2.44	11.15/6.48	43	18	0.00125	27184.6
2.55	9.03/4.37	35	18	0.00125	22126.9
2.45	9.08/5.97	35	12	0.005	8561.2

3.4.4. Crack Growth Measurements

Crack growth measurements were done using potential drop method [46]. As mentioned before three different wires were soldered to the sides of CT specimens and its notch (Figure 3-5). Wires on the sides were connected to the current supplier device which supplied the constant current of 10 (A). As the crack grows inside the sample the resistivity of the sample increases and the potential on the sides of the notch is increased as a result of constant current applied to the sample. The signal wires on the sides of the notch are connected to the signal reader device. Monitored potential changes were converted to crack length changes. Potential changes versus time (mV-Hr) curves were converted to crack size versus number of cycles (a-N) curves using ASTM E647-05 equations below:

$$V/V_r = A_o + A_1(a/W) + A_2(a/W)^2 + A_3(a/W)^3$$

$$a/W = B_o + B_1(V/Vr) + B_2(V/Vr)^2 + B_3(V/Vr)^3$$

Where V is the measured potential, Vr is the reference crack voltage corresponding to a/W=0.24, a is a crack length, W is the width of the sample and A and Bs are constants. First equation can be used to calculate the constant Vr from any reference a/W and its corresponding voltage and second equation is used to convert potential values to crack length values. Figure 3-6 summarizes potential drop method.

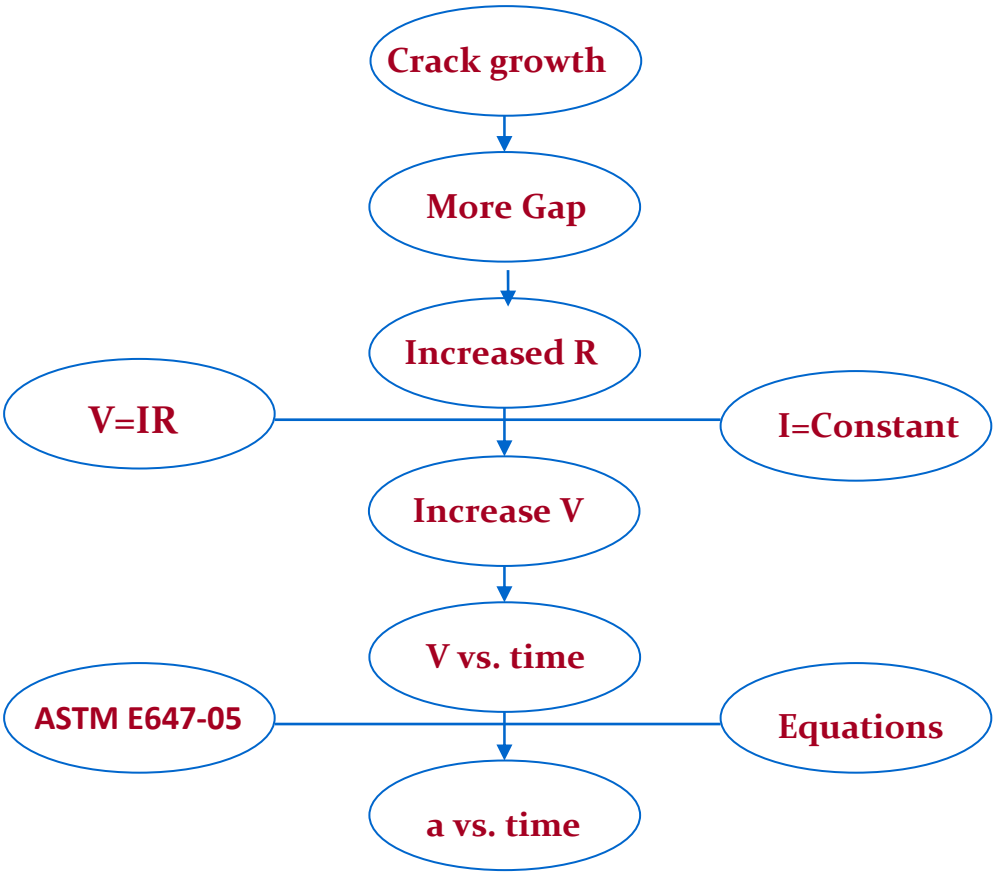

3-6: Potential drop test method.

3.4.5. Data Analysis:

Crack growth data obtained using the potential drop method were represented as crack growth per cycle (da/dN) data and rationalized using corrosion fatigue combined factor ($(\Delta K)^2 K_{max}/f^{\alpha}$). Using crack length (a) versus number of cycles (N) curves, crack growth per cycle could be obtained in different specific growth increments in a-N curves and an average crack length (a) can be used as a crack size representative of that increment. Figure 3-7 illustrates an example of the crack length-number of cycles curve for X52 pipeline steel obtained from potential drop data. Four different growth increments are shown on the curve with four straight trend lines fitted to them. The slope of these lines represents the crack growth per cycle (da/dN) in each increment. As it can be seen in figure below crack growth per cycle keeps increasing as the crack size increases (slopes of fitted lines increase).

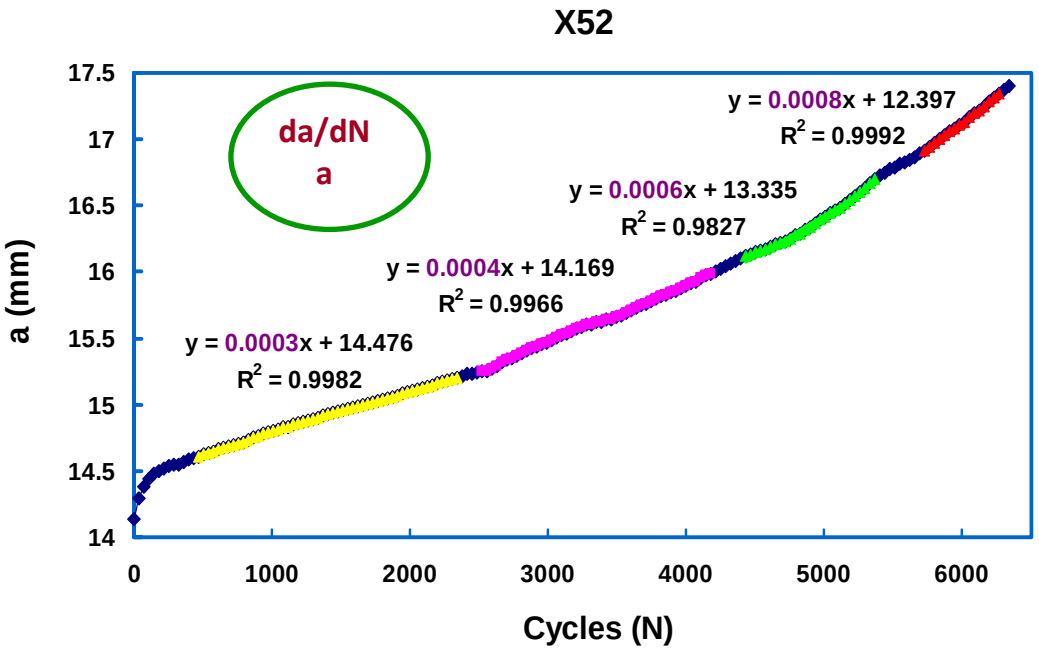

Figure 3-7: Crack length versus Number of cycles for X52 pipeline steel.

da/dN values were related to $(\Delta K)^2 K_{max}/f^{\alpha}$ values using average crack size (a) in each increment. K_{max} and ΔK equations for CT specimens are shown below. By replacing the equation of K_{max} and ΔK in $(\Delta K)^2 K_{max}/f^{\alpha}$, an equation is obtained with crack size as its only variable. The loading parameters (maximum and minimum loads and frequency) and specimen's dimensions are constant in equation below. Specific $(\Delta K)^2 K_{max}/f^{\alpha}$ values can be obtained using each average crack size (a) corresponds to the specific da/dN values.

$$K_{max} = \frac{P_{max}}{B\sqrt{W}} F(a/w)$$

$$\Delta K = \frac{\Delta P}{B\sqrt{W}} F(a/w)$$

$$\frac{(\Delta K)^2 K_{max}}{f^{\alpha}} = \frac{(\Delta P)^2 P_{max}}{B^3 \sqrt{W^3} f^{\alpha}} \times F(a/w)^3$$

3.5. Fatigue in Air Tests

Three fatigue tests in air were conducted on the samples of X52 and X80 pipeline steels to investigate the role of corrosive solution on corrosion fatigue crack growth by comparing the growth rate results. Cyclic loads were applied to CT specimens using Instron hydraulic loading device with different frequencies in each test including 0.5, 0.05, 0.005 and 0.001 Hz. Loading conditions of fatigue tests in air are shown in Table 3-8. Crack growth measurements were determined using optical pictures of the cracks on the sides of the samples after certain number of cycles (Table 3-9).

Table 3-8: Fatigue in air tests loading conditions.

Test No.	K_{max}	ΔK	R	$(\Delta K)^2 K_{max}$
1	33	15.3	0.53	7724.9
2	40	15.3	0.62	9363.6
3	33	16.8	0.489	9363.6

Table 3-9: Fatigue tests conditions.

Frequency (HZ)	Cycles (N)	Time (Hr)
0.5	1800	1
0.05	1800	10
0.005	3600	200
0.001	1800	500

4. Results and Discussion

4.1. Characteristics of Steels

Pipeline steels used in this research have different chemical compositions (Table 3-1). These pipeline steels can be categorized as low carbon steels with highest carbon content of 0.13 %wt in X65(I). Different content of carbon and alloying elements such as Mn, Mo and Cr leads to different microstructures and mechanical properties.

4.1.1. Microstructures and Mechanical Properties

Microstructures of all the steels were obtained using Scanning Electron Microscope. SEM pictures of steels microstructures are shown in Figure 4-1:

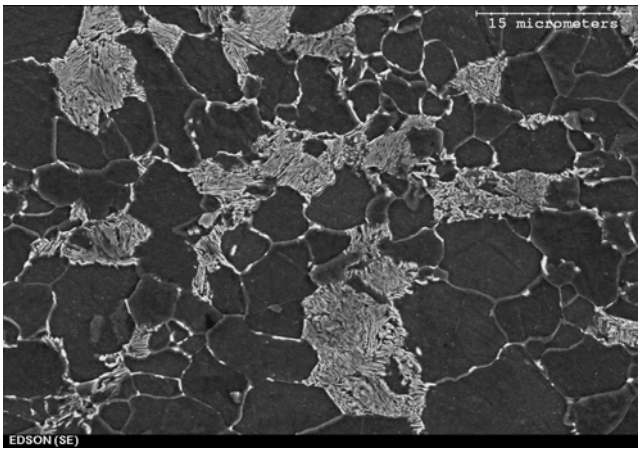

(a)

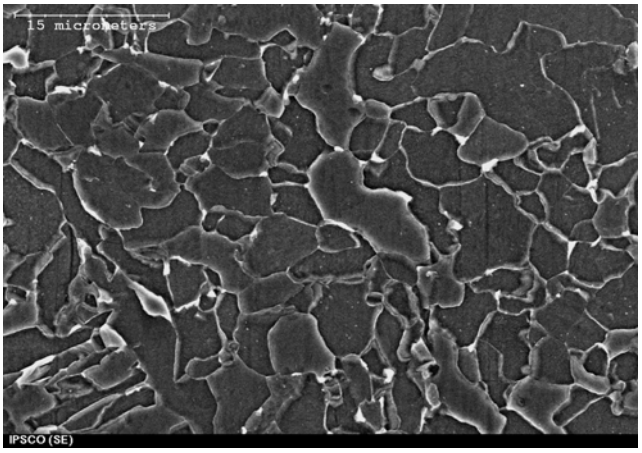

(b)

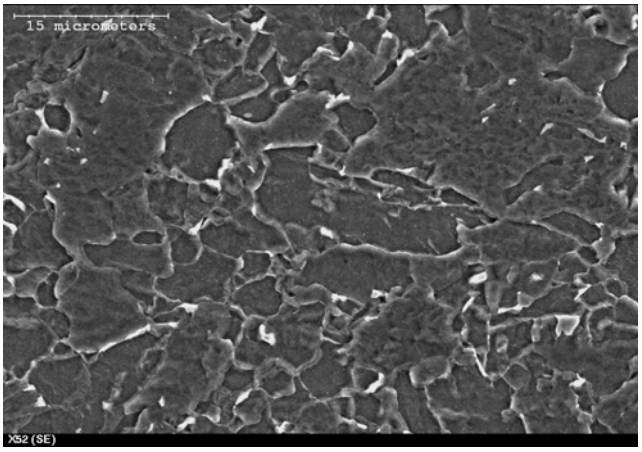

(c)

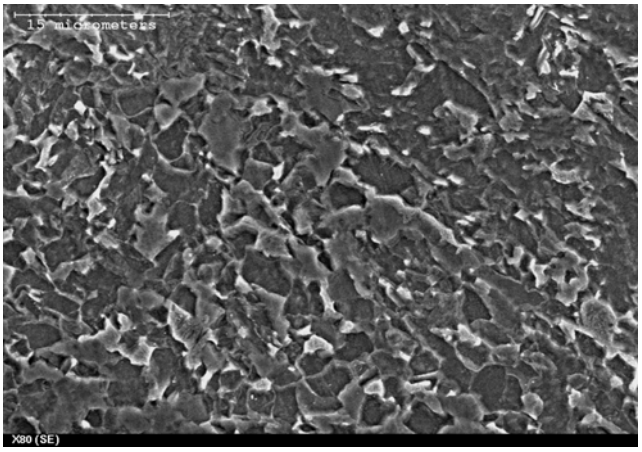

(d)

Figure 4-1: SEM picture (a) X65(I), (b) X65(II), (c) X52 and (d) X80.

As it can be seen in Figure 4-1, X65(I) is the only steel among the ones that were studied that has Pearlite structure, which agrees with the fact that X65(I) has the highest carbon content among the steels. Other steels have ferritic matrix with dispersed carbide particles. Another main difference in microstructures is the grain sizes. X52 has the largest grain size, while X80 has the smallest grain size. Microstructure and grain size of steels directly affect their mechanical properties. Table 4-1 lists tensile properties of the four steels:

Table 4-1: Mechanical properties of different steels.

Steel	Yield Strength (MPa)	Tensile Strength (MPa)	Total Elongation (%)
X80	619.5	705.1	20.6
X65(I)	522.8	607.8	24.3
X65(II)	450.7	544.6	30.1
X52	382.2	485.3	32.2

As it can be seen, X80 has the highest yield strength and tensile strength. On the other hand X52 represents the lowest yield strength and tensile strength with highest total elongation (ductility). Different mechanical properties of steels are a result of difference in their grain sizes, microstructures (second phases or particles) and their heat treatments. It is known that yield strength and tensile strength of the steels increases as their grain sizes decrease. It can be said that presence of pearlite affects X65(I)'s formability as it is known as a harder and less formable structure than its surrounding ferrite.

4.1.2. Corrosion Behavior

Corrosion behavior of different steels in C2 solution was compared using weight loss coupon tests. Figures 4-2 and 4-3 show the plotted steels weight loss data versus time. It can be seen in Figures. 4-2 and 4-3 that all the steels show almost the same amount of weight loss during the first 10 days but with longer exposure time they started to show different amount of weight loss. Coupon's weight loss is due to dissolution (corrosion occurrence) of their surfaces which are exposed to C2 solution. In other words weight loss data of steels represent their corrosion resistance. Figures. 4-2 and 4-3 below show that X80 and X65(II) have the lowest and the highest corrosion resistance among the steels, respectively, while X65(I) has lower corrosion resistance than X52 as it has higher amount of weight loss.

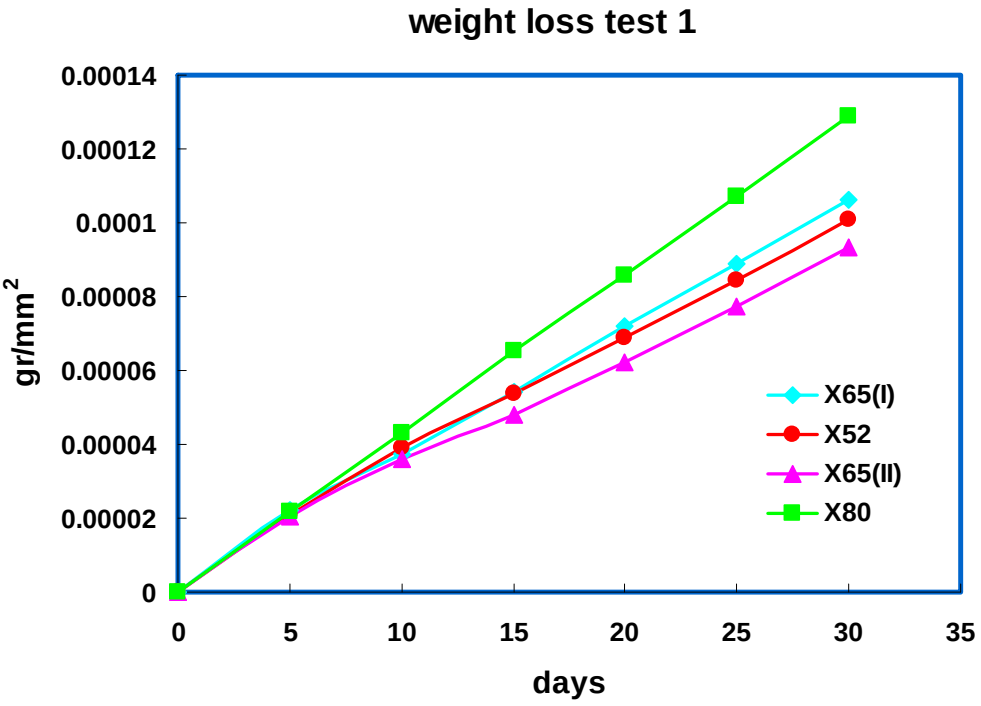

Figure 4-2: Weight loss test 1.

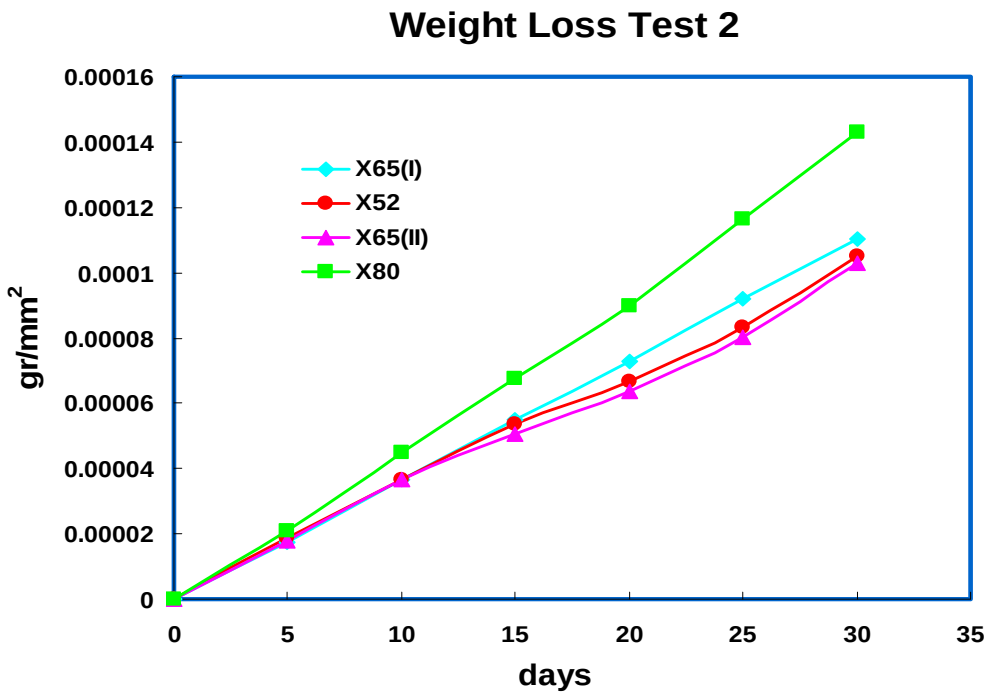

Figure 4-3: Weight loss test 2.

The ability of a steel to generate hydrogen can be related to weight loss data. Corrosion occurrence on the surface (dissolution of iron) generates electrons which reduce hydrogen ions to generate atomic hydrogen as a corrosion product. Hydrogen atoms generated on the surface tend to diffuse throughout the steels due to concentration gradient (Ficks Law). Hydrogen diffusion occurs with different rates in different steels due to their different microstructures. According to weight loss test results, it can be said that X80 has the highest source of diffusible hydrogen on its surface as more corrosion/dissolution occurs on its surface when it is exposed to the solution.

4.2. Corrosion Fatigue Crack Growth Curves

Potential changes were monitored by potential drop system. Crack growth curves were obtained by conversion of potential changes data to the actual crack sizes using ASTM E647-93 equations. Examples of crack growth curves for different steels are shown in Figures 4-4 to 4-7. These curves were used to illustrate the variation of crack growth per cycles (da/dN) versus ΔK or $(\Delta K)^2 K_{max}/f^{0.1}$.

Cracking in near-neutral pH environments was previously categorized as SCC and the growth rates were monitored by ΔK changes. It was shown in this research that crack growth rate data can not be rationalized by this factor individually. Figures 4-8 and 4-9 compare the growth rate data of X52 and X80 steels obtained from tests 7 and 8 using ΔK values. The initial ΔK and loading frequency were the same in these tests but initial K_{max} value of test 7 (43 $MPam^{0.5}$) is higher than its value in test 8 (35 $MPam^{0.5}$).

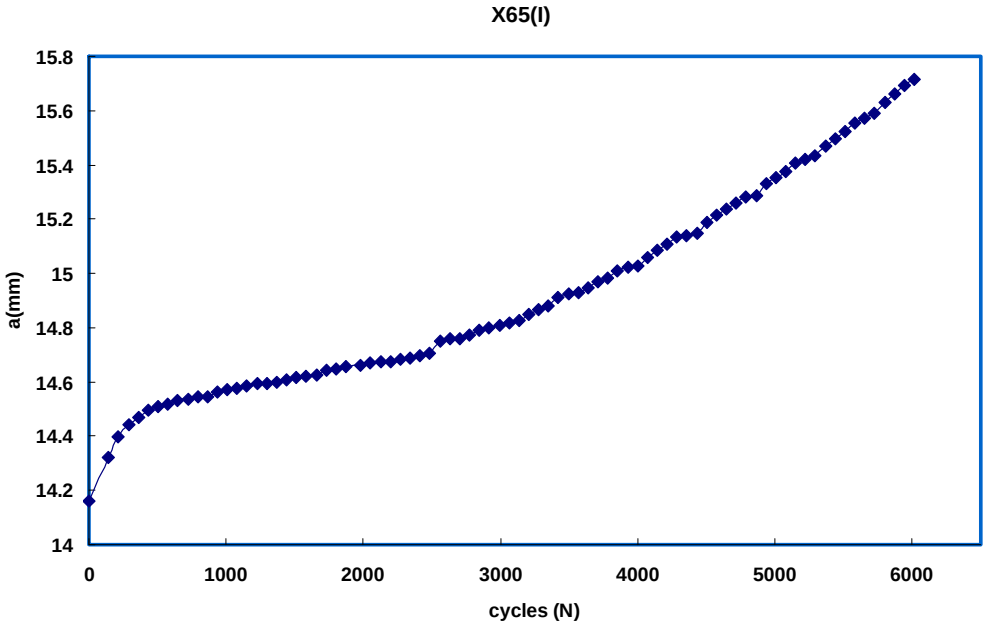

Figure 4-4: Crack growth curve of X65(I) pipeline steel (Test 1).

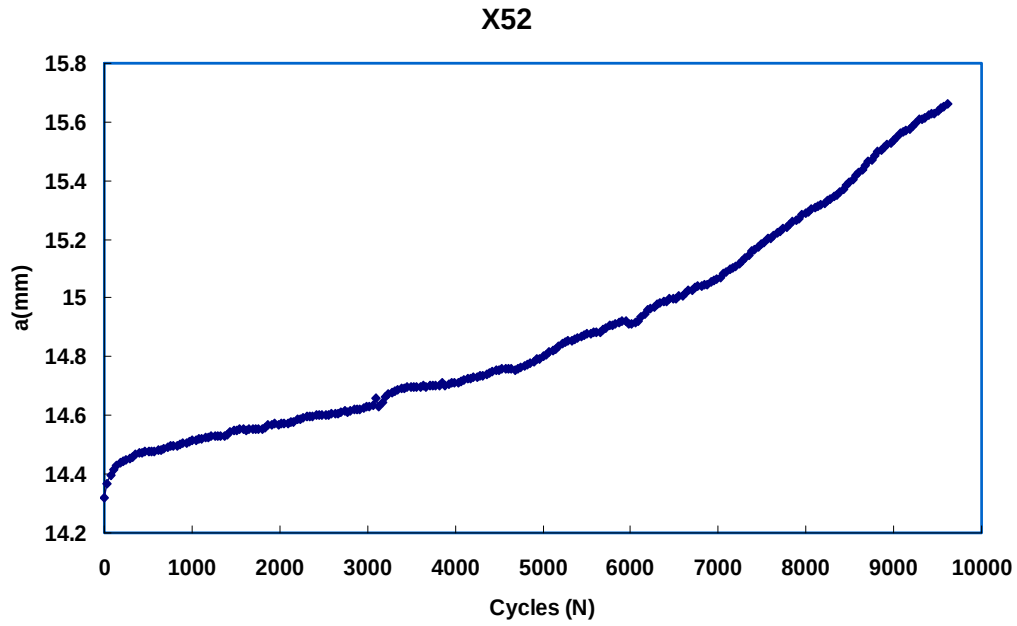

Figure 4-5: Crack growth curve of X52 pipeline steel (Test 3).

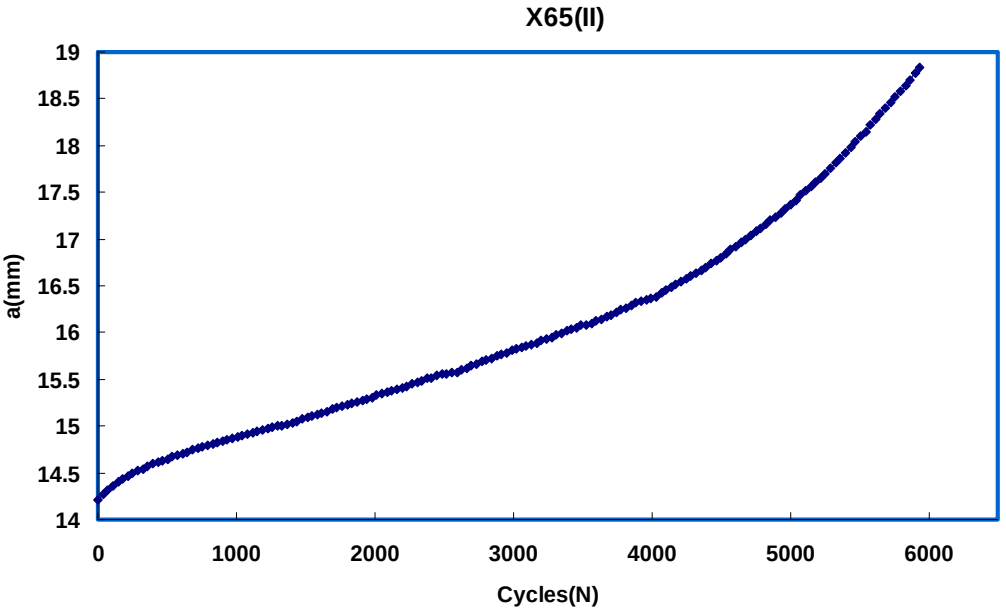

Figure 4-6: Crack growth curve of X65(II) pipeline steel (Test 5).

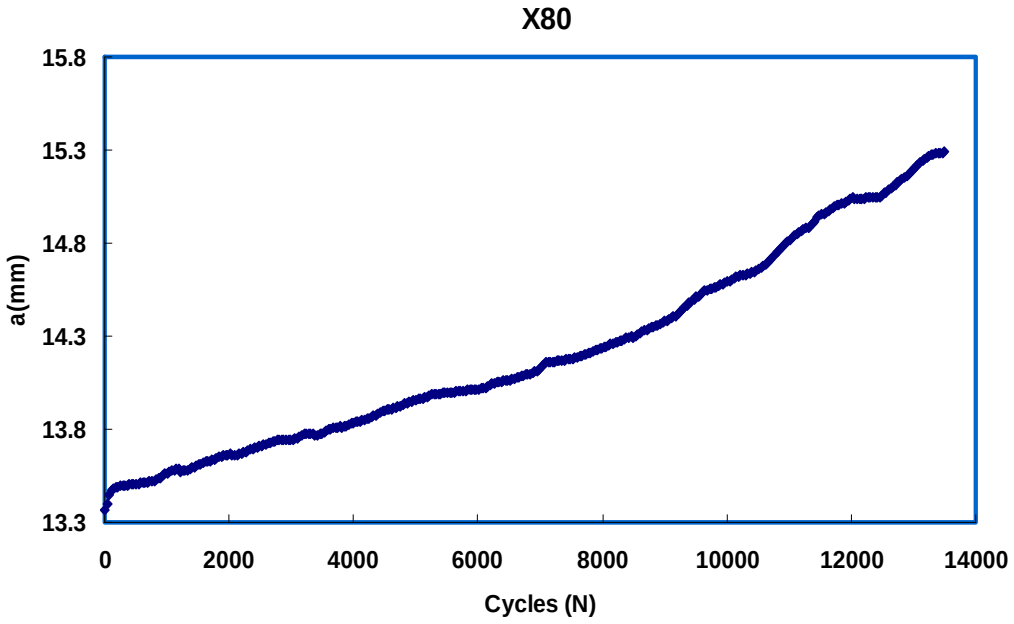

Figure 4-7: Crack growth curve of X80 pipeline steel (Test 6).

Figures 4-8 and 4-9 show that X52 and X80 pipeline steels reflect higher growth rates (da/dN), in all constant ΔK values, in the test with higher initial K_{max} which led to separate crack growth trends (paths) in these tests. ΔK can not provide complete description of crack growth behavior as K_{max} values (other fatigue cracking driving force) and environmental factors (hydrogen) also have a great influence on cracking. Cracking behavior of pipeline steels should be considered through a combined effect of ΔK, K_{max} and corrosive environment (hydrogen). For this purpose, $(\Delta K)^2 K_{max}/f^{0.1}$, as was proposed in Ref [25], was used for crack growth rate data analysis. The same growth rate data of tests 7 and 8 (Figures 4-8 and 4-9) were correlated to $(\Delta K)^2 K_{max}/f^{0.1}$ in Figures 4-10 and 4-11.

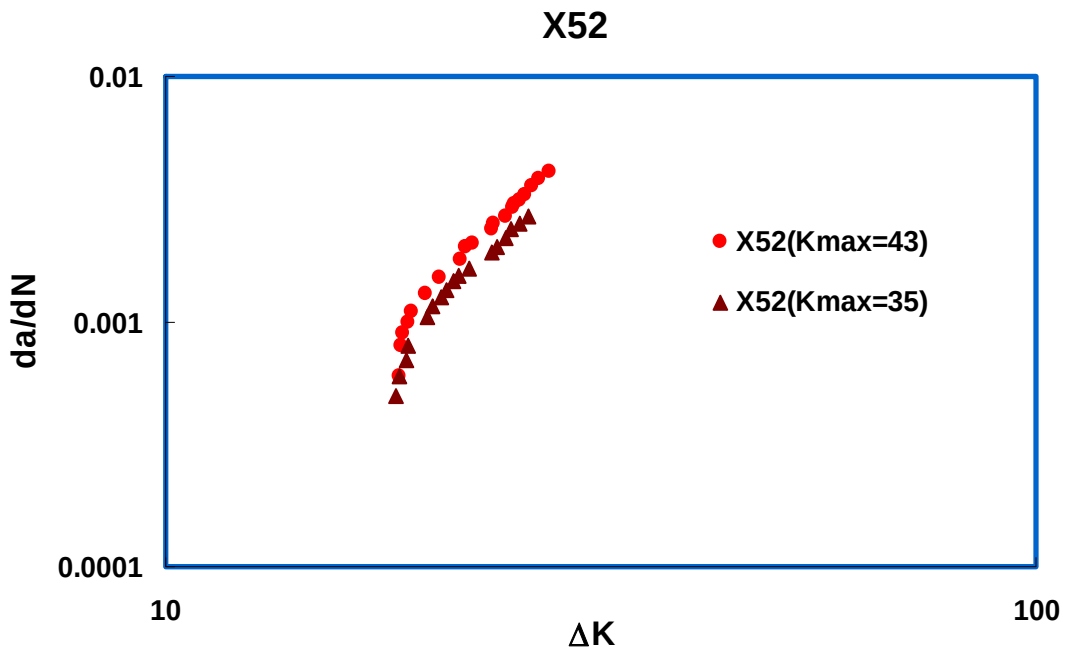

Figure 4-8: Crack growth rate da/dN as a function of ΔK for X52.

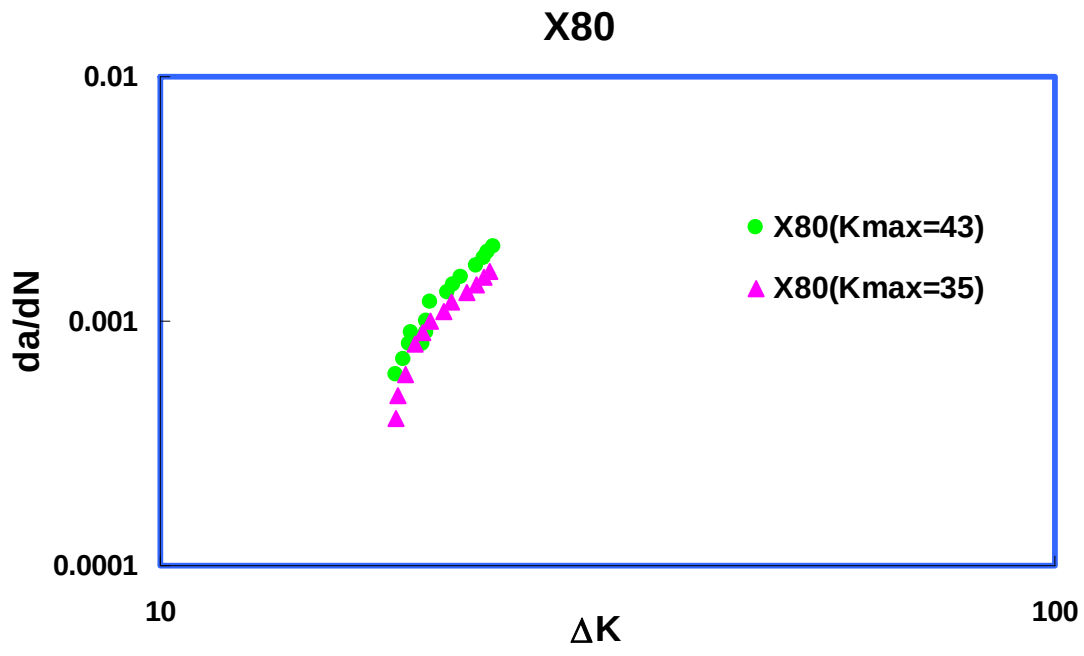

Figure 4-9: Crack growth rate da/dN as a function of ΔK for X80.

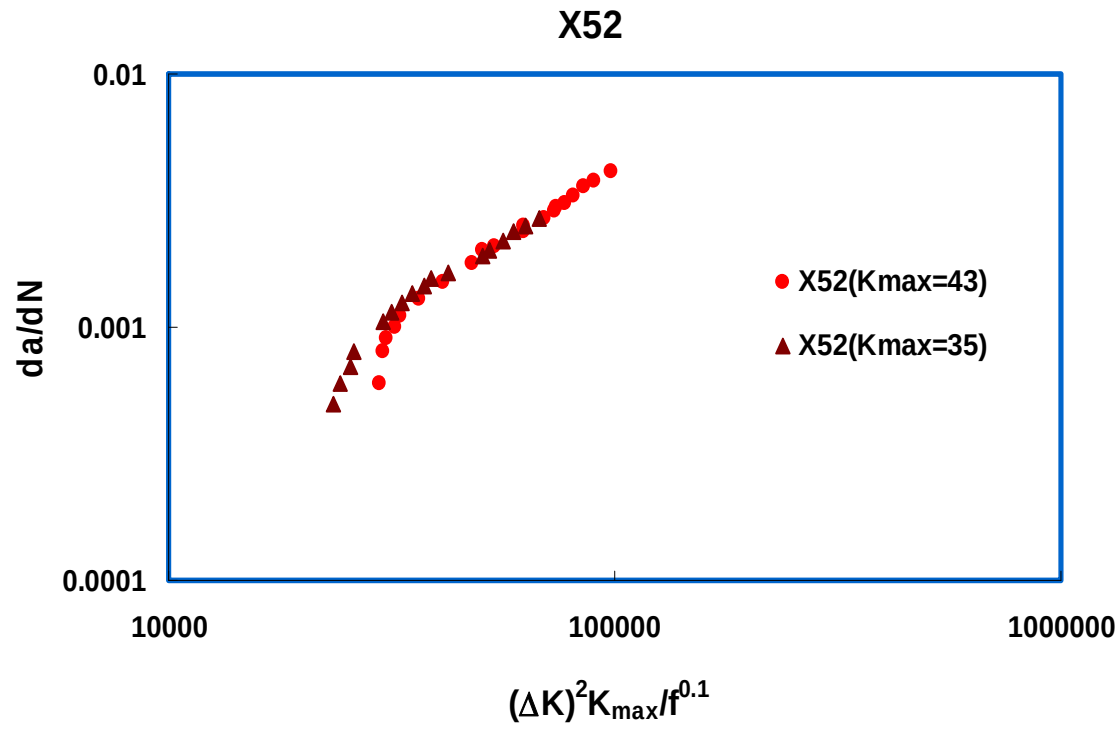

Figure 4-10: Crack growth rate da/dN as a function of $(\Delta K)^2 K_{max}/f^{0.1}$ for X52.

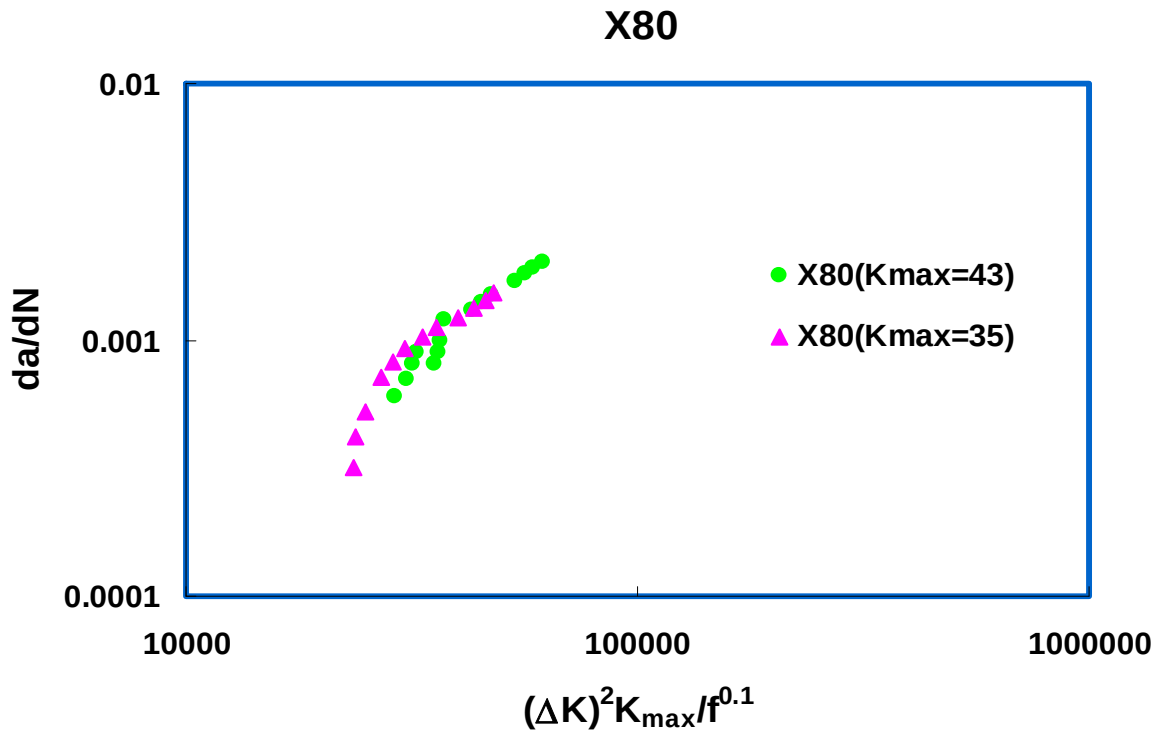

Figure 4-11: Crack growth rate da/dN as a function of $(\Delta K)^2 K_{max}/f^{0.1}$ for X80.

It can be seen that when the same growth rate data are correlated to $(\Delta K)^2K_{max}/f^{0.1}$, all the data points go along the same growth path and growth consistency can be obtained when growth rate data were rationalized using $(\Delta K)^2K_{max}/f^{0.1}$ combined factor.

Growth rate data (da/dN) of all steels in different loading conditions were correlated to $(\Delta K)^2K_{max}/f^{0.1}$ in this research. Crack growth curves of different steels obtained from different tests can be seen in Figures 4-12 to 4-15. It can be seen that cracking behavior of pipeline steels in near-neutral pH environment can be well explained by the behavior of corrosion fatigue cracking as the crack growth rate of all the steels in different loading conditions can be rationalized using $(\Delta K)^2K_{max}/f^{0.1}$ factor.

The crack growth curves can be divided into two different parts: the tail shaped part and a straight growth line following the tail shaped part. Also data points representing lower growth rates are present at the beginning of the crack growth curves of each individual test followed by data points representing higher growth rates joining to the straight linear growth region making small tail shape at the beginning of each test.

The resulted tail shape at the beginning of the tests represents the time required to achieve hydrogen equilibrium throughout the sample [29]. The Sample surface is the main source of hydrogen as corrosion occurs on the surface due to its exposure to the corrosive solution (C2). Generated atomic hydrogen on the surface diffuses throughout the sample due to concentration gradient (Ficks law). After some time depending on the hydrogen diffusion coefficient of the steel and the thickness of the CT specimen, the whole sample will be saturated with atomic hydrogen, achieving maximum effects of hydrogen on fatigue crack growth at the crack tip. A jump (tail) is seen when hydrogen effects start, and the linear region in the growth curves represents the occurrence of full hydrogen effects on crack growth. It is noticeable that the tail shape of the growth curve at the beginning of the tests becomes shorter in the test with more aggressive mechanical loading conditions (higher initial $(\Delta K)^2K_{max}/f^{0.1}$ values) as the effect of hydrogen (environment) becomes less noticeable in the presence of aggressive cyclic

stresses [24, 29]. According to Ref. [29], the time to achieve an equilibrium concentration of hydrogen in a similar steel pipeline CT specimen was about 275 hour. However, the tail part in some tests at low combined factor well exceeded this time period. This suggests that some other factors must be considered for the growth behaviour observed in the tail part, which will be discussed in the later sections.

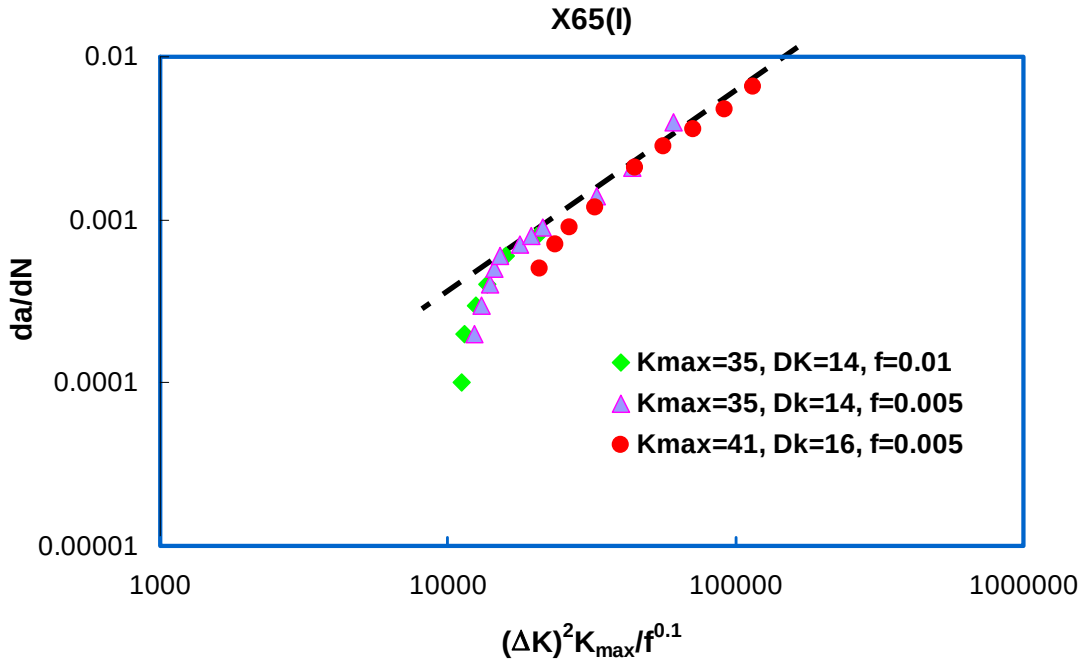

Figure 4-12: Crack growth rate da/dN as a function of $(\Delta K)^2K_{max}/f^{0.1}$ for X65(I).

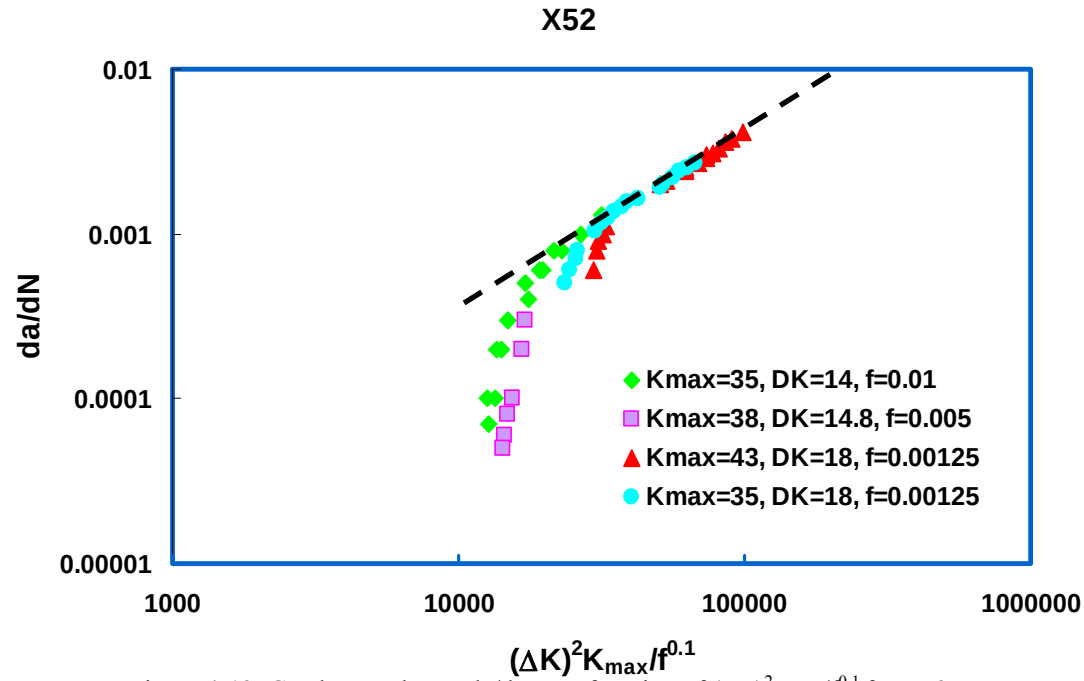

Figure 4-13: Crack growth rate da/dN as a function of $(\Delta K)^2K_{max}/f^{0.1}$ for X52.

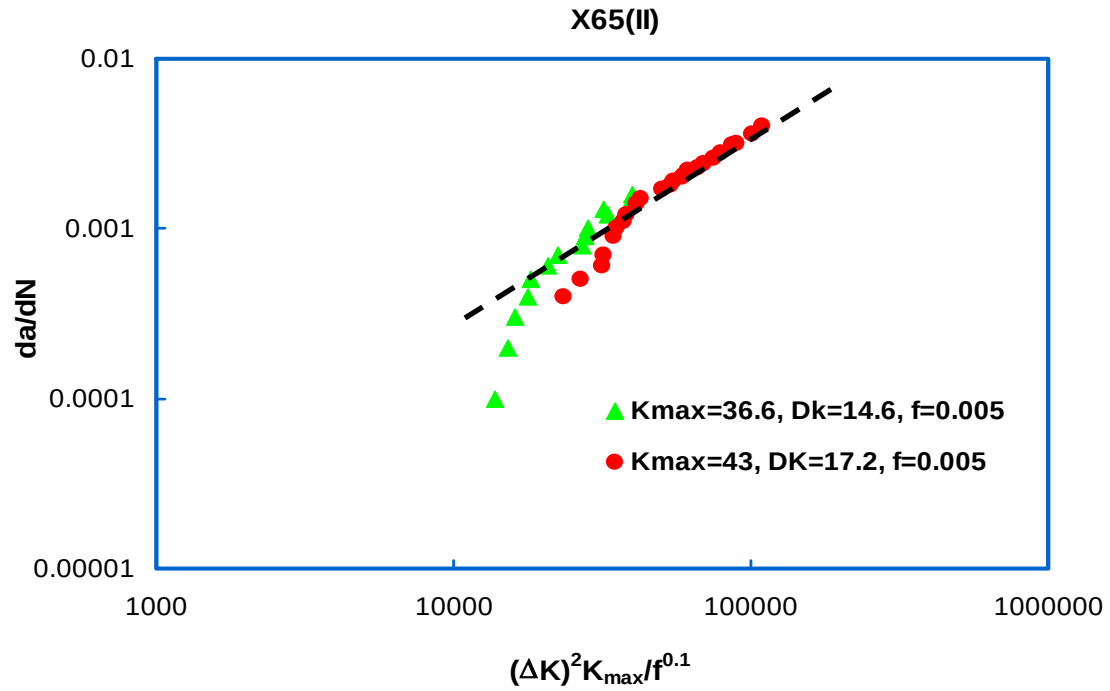

Figure 4-14: Crack growth rate da/dN as a function of $(\Delta K)^2 K_{max}/f^{0.1}$ for X65(II).

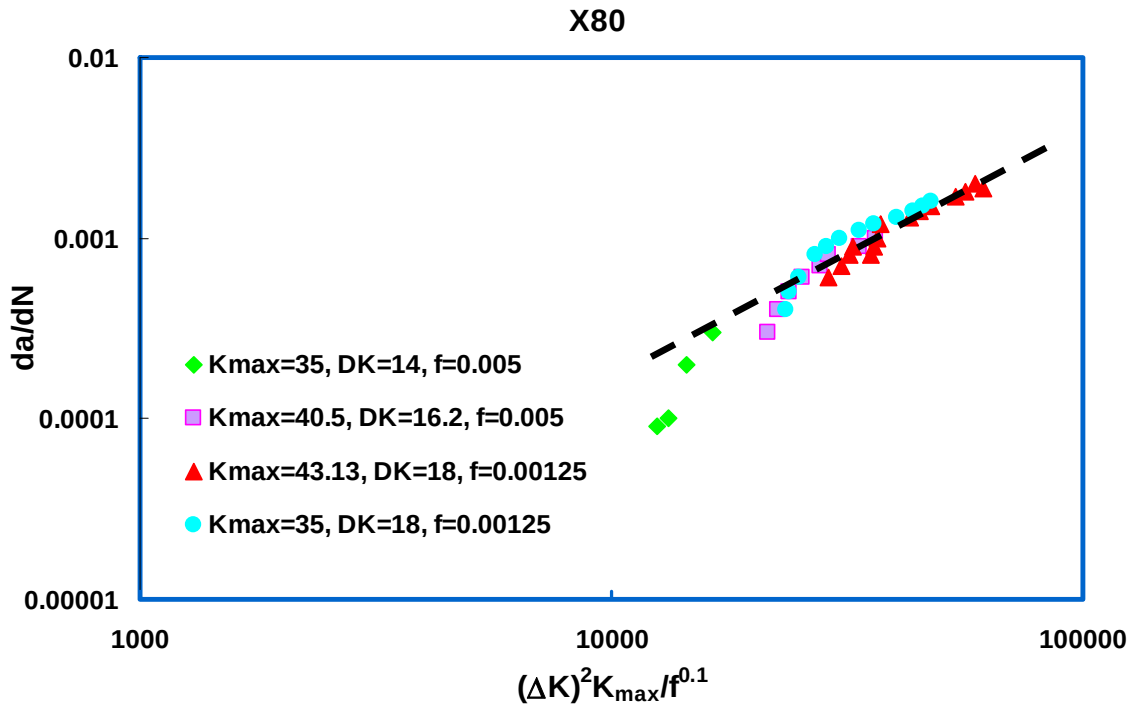

Figure 4-15: Crack growth rate da/dN as a function of $(\Delta K)^2 K_{max}/f^{0.1}$ for X80.

4.3. Material Dependency of Crack Growth Behavior

Corrosion fatigue crack growth curves of different steels are compared in Figure 4-16. Different steels represent different crack growth curves when growth rate data were correlated to $(\Delta K)^2 K_{max}/f^{0.1}$. In aggressive mechanical loading region of the curves (regions with high $(\Delta K)^2 K_{max}/f^{0.1}$ values), where linear dependence of crack growth data on the combined factor on log-log scale is obtained, the relative position and the slight difference in the slope of the curves represent the relative resistance to corrosion fatigue growth of the steels. X65(I) and X80 pipeline steels represent the highest and lowest crack growth rates, respectively, while X52 has higher crack growth rate than X65(II). In less aggressive loading conditions, big tails in the curves and different tail sizes and tail positions can be seen for different steels. All the tests were conducted in the same corrosive environment (C2 solution) and almost the same mechanical loading conditions so it can be concluded that difference in cracking behavior/growth rate is caused by different mechanical properties and microstructures of the steels. Further discussion will be made later on how corrosion fatigue growth rate of different steels is influenced by their properties and the microstructures of the steels.

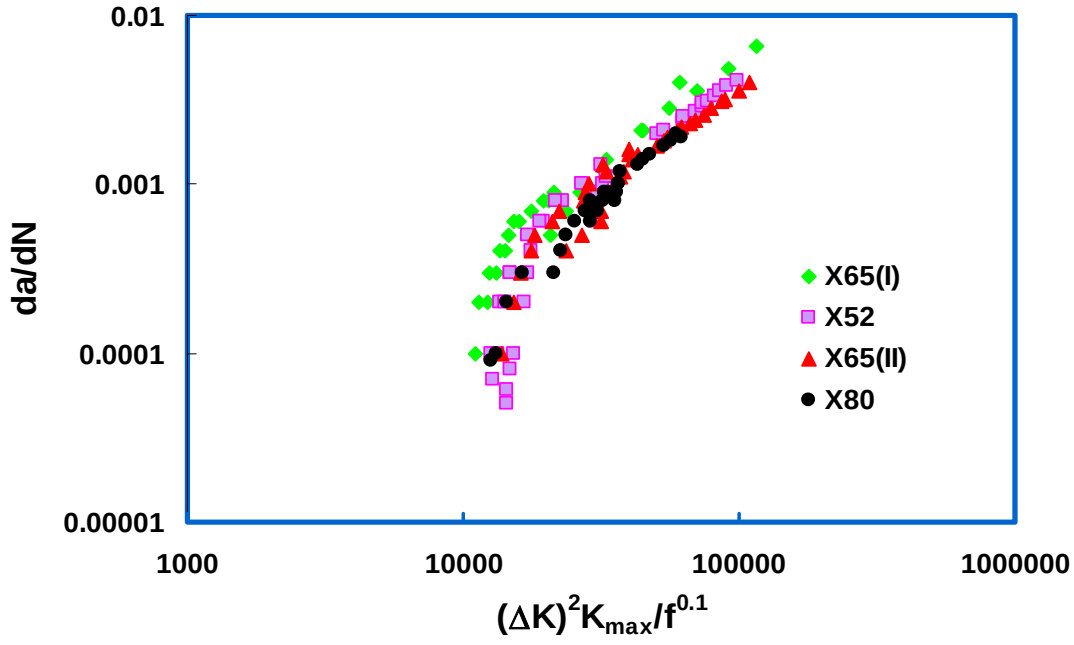

Figure 4-16: Comparison of Crack growth rate data da/dN as a function of $(\Delta K)^2 K_{max}/f^{0.1}$ for all the steels.

4.4. Corrosion Fatigue Cracking Behavior of Steels

Corrosion fatigue concepts were used to explain the relative resistance of the steels to crack growth through the corrosion fatigue combined factor, $(\Delta K)^2 K_{max}/f^{0.1}$. Corrosion fatigue is known to result from a synergistic interaction of corrosion occurrence and fatigue loading. In the present situation, fatigue crack growth can also be enhanced by hydrogen. Figure 4-17 illustrates the interaction of corrosion and fatigue and their influences on corrosion fatigue cracking including the important role played by hydrogen during the process of cracking.

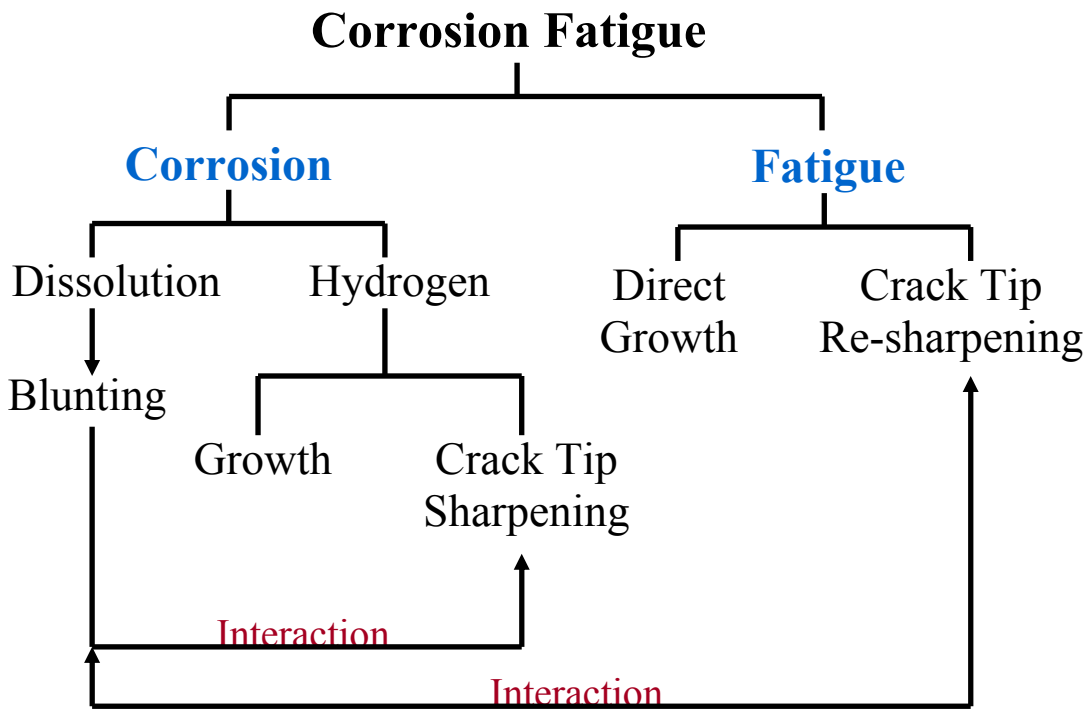

Figure 4-17: Corrosion and fatigue contributions in corrosion fatigue cracking.

Elimination of either fatigue loading or corrosion occurrence limits the occurrence of corrosion fatigue. Corrosion fatigue represents more severe cracking than fatigue cracking as a result of hydrogen contribution in the cracking process which enhances fatigue cracking by the hydrogen embrittlement effect.

Existing crack primarily tends to grow under applied cyclic loadings as the main crack growth driving force (fatigue part). Corrosion occurrence has a dual effect on the cracking process. Corrosion generates hydrogen and corrosion products as a result of the steel's dissolution. Dissolution at the crack tip may cause crack tip blunting. When corrosion products are formed in the crack crevice, crack closure due to the contact of crack faces above the minimum stress of the cycle may also occur. Both the factors would lead to a reduced crack growth rate. On the other hand generated hydrogen atoms enhance the crack growth as they diffuse into the plastic zone in front of the crack tip (triaxial stress zone) and enhance the growth of crack by embrittling the region. Toughness and ductility of steel are reduced dramatically when hydrogen is introduced to the microstructure so that cracking potential is increased and the crack can propagate easier under the same mechanical loading condition. Besides the direct hydrogen effect as indicated above, segregation of hydrogen can also directly induce micro-cracks in the plastic zone, which may propagate to the root of main crack and re-sharpen the crack if it has been blunted.

Based on the above arguments, corrosion resistance (also inversely related to hydrogen generating ability) and fatigue resistances of steels are the important factors that can define corrosion fatigue cracking resistance of steels. As hydrogen has a key role in the cracking process the amount of available hydrogen (corrosion resistance) which can contribute in cracking of steels causes major differences in cracking behavior of steels. Steels with different microstructures and different mechanical properties are expected to have different corrosion behavior (corrosion resistance) and different fatigue resistance which leads to different corrosion fatigue cracking resistance.

According to the above discussions, comparative investigation of fatigue cracking behavior in air and corrosion resistance (coupon tests) of steels can lead to some insights on corrosion fatigue crack growth and the effect of steel mechanical property and microstructure on corrosion fatigue crack growth rate.

4.5. Fatigue in Air Tests:

Mechanical conditions in fatigue in air tests were selected to be consistent with those in the tail part of corrosion fatigue curve, where hydrogen is considered to play a dominant role in cracking process. Since corrosive environment is not present in fatigue in air (α=0), the combined corrosion fatigue factor $(\Delta K)^2 K_{max}/f^{\alpha}$ is reduced to $(\Delta K)^2 K_{max}$. X52 and X80 pipeline steels were used in these tests in three different initial loading conditions in which two of them lead to the same $(\Delta K)^2 K_{max}$ initial value (Table 3-8) . As no frequency effect is included in this term, tests were conducted at different loading frequencies to investigate the effect of frequency on fatigue crack growth in air (Table 3-9).

Fatigue crack growth rate data in air were plotted as a function of frequency in Figures 4-18 and 4-19 for X52 and X80 pipeline steels respectively including initial K_{max} and ΔK of each test. It is seen that crack growth rate decreases rapidly with decreasing frequency at low frequency loading while crack growth rate is less sensitive to the change of loading frequency at high loading frequencies. These observations are consistent with the general observation that crack growth rate is not affected by loading frequency in high frequency regime. Crack growth rate data in air for both the steels were normalized by $(\Delta K)^2 K_{max}$ in an attempt to reveal the true effect of loading frequency. Plotted curves in Figures 4-20 and 4-21 show that normalized crack growth rate are also frequency dependent and substantial reduction in normalized crack growth rate can be observed when loading frequency was below 0.01 Hz.

It is believed that reduced crack growth rate is primarily due to the increased creep deformation at the tip of the crack which causes crack tip blunting. Considering the same number of loading cycles, lower loading frequencies lead to longer time period of applied loads which can lead to the occurrence of time dependent plastic deformation (creep). Creep occurrence creates excessive plastically deformed area at the tip of crack which tends to blunt the crack tip. The existent crack can turn to the situation of mechanical dormancy in these mechanical loading regimes.

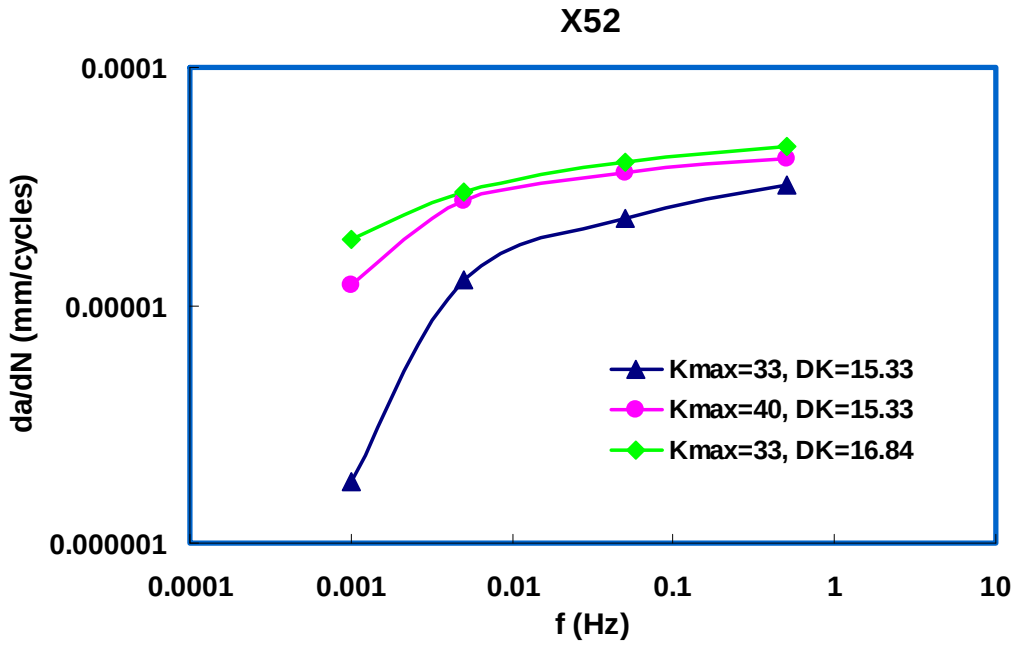

Figure 4-18: Fatigue in air crack growth rate vs. frequency for X52 pipeline steel.

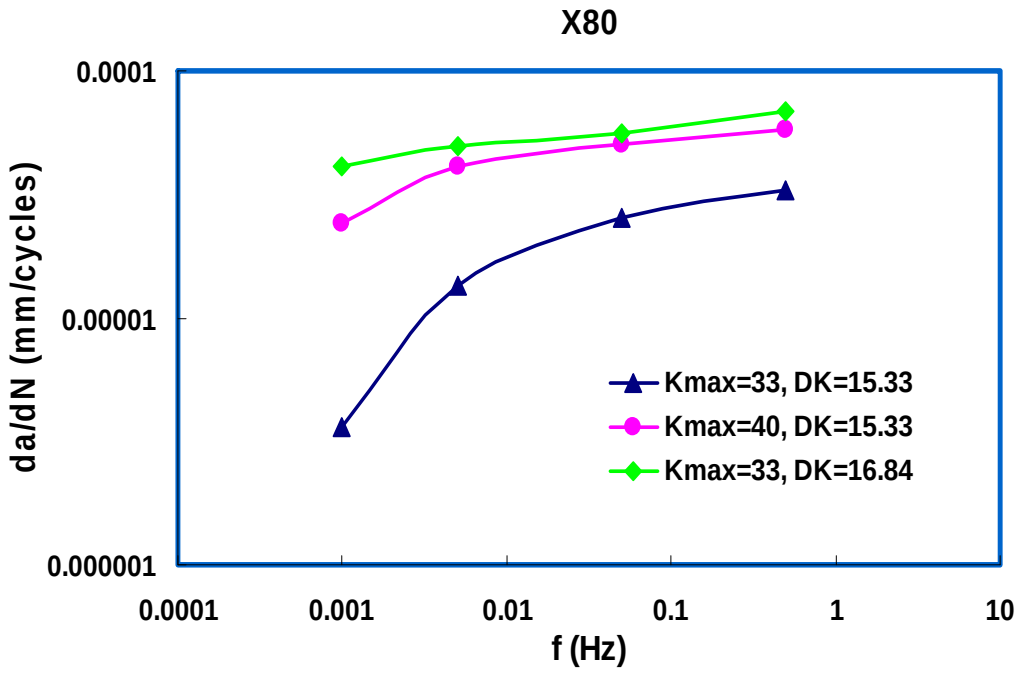

Figure 4-19: Fatigue in air crack growth rate vs. frequency for X80 pipeline steel.

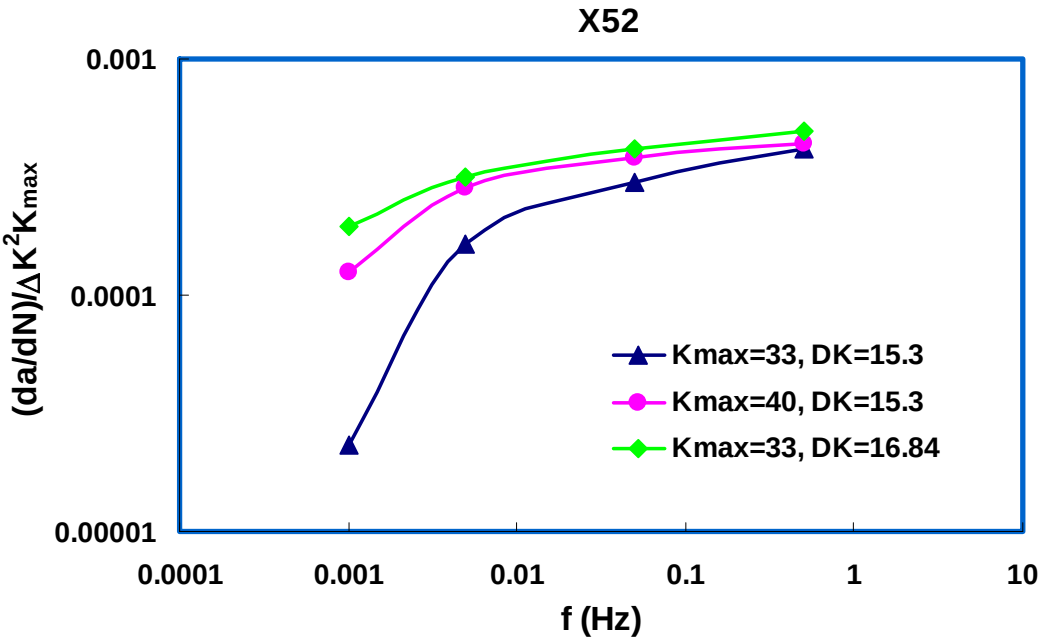

Figure 4-20: Normalized fatigue in air crack growth rate vs. frequency for X52 pipeline steel.

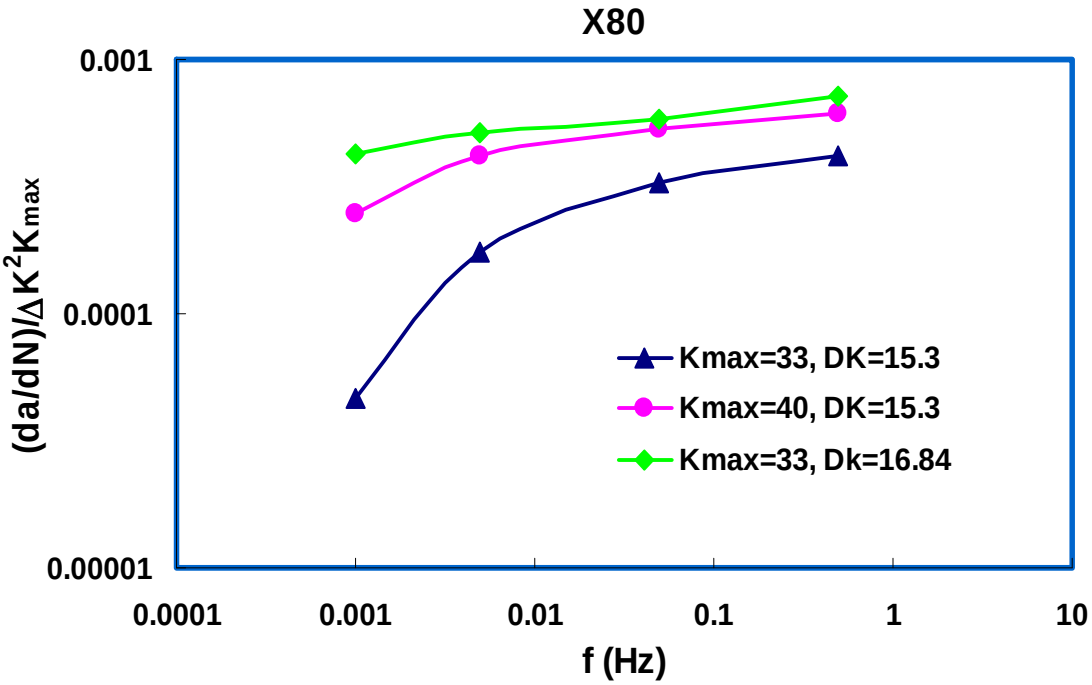

Figure 4-21: Normalized fatigue in air crack growth rate vs. frequency for X80 pipeline steel.

4.6. Hydrogen Effects

As seen in Figures. 4-18 – 4-21, crack growth rate in air are lower than the corrosion fatigue crack growth rates of the same loading conditions by one order of magnitude which is believed to be the result of hydrogen atoms contribution in corrosion fatigue cracking process. It was also seen that fatigue crack growth rates in air and corrosion fatigue crack growth rates have opposite dependence to the loading frequency. The crack growth rate in near neutral pH environments for all steels could be well rationalized by $(\Delta K)^2 K_{max}/f^{\alpha}$ which indicates an increase of crack growth rate with decreasing loading frequency while fatigue crack growth rate in air decreases with decreasing loading frequency. This inconsistency clearly suggests the presence of two competitive processes concurrently occurring during corrosion fatigue of pipeline steels in near neutral pH environments.

One of the competitive processes, as defined in previous section, is the mechanical dormancy arising from crack tip blunting by low temperature creep. The other process is known to be related to the hydrogen effects. In corrosion fatigue cracking hydrogen atoms diffuse to the plastically deformed area at the crack tip mainly during the loading period rather than unloading period to have their effect on cracking, for example, to re-sharpen blunted crack tip caused by low temperature creep. A higher loading-unloading rate allows less hydrogen to diffuse to the crack tip so that the effect of hydrogen (corrosive environment) will become minor in high frequency loading conditions. It should be noted that the small tails observed in the region with high $(\Delta K)^2 K_{max}/f^{\alpha}$ loading should be primarily related to the time period required for achieving hydrogen equilibrium throughout the CT specimen.

Using the above discussion, the corrosion fatigue curves of steels as normalized by $(\Delta K)^2 K_{max}/f^{\alpha}$ can be better understood. Corrosion fatigue curves are featured with a liner stage at the high combined factor. This represents a mechanically driven process, in which mechanical loading is aggressive enough to prevent the occurrence of mechanical dormancy. The presence of hydrogen in the steel under the loading condition has simply enhanced the crack growth rate. The long tailed

region at the intermediate combined factor reflects the competitive situation between the mechanical dormancy and the hydrogen-assisted cracking.

It was shown by Chen et al [25] that the $(\Delta K)^2 K_{max}/f^{0.1}$ combined factor can define the boundary of growth and dormancy. It was revealed that any combination of K_{max}, ΔK and f which results in lower $(\Delta K)^2 K_{max}/f^{0.1}$ value than the threshold value leads to crack dormancy. This situation can be explained as a benign mechanical loading situation which leads to mechanical dormancy and even hydrogen assisted cracking cannot make the crack growth occur. At slightly higher combined factors than threshold values competitive situation between the mechanical dormancy and the hydrogen-assisted cracking starts, which can be represented as a dormant growth region. When hydrogen is absent in the material in this region, the current mechanical loading should lead to the occurrence of mechanical dormancy. However, the presence of hydrogen has enhanced the aggressiveness of the mechanical loading, so that crack growth can be possible, probably at some selected locations, for example, the weakest links in the plastic zone, such as pearlite-ferrite interfaces, grain boundaries, and inclusions (microstructural effects). In this situation a total dormancy will not occur and crack tip is frequently in transition between the blunted and sharp conditions which leads to very low crack growth rates in near neutral pH environments.

Figure 4-22 represents the crack growth curves of X65(I) and X65(II) pipeline steels in dormant growth region obtained from test 9 (Table 3-3), which had an initial combined factor slightly higher than the threshold value. In this test, X65(I) and X65(II) pipeline steels were exposed to the corrosive solution (C2) for a long time (almost 90 days) while cyclic loads were applied to them. It was seen that X65(II) represents a continuous slow growth rate which led to a total crack growth of less than a millimetre. On the other hand an increase in growth rate was seen in X65(I) after almost 42 days of exposure. Crack growth rate data obtained from the growth curves of these steels were plotted in Figures 4-23 and 4-24 using $(\Delta K)^2 K_{max}/f^{0.1}$ combined factor. It is noted that growth behaviour of X65(I) is consisted with its obtained growth curve in previous test as the growth data join the main curve as $(\Delta K)^2 K_{max}/f^{0.1}$ increases.

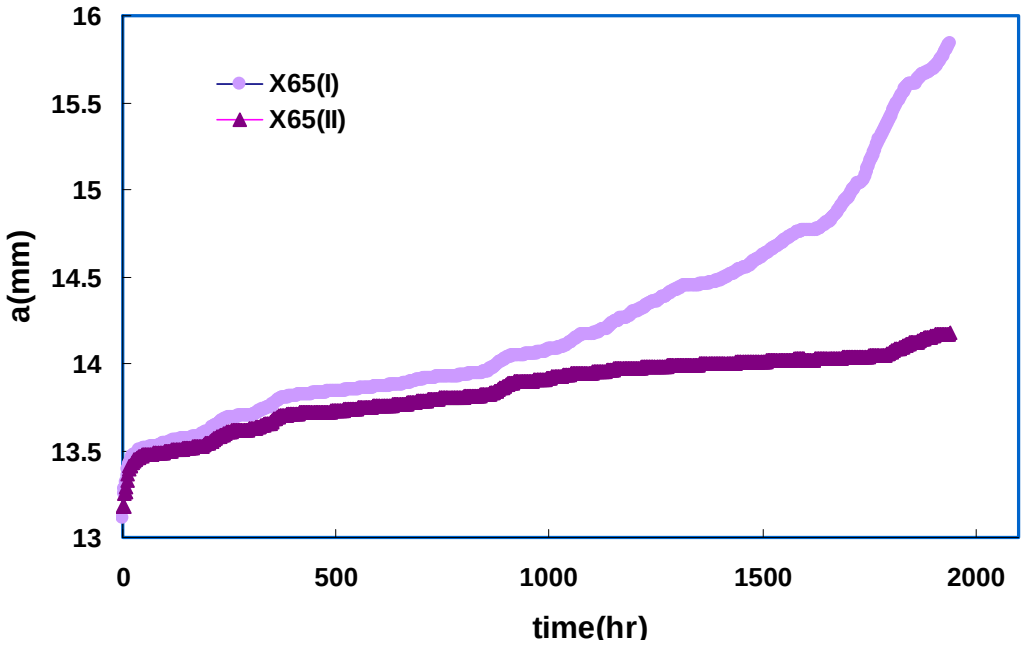

Figure 4-22: Crack size vs. time (Hr) curves for X65(I) and X65 (II) in low loading condition (test 9).

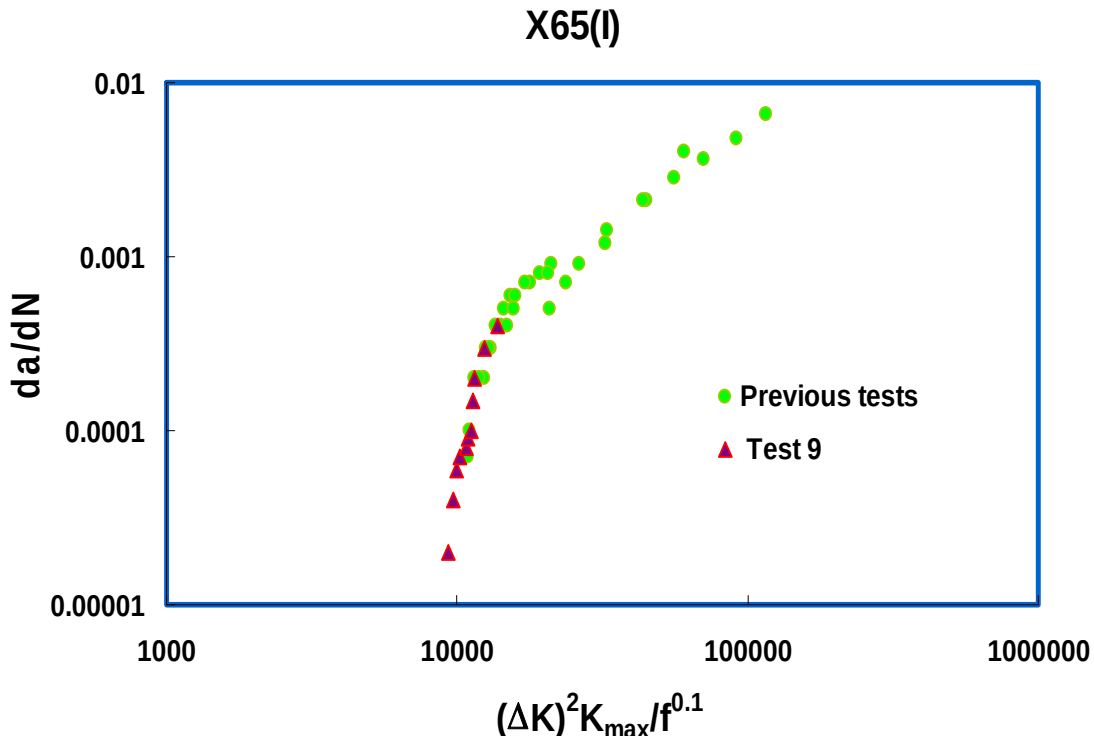

Figure 4-23: Dormant growth crack growth rate data da/dN vs. $(\Delta K)^2K_{max}/f^{0.1}$ for X65(I) pipeline steel.

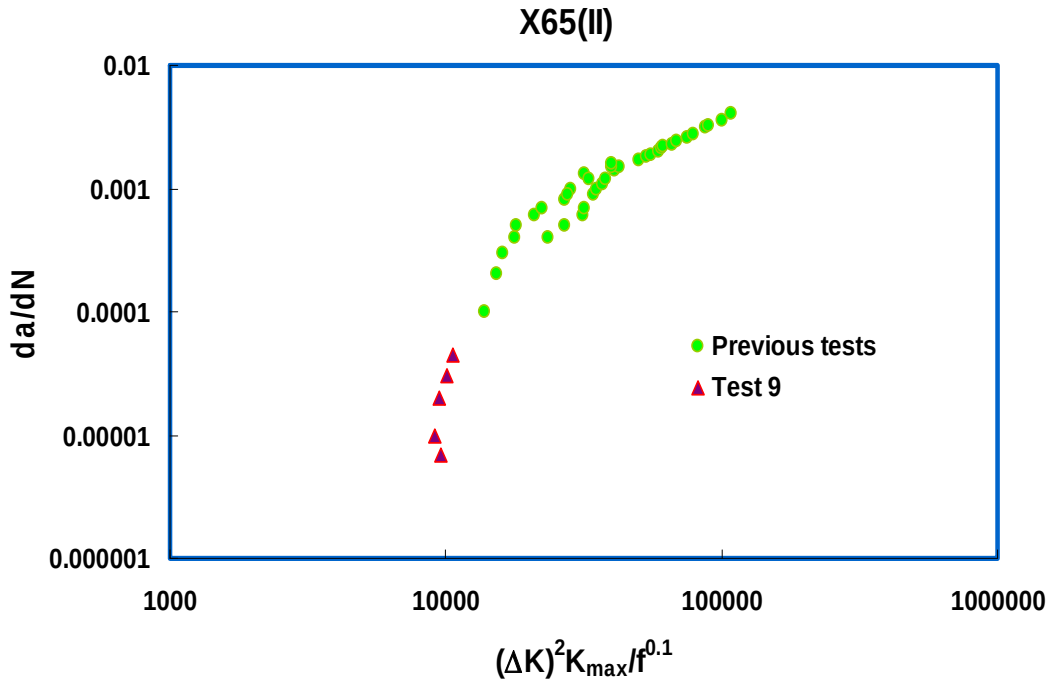

Figure 4-24: Dormant growth Crack growth rate data (da/dN) vs. $(\Delta K)^2K_{max}/f^{0.1}$ for X65(I) pipeline steel.

The increase in crack growth rate of X65(I) pipeline steels is related to its microstructure (pearlite phases) as a result of increased probability of cracking at selected regions of structure (weakest links in the plastic zone) such as pearlite-ferrite interfaces which was mentioned before.

Figure 4-25 represents the cross section image of X65(I) pipeline steels sample tested in test 9. A branched crack seen in the picture is a evidence of crack growth difficulty due to lack of desirable crack growth paths but it can be seen in Figure 4-26 that transgranular crack started to grow from the branched tip which was related to the presence of pearlite phase and local corrosion (hydrogen generation) in its interface with the matrix.

The same test was repeated (test 10) using X80 and X52 pipeline steels. Dormant growth behaviour was seen in cracking behaviour of both steels in this region which led to very low crack growth rate of less than 0.2 mm in almost 105 days (Figures 4-27 and 4-28).

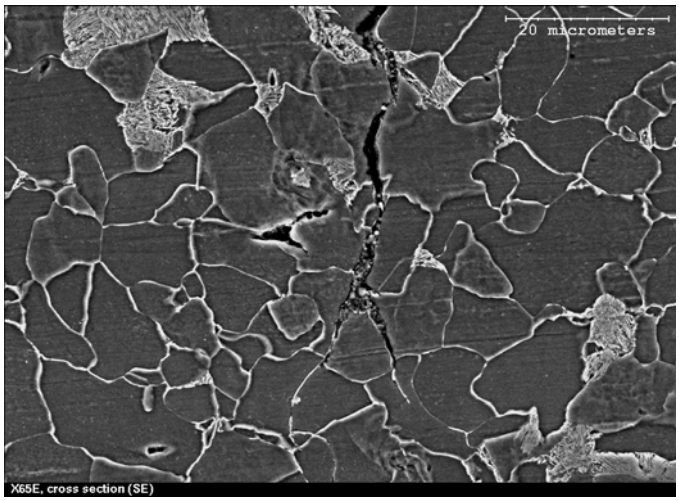

Figure 4-25: SEM picture of a crack which was propagated in X65(I) pipeline steel.

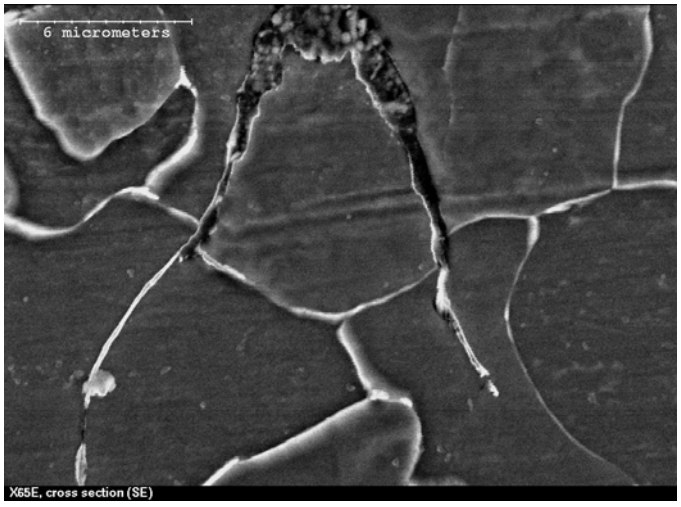

Figure 4-26: SEM picture of a crack which was propagated in X65(I) pipeline steel.

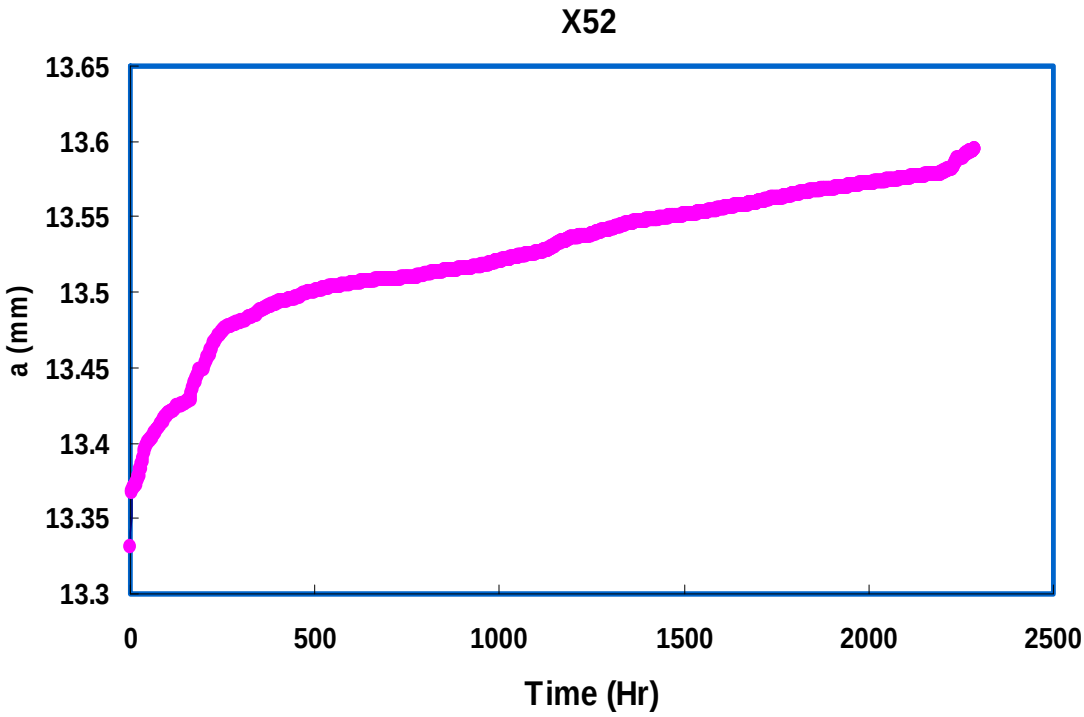

Figure 4-27: Crack length change vs. time for X52 pipeline steel.

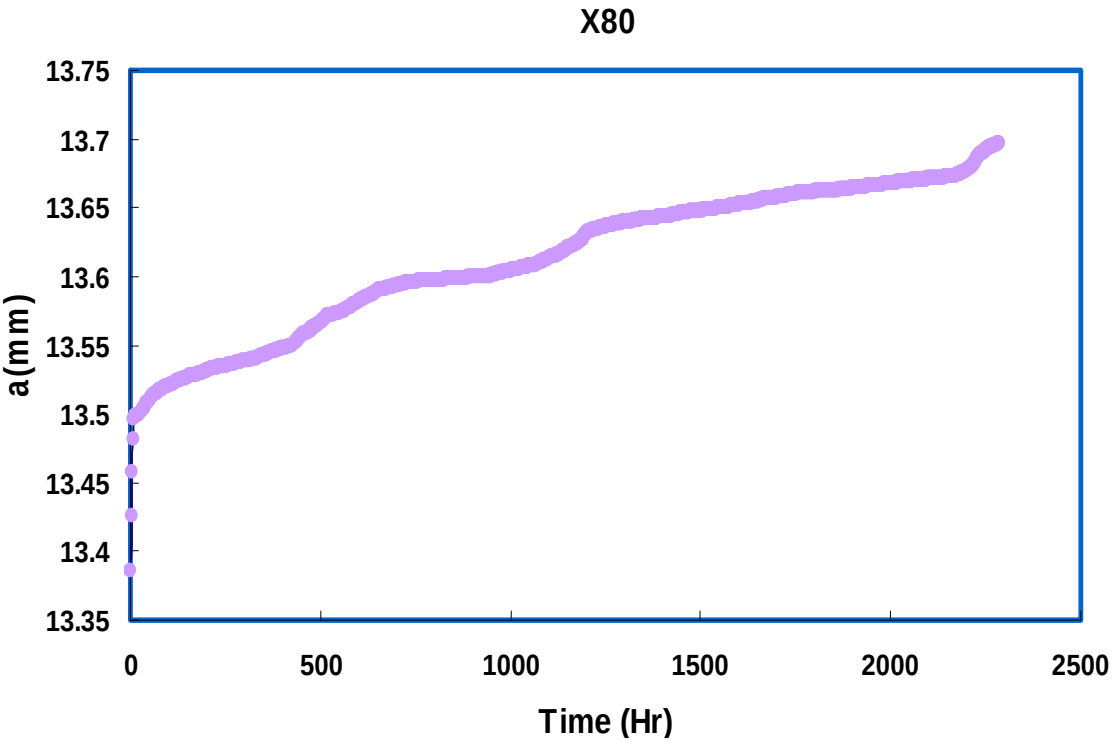

Figure 4-28: Crack length change vs. time for X80 pipeline steel.

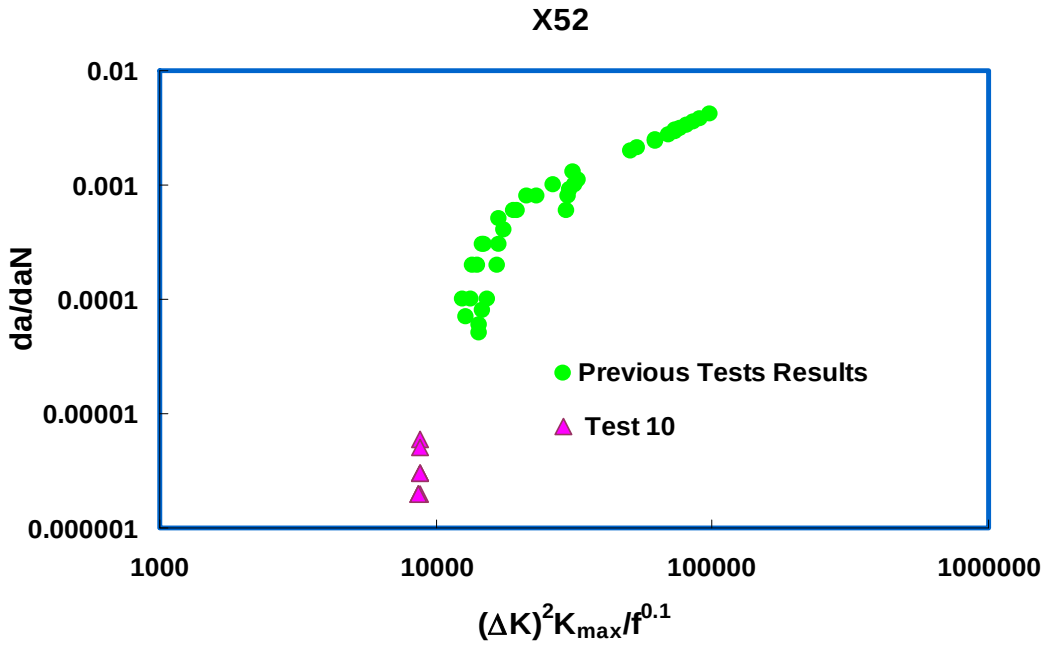

Figure 4-29: Dormant growth crack growth rate (da/dN) vs. $(\Delta K)^2K_{max}/f^{0.1}$ for X52 pipeline steel.

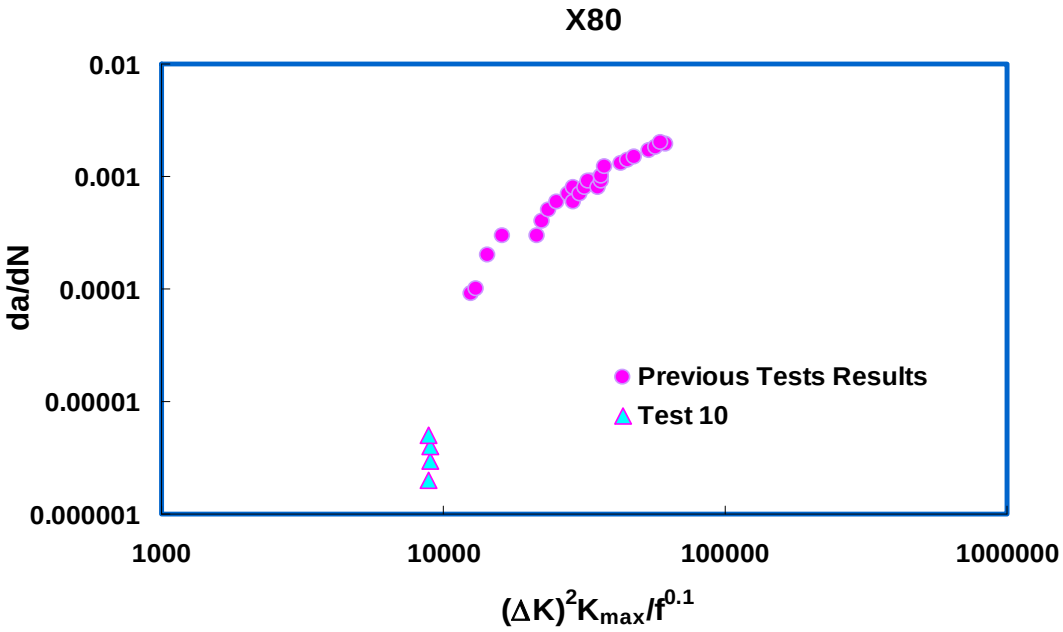

Figure 4-30: Dormant growth crack growth rate (da/dN) vs. $(\Delta K)^2K_{max}/f^{0.1}$ for X80 pipeline steel.

Crack growth rate data obtained from test 10 were plotted vs. $(\Delta K)^2 K_{max}/f^{0.1}$combined factor in figures 4-29 and 4-30 representing the dormant growth region. Cross section image of a crack which was propagated in X80 pipeline steel in dormant growth region (test 10) can be seen in figure 4-31. The competitive growth and dormancy occurred in dormant growth region can be clearly seen in this figure. It can be seen that crack reaches a pit-like region where its tip can become blunted and crack dormancy is probable to occur but it restarted its growth from the bottom of the pit.

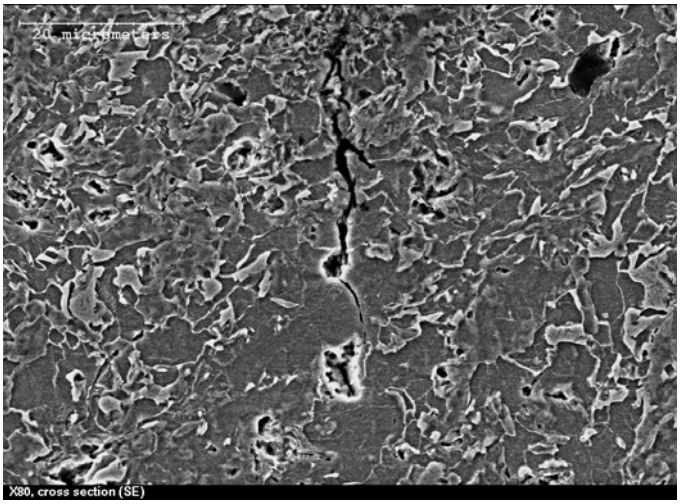

(a)

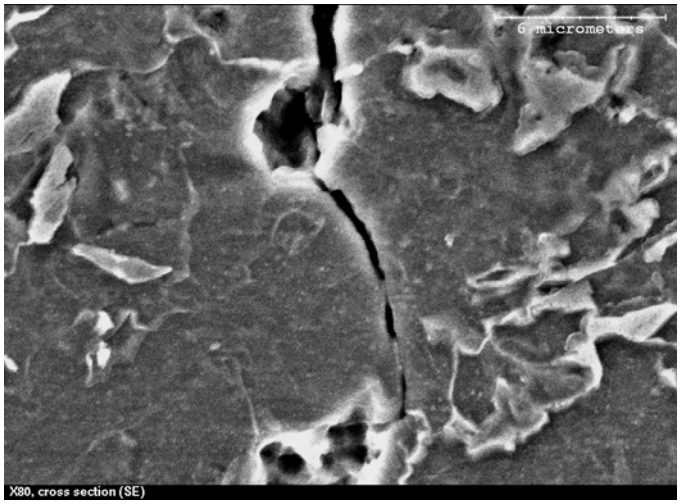

(b)

Figure 4-31: Dormant growth crack growth rate (da/dN) vs. $(\Delta K)^2 K_{max}/f^{0.1}$ for X52 pipeline steel.

The great role of hydrogen in corrosion fatigue cracking of pipeline steels in near neutral pH environments was revealed according to the above discussion. It can be concluded that corrosion occurrence and hydrogen generating ability of steels should be considered as a key point in explaining the crack growth rate ordering of steels.

4.7. Steel Dependence of Corrosion Fatigue Crack Growth Rate

Crack growth rate of each steel could be well rationalized by $(\Delta K)^2 K_{max}/f^{\alpha}$ combined factor and hydrogen effects on cracking could also be well explained. Corrosion fatigue crack behaviour of pipeline steels in near neutral pH environments as expressed using $(\Delta K)^2 K_{max}/f^{\alpha}$ combined factor will be further discussed in terms of their mechanical properties and microstructures.

As all the steels were tested in the same mechanical loading conditions, their corrosion resistances should be compared as a factor revealing the amount of hydrogen assistance for cracking. Figures 4-2 and 4-3 illustrate the comparative corrosion resistance of steels in terms of their weight loss with time. It can be seen that the relative corrosion resistance of X65(I), X52 and X65(II) in terms of weight loss is in the same order as their corrosion fatigue crack resistance measured by corrosion fatigue growth rates, that is, lower corrosion resistance would result in higher crack growth rate. However, X80 has the lowest corrosion resistance (highest corrosion rate) while it represents the lowest corrosion fatigue crack growth rate among the steels.

This inconsistency can be explained referring to the fact that weight loss represents the corrosion occurrence on the surface of the samples, and the amount of hydrogen generated at the surface (source of hydrogen atoms). It should be noted that hydrogen atoms contribute to cracking only when they can diffuse through the steel to reach the crack tip. Hydrogen atoms can be trapped in microstructural defects such as voids, grain boundaries, inclusions or second phase particles interfaces as they diffuse through the steels. Therefore, the amount

of hydrogen that can be directly related to cracking should depend on both the steels corrosion resistance (hydrogen source) and its microstructure (hydrogen diffusion path).

Environmental influences on corrosion fatigue crack growth behaviour is reflected by α values in $(\Delta K)^2 K_{max}/f^{\alpha}$ combined factor. In other words, α values reflect the combined effect of the steel's corrosion resistance and microstructures on their corrosion fatigue crack growth behaviour. Based on this discussion, mechanical factors influencing crack growth were neglected and crack growth rate data of all steels were normalized to the single crack growth curve of X65(I) as a reference (α=0.1) by introducing individual new α values to different steels (Figure 4-32).

As all the steels were tested in the same corrosive solution (C2), different α values of steels represents different hydrogen contribution in cracking of steels due to their different corrosion resistance and microstructures. New α values and corrosion rates (weight loss tests) of steels were shown in Table 4-2 in the order of their crack growth rates. It is seen that α values are consistent with crack growth rate orders as X65(I) has the highest α value and X80 has the lowest α value regardless of its highest corrosion rate. It can be concluded that although X80 has the highest amount of available diffusible hydrogen on its surface less amount of hydrogen atoms will contribute in its cracking due to its micrsotrucral effects on hydrogen diffusion.

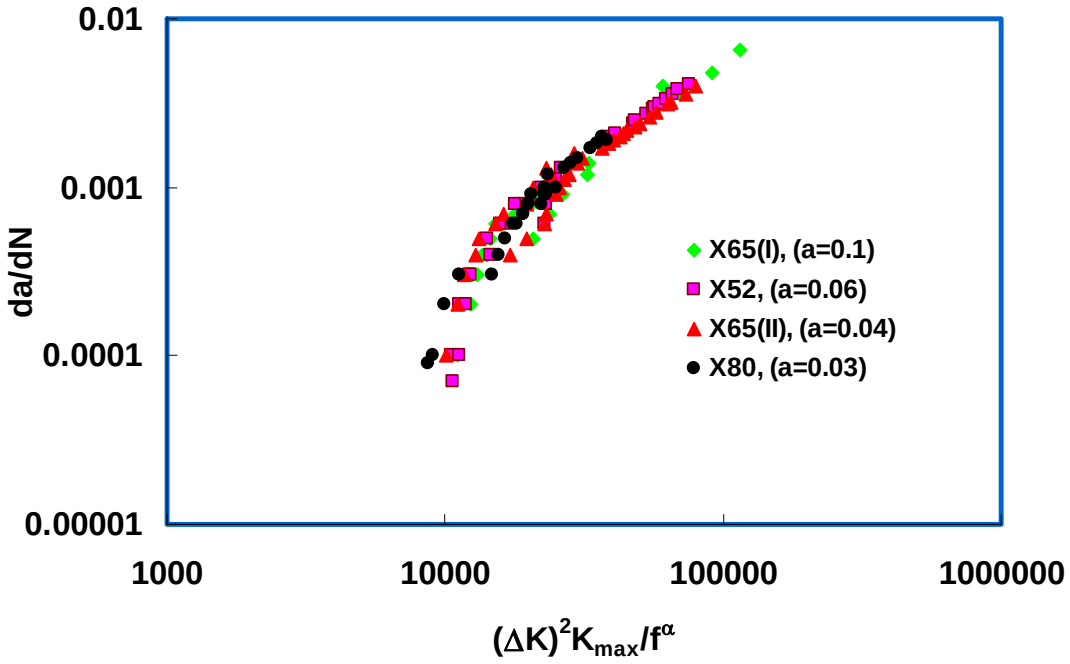

Figure 4-32: New α value of steels resulting in obtaining same crack growth curves.

Table 4-2: Environmental factors (α) and corrosion rates of different steels.

Steels	Environmental Factor (α)	Corrosion rates gr.mm^2/days
X65(I)	0.1	4×10^{-6}
X52	0.06	3×10^{-6}
X65(II)	0.04	3×10^{-6}
X80	0.03	5×10^{-6}

4.8. Microstructure Effect

Steel's microstructure has a great influence on its corrosion fatigue crack growth behaviour. It is believed that steels with more uniform microstructures have higher cracking resistance. This is related to the influence of steels microstructure on hydrogen diffusion. Hydrogen atoms can be trapped in microstructure obstacles with strong affinity with hydrogen such as voids, dislocations, grain boundaries and second phases or particles interfaces with the matrix. High dislocation density in grain boundaries due to lattice mismatch generates welcoming distorted areas for hydrogen atoms to diffuse in. The same role applies to interface of second phases or particles with the matrix. The probability of hydrogen trapping in second phases interfaces with matrix is even higher when the steels are under external stresses. Microplastic deformations can occur in the interfaces due to different formability and mechanical properties of phases. Plastically deformed areas are known as other plausible spots for hydrogen atoms to be trapped in due to the locally increased distortion and dislocation density.

Second phases and particles present in the microstructure can also increase the amount of hydrogen atoms generation in the microstructure locally. Different phases and particles can make local galvanic corrosion cells when they are exposed to the corrosive solution as an electrolyte due to their different chemical properties. Iron dissolution and hydrogen generation can result from the generated galvanic cells which increases local hydrogen concentration in the microstructure.

The balance of the above effects represents the hydrogen diffusion and trapping pattern in different steels. Considering this pattern and the initial available amount of diffusible hydrogen on the samples surface (hydrogen source) of different steels (weight loss tests) comparative amount of hydrogen atoms which can be present at the tip of a crack propagated in steel's microstructure to have contribution in cracking procedure can be predicted.

X65(I) has the most un-uniform microstructure due to presence of pearlite structures in the ferritic matrix of its microstructure (Figure 4-1). Presence of pearlite structure can be responsible for X65(I)'s lowest corrosion fatigue cracking resistance which leads to its highest crack growth rate (Figure 4-16). Pearlite has higher hardness and lower formability compared to its surrounding ferrite so that microplastic deformation occurs at pearlite-ferrite interfaces under the applied cyclic stresses. In addition to the available diffused hydrogen atoms in the microstructure, hydrogen atoms generated from galvanic corrosion between pearilte and ferrite can also be trapped in the plastically deformed region in their interfaces. As a result, pearlite-ferrite interfaces turn to be potent and plausible spots for crack growth. Figure 4-33 shows the cross section SEM image of a crack in X65(I) pipeline steel (Test 3). It can be seen that the crack, which was propagated in ferrite regions, tended to change its growth path through the region where pearlite is present due to high amount of hydrogen atoms present in that region which facilitates the crack growth by hydrogen embrittlement effect.

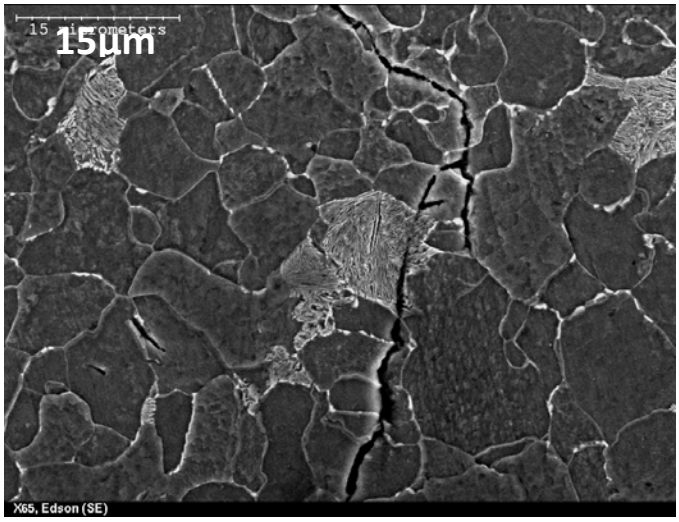

Figure 4-33: SEM picture of a crack which was propagated in X65(I) pipeline steel.

Figure 4-34 shows SEM picture taken from tip of a crack which was propagated in X65(I) pipeline steel's sample. A sharp crack tip which can be seen in this picture represents the high amount of hydrogen atoms present in the microstructure. It was mentioned before that hydrogen atoms are known as a crack tip re-sharpeners as they can generate new desirable paths for a blunted crack to grow due to their embrittlement effect. High amount of hydrogen atoms in the microstructure helps the crack tip to remain sharp so that the crack can grow easily. High amount of hydrogen atoms available in X65(I)'s microstructure to contribute in cracking process lead to its highest crack growth rate which is consistent with its highest comparative α value.

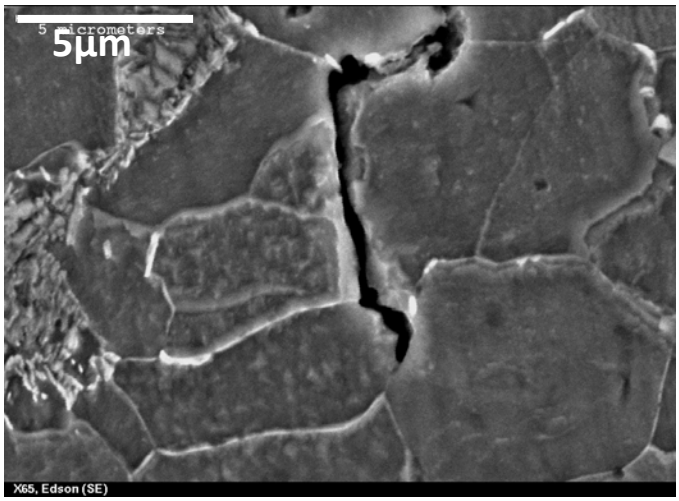

Figure 4-34: SEM picture of a crack tip in X65(I) pipeline steel specimen.

X52, X65(II) and X80 pipeline steels have more uniform microstructure than X65(I). Microstructure of these steels contains dispersed carbides in a ferritic matrix. Low possibility of localized corrosion occurrence in these steel's microstructures, makes diffused hydrogen atoms from the surface to be known as dominant hydrogen atoms portion which contribute in cracking process. On the other hand, grain boundaries are known as the dominant hydrogen trapping sites in these steels microstructures. Steels grain sizes can define their comparative hydrogen trapping ability in their microstructures. Smaller grain sizes leads to longer grain boundaries and increased hydrogen trapping sites in microstructure.

X52 and X65(II) pipeline steels represent lower amount of available diffusible hydrogen than X65(I) as a result of their lower corrosion rate (weight loss test). This can explain their lower crack growth than X65(I) as less amount of hydrogen atoms contribute in cracking procedure in these steels than X65(I). A crack which was propagated in X52 pipeline steels is seen in Figure 4-35. Crack tip branching which was occurred during cracking procedure represents crack growth difficulties that can be related to the low amount of hydrogen present in the microstructure to build plausible growth regions so that branching occurs with the goal of finding the best growth path.

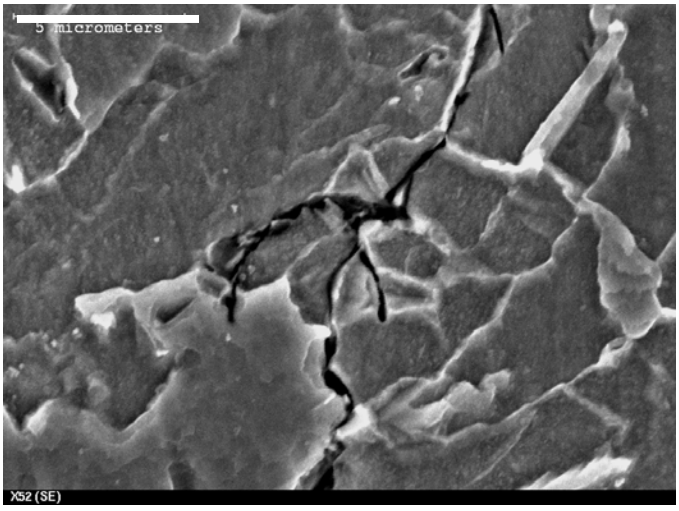

Figure 4-35: SEM picture of crack which was propagated in X52 pipeline steel.

Lower crack growth rate of X65(II) than X52 can also be explained using the above scenario. It can be expected that less amount of hydrogen atoms contribute in cracking process of X65(II) as it has smaller source of hydrogen as a result of its lower corrosion rate (Weight loss tests). X65(II) also has more trapping sites inside its microstructure (lower grain size and longer grain boundary area) compared to X52 pipeline steels where diffused hydrogen atoms can be trapped in instead of reaching to the crack tip to contribute in cracking procedure.

X80 represents lowest crack growth rate while it has the highest corrosion rate among the steels used in this research. This can be related to X80's lowest grain size. It was seen in figure 4-1 that X80 has a very fine grain microstructure and it has the lowest grain size among the steels which results in having the longest grain boundary area. It can be concluded that a great majority of hydrogen atoms which were diffused through X80 will be trapped in the microstructure (grain boundaries) and little portion of generated hydrogen on the surface reaches the crack tip to contribute in cracking process. As a result X80, represents lowest crack growth rate which is consistent with its lowest α value (Table 4-15) as a factor which reflects the amount of hydrogen contributes in cracking procedure considering both hydrogen generating ability of steel and steels microstructures hydrogen trapping ability.

5. Conclusions:

This work has focused on the cracking behavior of pipeline steels in near-neutral pH environment (C2 solution) using $(\Delta K)^2K_{max}/f^{\alpha}$ combined factor to investigate the dependence of crack growth behavior to the microstructure and mechanical properties of steels. Firstly several tests were done to obtain the growth curve of all the steels. The growth rates were compared and growth rates ordering of steels were further investigated by doing separate fatigue in air tests and weight loss corrosion coupon tests. The following is a list of the conclusions of this work:

1. Crack growth behavior of pipeline steels in near neutral pH environments is consistent with the behavior of corrosion fatigue cracking.

2. Crack growth in near neutral pH environments can be well rationalized by a combined factor, $(\Delta K)^2K_{max}/f^{\alpha}$, which reflects the synergistic interaction between the mechanical driving force and hydrogen effects.

3. Hydrogen plays a decisive role in terms of crack growth in pipeline steels exposed to near neutral pH environments.

4. $(\Delta K)^2K_{max}/f^{0.1}$ combined factor can define the boundary of growth and dormancy. Any combination of K_{max}, ΔK and f which results in lower $(\Delta K)^2K_{max}/f^{0.1}$ value than the threshold value leads to crack dormancy. This situation can be explained as a benign mechanical loading situation which leads to mechanical dormancy.

5. At slightly higher combined factors than threshold values competitive situation between the mechanical dormancy and the hydrogen-assisted cracking starts, which is represented as a dormant growth region.

6. In the situation which results in high $(\Delta K)^2 K_{max}/f^{0.1}$ mechanically driven process controls the cracking procedure and hydrogen atoms just enhance the crack growth.

7. Crack growth behaviour of pipeline steels in near neutral pH environments is material dependent.

8. Steel's microstructure has a great influence on its cracking behaviour. Steels with more uniform microstructure represent higher crack growth resistance.

9. Hydrogen atoms which can contribute in cracking procedure can be trapped in microstructural defects such as voids, grain boundaries, inclusions or second phase particles interfaces as they diffuse through the steels.

10. Higher crack growth rate will result in the steel in which higher amount of hydrogen atoms can be provided to the tip of a crack propagating in the microstructure.

11. X65(I) represents highest crack growth rate. Presence of pearlite structure in X65(I)'s microstructure increases hydrogen content of its microstructure by generating local pearlite-ferrite galvanic corrosion cells.

12. X80 represents lowest crack growth rate. Fine grain sizes in X80's structure provides long grain boundary areas where hydrogen atoms can trap in result in decreased amount of hydrogen atoms contributing in cracking process at the crack tip.

References:

[1] Anderson, T. L. “Fracture Mechanics: Fundamentals and Applications”, 3rd edition, Boca Raton, FL: CRC Press, (2005).

[2] Ramsamooj, D. V., and T. A. Shugar. "Modeling of Corrosion Fatigue in Metals in an Aggressive Environment" International Journal of Fatigue, Supplement 1 (2001): 301-9.

[3] Jones, D. A. “Principles and Prevention of Corrosion”, 2nd edition, Upper Saddle River, NJ: Prentice Hall, (1996).

[4] Fang, B. Y., Atrens, A., Wang, J. Q., Han, E. H., Zhu, Z. Y. and Ke, W. "Review of Stress Corrosion Cracking of Pipeline Steels in “low” and “high” pH Solutions." Journal of Materials Science, Vol. 38, No. 1 (2003): 127-32.

[5] National Energy Board, “Report of the Inquiry Concerning Stress Corrosion Cracking on Canadian Oil and Gas Pipelines”, (1996).

[6] Colwell, J. A., Leis, B. N. and Singh. P. M., "Crack Initiation of Line Pipe Steels in Near-Neutral pH Environments" Environment-Induced Cracking of Materials, Ed. S.A. Shipilov, et al. (2008): 233-242.

[7] Parkins, R.N., “Stress Corrosion in Buried Pipelines”, TCPL, (1990).

[8] Beavers, J. A., and Harle, B. A. "Mechanisms of High-pH and Near-Neutral-pH SCC of Underground Pipelines", Journal of Offshore Mechanics and Arctic Engineering, Vol.123 No.3 (2001): 147-152.

[9] Fang B., Han E., Zhu Z., Wang J., Ke W. "Stress Corrosion Cracking of Pipeline Steels", Journal of Materials Science and Technology, Vol. 18, No. 1 (2002): 3-6.

[10] Parkins, R.N., "Environment Sensitive Cracking of High-Pressure Pipelines in Contact with Carbon-Dioxide-Containing Solutions", AGA (1992): 61-66.

[11] Parkins, R.N., Blanchard, W.K.J. and Delanty, B.S. Corrosion 50, (1994) p. 394.

[12] CEPA, Submision to the National Energy Board. 1996.

[13] Parkins, R.N. Blanchard Jr., W.K. and Delanty, B.S. "Transgranular Stress Corrosion Cracking of High-Pressure Pipelines in Contact with Solutions of Near Neutral pH.", NACE International, Corrosion, Vol.50, No. 05 (1994): 394-408.

[14] Troiano, A. R., "The Role of Hydrogen and Other Interstitials in the Mechanical Behavior of Metals", Trans. Soc. Metall. 52, (1960): 54-80.

[15] Chattoraj, I. "The Effect of Hydrogen Induced Cracking on the Integrity of Steel Components." Sadhana, Vol. 20, No. 1, (1995): 199-211.

[16] Zapffe, C. A., Sims, C. E., "Hydrogen Embrittlement Internal Stress and Defects in Steels", Trans. Am. Inst. Metall. Eng. 145, (1941): 225-259.

[17] Been, J., King, F., Sutherby, R., “Environmentally Assisted Cracking of Pipeline Steels in Near-Neutral pH Environments”, Environment-Induced Cracking of Materials, (2008): 221-230.

[18] Harle, B. A., and Beavers, J. A., “Low-pH Stress Corrosion Crack Propagation in API X-65 Line Pipe Steel”, Corrosion, Vol. 49, No. 10, (1993): 861-863.

[19] Asher, S. L. and Singh, P. M., "Role of Stress in Transgranular Stress Corrosion Cracking of Transmission Pipelines in Near-Neutral pH Environments" Corrosion, Vol. 65, No. 2, (2009): 79-87.

[20] Li, X. C., Eadie, R. L. and Luo, J. L., “Influence of Plasticity on Corrosion and Stress Corrosion Cracking Behavior in Near Neutral pH Environment”, Corrosion Engineering, Science and Technology, Vol. 43, No. 4, (2008): 297-303.

[21] Van Boven, G., Chen, W. and Rogge, R., "The Role of Residual Stress in Neutral pH Stress Corrosion Cracking of Pipeline Steels Part I: Pitting and Cracking Occurrence", Acta Materialia Vol. 55, No.1, (2007): 29-42.

[22] Chen, W., Van Boven, G., and Rogge, R., "The Role of Residual Stress in Neutral pH Stress Corrosion Cracking of Pipeline Steels – Part II: Crack Dormancy" Acta Materialia, Vol. 55 No.1, (2007):43-53.

[23] Qiao, L. J., Luo, J. L., and Mao, X., "The Role of Hydrogen in the Process of Stress Corrosion Cracking of Pipeline Steels in Dilute Carbonate-Bicarbonate Solution", Journal of Materials Science Letters, Vol. 16, No. 7, (1997): 516-20.

[24] Wang, S., Zhang, Y., and Chen, W., "Room Temperature Creep and Strain-rate-Dependent Stress-Strain Behavior of Pipeline Steels", Journal of Materials Science, Vol. 36, No. 7, (2001): 1931-1938.

[25] Chen, W., Eadie, R. L. and Sutherby, R. L. "Environmental Effects on Near-Neutral pH Stress Corrosion Cracking in Pipelines." Environment-Induced Cracking of Materials, (2008): 211-220.

[26] Chen, W., King, F., Jack, T. R. and Wilmott, M. J., "Environmental Aspects of Near-Neutral pH Stress Corrosion Cracking of Pipeline Steel", Metallurgical and Materials Transactions A, Vol. 23, No. 5 (2002): 1429-36.

[27] Chen, W., and Sutherby, R. L., "Crack Growth Behavior of Pipeline Steel in Near-Neutral pH Soil Environments", Metallurgical and Materials Transactions A, Vol. 38, No. 6 (2007): 1260-1268.

[28] Been, J., Lu, H., King, F., Jack, T., and Sutherby, R., "The Role of Hydrogen in EAC of Pipeline Steels in Near-Neutral pH Environments" Environment-Induced Cracking of Materials, (2008): 255-266.

[29] Cialone, H. J., and Holbrook, J. H., "Effects of Gaseous Hydrogen on Fatigue Crack Growth in Pipeline Steel", Metallurgical Transactions A, Vol. 16, No. 1 (1985): 115-22.

[30] Gu, B., Luo, J., and Mao, "Hydrogen-Facilitated Anodic Dissolution-Type Stress Corrosion Cracking of Pipeline Steels in Near-Neutral pH Solution", Corrosion, Vol.55, No. 1, (1999): 96-106.

[31] Chen, W., Kania, R., Worthingham, B. and Van Boven, G., "Transgranular Crack Growth in the Pipeline Steels Exposed to Near-Neutral Soil Aqueous Solutions – Role of Hydrogen", Acta Materialia, 57, 2009, pp. 6200-6214.

[32] Chu, R., Chen, W., Wang, S., King, F., Jack, T. R., and Fessler, R. R., "Microstructure Dependence of Stress Corrosion Cracking Initiation in X-65 Pipeline Steel Exposed to a Near-Neutral pH Soil Environment", Corrosion, Vol. 60, No. 3 (2004): 275-83.

[33] Kushia, T., Nose, K., Asahi, H., Kimura, M., Yamane, Y., Endo, S., and Kawano, H., "Effects of Metallurgical Factors and Test Conditions on Near Neutral pH SCC of Pipelines Steels", Corrosion, (2001): Paper No. 01213.

[34] Bulger, J. T., Lu, B. T., Luo, J. L., "Microstructural Effect on Near-Neutral pH Stress Corrosion Cracking Resistance of Pipeline Steels" Journal of Materials Science, Vol. 41, No. 15, (2006): 5001-5005.

[35] Martínez-Madrid, M., Chan, S. L. I., Charles, J. A., López L., J. A., and Castaño, V., "Effect of Grain Size and Second Phase Particles on the Hydrogen Occlusivity of Iron and Steels", Materials Research Innovations, Vol. 3, No. 5, (2000): 263-270.

[36] Lu, B.T., and Luo, J. L., "Relationship between Yield Strength and Near-Neutral pH Stress Corrosion Cracking Resistance of Pipeline Steels: An Effect of Microstructure", Corrosion, Vol. 62, No. 2 (2006): 129-140.

[37] Lessar, J. F., and Gerbrich, W. W., "Grain Size Effects in Hydrogen-Assisted Cracking", Metallurgical Transaction A, Vol. 7A, No. 6, (1976): 953-60.

[38] Chan, S. L. I., "Hydrogen Trapping Ability of Steels With Different Microstructures", Journal of the Chinese Institute of Engineers, Vol. 22, No., 1, (1999): 43-53.

[39] Park, G. T., Koh, S. U., Jung, H. G., and Kim, K. Y., "Effect of Microstructure on the Hydrogen Trapping Efficiency and Hydrogen Induced Cracking of Line pipe Steel", Corrosion Science, Vol. 50, No. 7, (2008): 1865-1871.

[40] Beavers, J. A., "Near-Neutral pH SCC: Dormancy and Re-Initiation of Stress Corrosion Cracks", CC Technologies Report, 2004.

[41] Shoji, T., Suzuki, S., and Ballinger, R. G., "Theoretical Prediction of SCC Growth Behavior-Threshold and Plateau Growth Rate" Proc. 7th Symp on

Environmental Degradation of Materials in Nuclear Power Systems, NACE, Houston, Vol. 2, (1995): 881-891.

[42] Parkins, R. N., and Beavers, J. A., "Some Effects of Strain Rate on the Transgranular Stress Corrosion Cracking of Ferritic Steels in Dilute Near-Neutral-pH solutions", Corrosion, Col. 59, No. 3, (2003): 258-273.

[43] Been, J., and Sutherby, R. L., "Effects of Loading Frequency on Near-Neutral pH Crack Growth on Operating Pipelines", NACE Northern Area Conference, Calgary, Canada, Feb. 7-8, 2006.

[44] Plumtree, A., Williams, B. W., Lambert, S. B., and Sutherby, R., "SCC Growth in Pipeline Steel", Environment-Induced Cracking of Materials, (2008): 199-210.

[45] Wang, Y. Z. "Corrosion Fatigue", Uhlig's Corrosion Handbook. Ed. R. Winston, Revie. 2nd edition, John Wiley & Sons, Inc. 221-232.

[46] Gangloff, R. P. "Environmental Cracking-Corrosion Fatigue", In: Baboian R, editor, Corrosion Tests and Standards: Application and Interpretation, West Conshohocken: ASTM International, (2005): 302-321.

[47] Sadananda, K., and Vasudevan, A. K., "Crack Tip Driving Forces and Crack Growth Representation Uder Fatigue", International Journal of Fatigue, Vol. 26, No. 1, (2004): 39-47.